Chapter 12
The Bushveld Complex, South Africa

R. Grant Cawthorn

Abstract The mafic rocks of the Bushveld Complex, South Africa, were emplaced into a stable cratonic shield some 2.06 b.y. ago, and have remained remarkably well preserved from deformation, metamorphism and low temperature alteration, at least partly by its isostatic impact on the entire crustal thickness. The generation and emplacement of possibly 1 million km^3 of magma within 65,000 years and the lateral continuity of layering (for up to 100 km) remain intriguing challenges to understanding the evolution of this igneous body. The intrusion is exposed as a three-lobed body, up to 7 km thick, with inward dipping layers that range from dunite to monzonite. Platinum-group element-rich orthopyroxenite, chromitite and vanadiferous magnetitite layers contain vast proportions of the World's deposits of these commodities. Modal layering, on scales from mm to tens of m, ranges from well-developed in some vertical sections to virtually absent in others. Distinctive layers (ranging from mm to many tens of m) can be identified in two or even three lobes testifying to their connectivity. Feeders to the intrusion cannot be identified, and the exact compositions (and numbers) of the parental magmas are still debated. Rates and effectiveness of their mixing also require resolution. Models of magma additions and extents of mixing lead to very conflicting interpretations in terms of rapidity and vertical extents of the sequence affected. As the largest known mafic intrusion it represents an end-member in terms of magmatic chamber processes.

I make the following variably contentious suggestions and conclusions. Many long vertical sections that show modal graded bedding (from orthopyroxenite to anorthosite) with no tendency for minerals to occur in their cotectic proportions may be best explained by grain settling and sorting due to gravity (applying Stokes' Law). In contrast, in the chromitite and magnetitite layers marked vertical changes in composition have been attributed to in situ growth. Magma additions may be inferred from upward reversals in the mg# in olivine and pyroxene in the Lower and Main Zones, and upward increase in the An content of plagioclase in the Main Zone. Such reversals are not abrupt, but are preserved through thicknesses of 100 s of metres. Chromitite layers usually have sharp basal contacts and show no change in the mg# of the mafic mineral above, compared to below, each layer. Models of

R. G. Cawthorn (✉)
School of Geosciences, University of the Witwatersrand,
PO Wits, Johannesburg 2050, South Africa
e-mail: Grant.Cawthorn@wits.ac.za

B. Charlier et al. (eds.), *Layered Intrusions,* Springer Geology,
DOI 10.1007/978-94-017-9652-1_12

magma addition and rapid mixing appear inconsistent with such observations and mineral data. Orthopyroxenites in the Upper Critical Zone have an mg# <82 that demonstrates that these minerals formed in equilibrium with plagioclase, but that plagioclase did not co-accumulate with pyroxene. Hence, these pyroxenites did not form from a magma saturated only in pyroxene. At the top of the Critical Zone there is Sr isotopic evidence for major addition of magma, but calculations using the Cr contents of pyroxene preclude any mixing between the magmas. The Cr content of magma needed for chromite saturation and the stability of olivine in the MELTS computer model do not produce crystallization sequences that match actual experimental observations on the MgO- and SiO_2-rich liquids that have been proposed for the parental magmas to the Bushveld Complex

As a consequence of the very slow accumulation rates of grains at the base of the chamber, combinations of Ostwald ripening and annealing caused consolidation into an essentially solid framework close to the grain-magma interface (no more than a few metres). Within most of the layered sequence, the small proportion of interstitial liquid that remained was effectively trapped. During its final solidification, this trapped liquid caused significant changes in mineral compositions, namely (i) decrease in mg# in pyroxenes where present in low abundance, and (ii) incompatible trace-element enrichment in all minerals relative to their original cumulus composition. These effects limit the ability to undertake geochemical modelling based on trace element abundances.

Models that envisage introduction of grain slurries into their present locations either from below or from the sides create more problems than they solve, primarily in terms of producing distinctive layers of near-constant thickness over enormous areas, again by application of Stokes' Law. Furthermore, the low Al_2O_3 content of orthopyroxene is inconsistent with their derivation from a deeper magma chamber.

This chapter summarizes some of the main features of the Bushveld Complex, and then examines some of the main debates and challenges to understanding its magmatic history. Aspects of platinum-group element mineralization are reviewed in a companion chapter. Possibly we (I) err in trying to identify a single (or dominant) process, whereas many mechanisms may have been working in tandem with each being more effective in different situations. Many enigmas remain to be resolved, and there is little agreement regarding almost all aspects of the genesis of this huge body of rock.

Keywords Layering · Cumulate rock · Platinum · Magnetitite · Trapped liquid

History

The first mention of igneous rocks and minerals in the area of South Africa to become famous as the Bushveld was to norite, chromite and magnetite on a map by a German explorer, Carl Mauch, in the late 1860s (Hargar 1934). The first use of the word Bushveld (which refers to savannah with smallish trees—often acacia thornbush—typical on the high plateau north of Pretoria), was the "Plutonic series of the

Bushveld" by Molengraaff (1901). Hall (1932) published a 532-page monograph that included 184 publications on the Bushveld, and by 1976 Molyneux et al. compiled an index of 541 papers and 113 theses, with an addendum (Knowles 1978) of a further 101 publications. It is impossible to speculate on the number of publications now about these rocks. Thus, numerous publications and authors must go unrecognised here, their efforts synthesised by Willemse (1964), Wager and Brown (1968) and Eales and Cawthorn (1996), and recently, primarily on the origin of its ores by Maier et al. (2012). Possibly the single most memorable event was the discovery of the platiniferous Merensky Reef in 1924 that hosts about 75 % of the World's platinum-group element deposits, although platinum-bearing chromitites were known by 1908 (Cawthorn 1999).

Location

The Kaapvaal craton (Fig. 12.1a) became stabilized between 3 and 2.7 b.y., ago and has been intermittently submerged (and rocks in the volcano-sedimentary basins—Witwatersrand, Ventersdorp, Transvaal, Waterberg and Karoo—accumulated), but has not been subsequently significantly deformed or disrupted. Considerable time after the Transvaal sedimentary rocks had formed there were the following events:

- intrusion into the Transvaal sedimentary rocks of mafic sills (totalling at least 2 km in thickness) and eruption of mafic to felsic volcanic rocks (Dullstroom and Rooiberg Groups) up to 3 km thick, although relative ages of the sills and volcanic rocks are unresolved,
- intrusion of the layered ultramafic-monzonitic rocks (Bushveld Complex) up to 7 km thick, and
- intrusion of granites (Lebowa Granite Suite), possibly 2 km thick.The South African Committee on Stratigraphy (SACS 1980) proposed that the term "Bushveld Complex" be applied to all the above-mentioned igneous events occurring within a short time interval at about 2.06 b.y. They proposed the name Rustenburg Layered Series for the mafic rocks. For simplicity, and in keeping with many international publications, I will retain the terminology Bushveld Complex for the layered mafic rocks described here.

The preserved extent of the Bushveld Complex, a schematic section showing relations to country rocks, the Bouguer gravity anomaly map and an inferred cross-section are shown in Figs. 12.1b, c, d and e respectively.

Morphology

Floor and Roof

Almost everywhere the Bushveld Complex has intruded into the Transvaal Supergroup, more specifically the alternating quartzites and shales of the Pretoria Group.

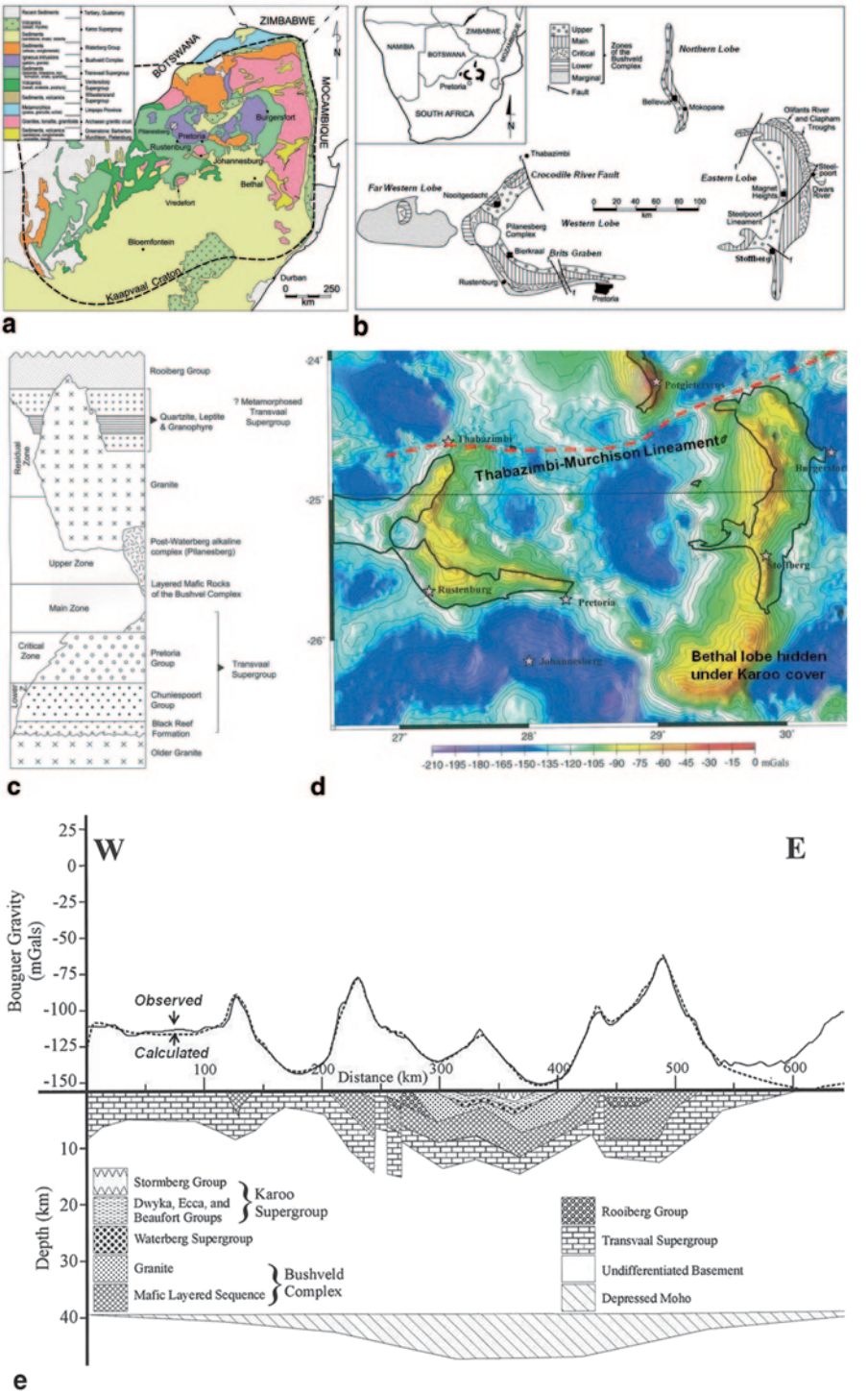

Fig. 12.1 Maps of Bushveld Complex. **a** Regional map showing the Archaean Kaapvaal craton and major sedimentary basins and igneous rocks. **b** Simplified map of the mafic rocks of the

In the west and northeast, emplacement was essentially concordant at the level of the Magaliesberg Quartzite, whereas from Steelpoort (Fig. 12.1b) southward the emplacement was discordant, being emplaced into higher stratigraphic units (Button 1976; Cawthorn 1998). Conversely, in the northern lobe the intrusion was into deeper levels, including the dolomitic Chuniespoort Group and the basement granitic gneisses. All floor rocks have been metamorphosed and variably partially melted (Johnson et al. 2003).

The nature of the roof represents a more enigmatic problem. It is impossible to envisage a mechanically rigid roof of dimensions of over 300 km north-south and east-west atop a magma chamber at up to 1300 °C. The observations of von Gruenewaldt (1972) might be (rather liberally) simplified here to suggest that the roof was composed of the Rooiberg felsic volcanic rocks that were dismembered into enormous blocks that floated on the mafic magma chamber (Cawthorn 2013a). They were continuously melted at their bases, the melt being injected upwards between the blocks, producing granophyres. Residual material was highly metamorphosed, destroying most primary volcanic features. The question of the nature of the original roof rocks is further complicated by the intrusion of the Bushveld Granites close to this boundary.

Vertical and Lateral Extents

The preserved, probably contiguous, sequence can be traced around an area of about 40,000 km^2 (exposed west, east and north lobes), but it is has been proven by drilling of gravity anomalies to occur under Karoo cover in the southeast (called the Bethal lobe; Fig. 12.1a) and immediately north of Thabazimbi (Fig. 12.1b, increasing its extent greatly. Furthermore, its metamorphic aureole can be traced much further outward in the west and east, and the original extent of mafic rocks must have been even greater (Cawthorn and Walraven 1998). They calculated that the volume of this body may be in the order of 1 million km^3.

A stratigraphic column is shown in Fig. 12.2. It implies a maximum thickness of 8 km. However, in many areas various sections, especially of the bottom part, are not developed, and so most profiles do not preserve the entire succession. It cannot be proven but it is now generally accepted that eastern and western lobes are connected through the centre at depth (Nguri et al. 2001), but whether the northern lobe was ever contiguous with the other two is unknown. Very simplistically, the combined eastern and western lobs may be considered to have the shape of a very wide, but irregular funnel with each zone, in places overlapping underlying zones (Kruger 2005). Furthermore, a combination of poor exposure and lack of layering to measure dip, especially in the Main Zone, makes estimates in any profile uncertain.

Bushveld Complex showing the major zones and lobes. At this scale, the outcrop of the Residual or Roof Zone near Stoffberg is too small to demarcate. **c** Schematic block diagram largely taken from Willemse (1964) of the relationships between the major rock formations. **d** Regional Buouger anomaly gravity map including the outcrop of the Bushveld Complex (outlined) as compiled by the Council for Geoscience. **e** West-east section, shown on Fig. 12.1d of gravity data and inferred structure (from Cawthorn et al. 1998). Dotted and solid lines are calculated and observed gravity respectively

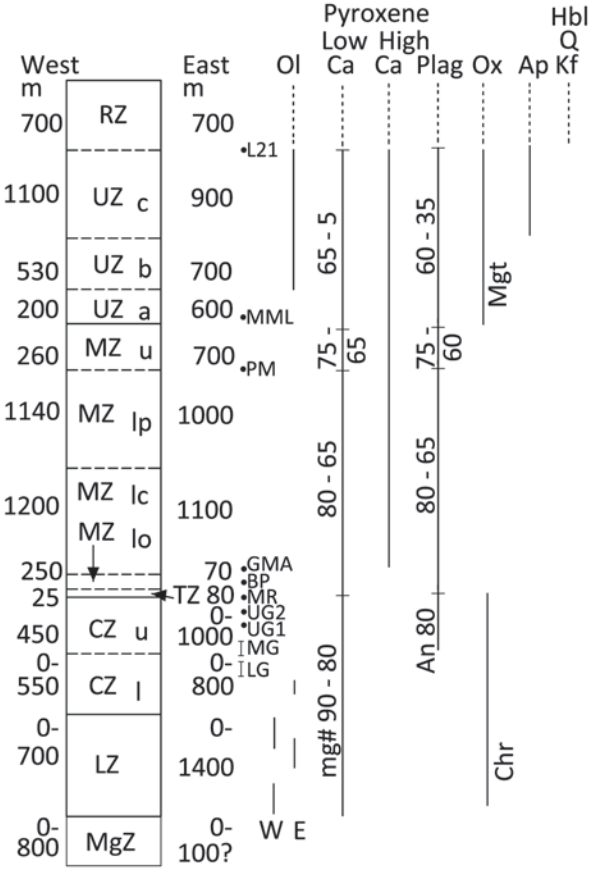

Fig. 12.2 Stratigraphic section through the Bushveld Complex (adapted and enlarged after Cawthorn 2013a). The maximum thicknesses are shown, and should not be summed to obtain actual total thickness anywhere. The solid lines denote cumulus mineral assemblages, dotted lines intercumulus status. Abbreviations of the zones: *MgZ* Marginal, *LZ* Lower, CZ_l Lower Critical, CZ_u Upper Critical, *TZ* Transition, MZ_{lo} Lower Main (primary orthopyroxene), MZ_{lc} Lower Main (cumulus clinopyroxene and orthopyroxene), MZ_{lp} Lower Main (primary pigeonite), MZ_u Upper Main, UZ_a Upper a, UZ_b Upper b, UZ_c Upper c, *RZ* Residual (or Roof). Mineral abbreviations: *Ol* olivine, Low Ca low-calcium pyroxene (orthopyroxene, inverted clinobronzite and inverted pigeonite), high Ca high-calcium clinopyroxene, *Plag* plagioclase, *Ox* oxide (*mgt* magnetite, *chr* chromite), *Ap* apatite, *Hbl* hornblende, *Q* quartz, *Kf* potassium feldspar. W and E in the olivine column refer to west and east lobes. Important marker horizons are indicated: *LG*, *MG UG* Lower, Middle and Upper Group Chromitites, *MR* Merensky Reef, *BP* Bastard Pyroxenite, *GMA* Giant Mottled Anorthosite, *PM* Pyroxenite Marker, *MML* and *L21* Main Magnetitite Layer and magnetitite layer 21. Generalized cumulus compositional trends are shown for low-calcium pyroxene (mg#) and plagioclase (anorthite content)

The vertical succession is divided into zones based mainly on mineral assemblages. The Lower Zone may reach 2 km thick, but is only present in a series of troughs. The most spectacular outcrops (Fig. 12.3a) are developed in the Olifants River section (Fig. 12.1b), described by Cameron (1978). Another detailed study

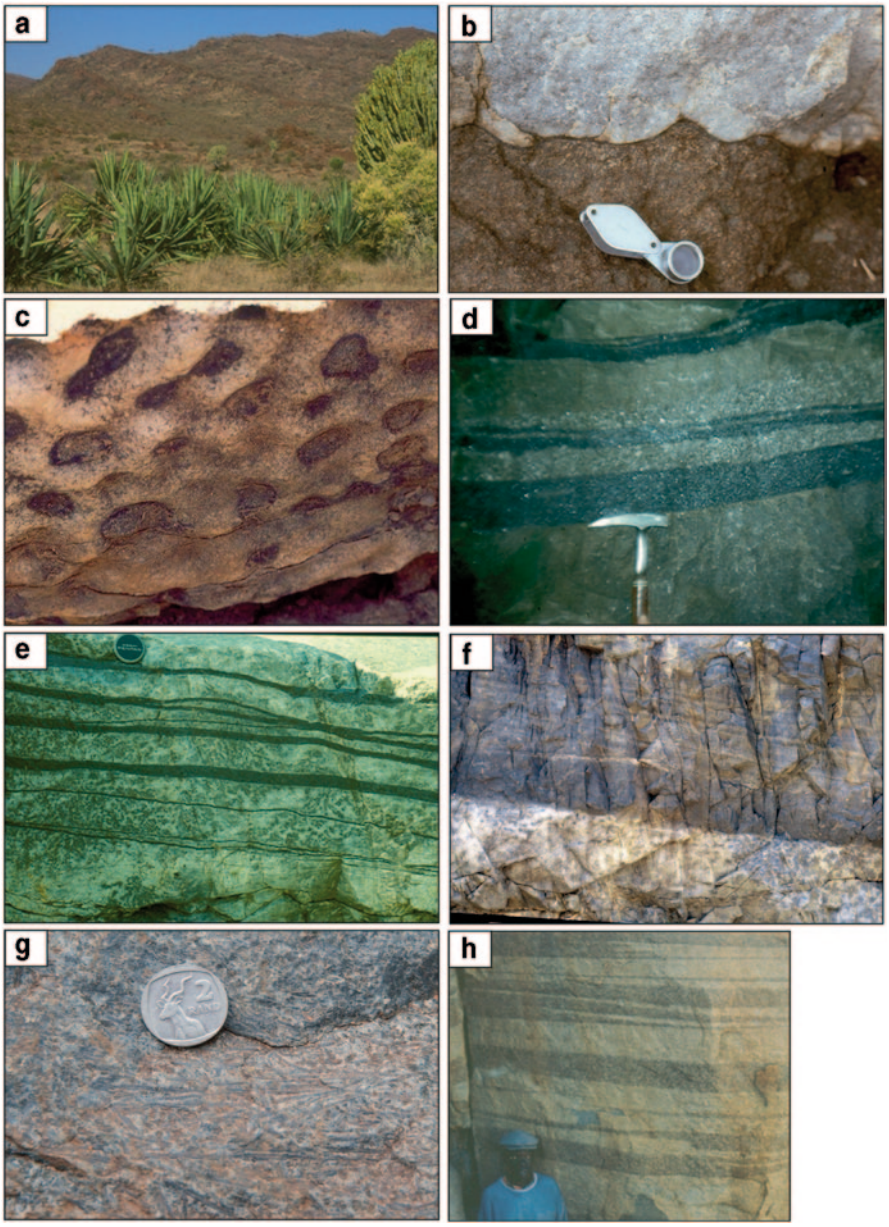

Fig. 12.3 Assorted photographs of aspects of the layering of the Bushveld Complex. **a** Dunite-pyroxenite layering on a scale of tens of m in the Lower Zone in the Olifants River trough. **b** and **c** Boundary between Lower Critical Zone and Upper Critical Zone on Jaglust (Cameron 1978). Feldspathic pyroxenite is overlain by a thin chromitite layer (MG2) and leuconorite. The chromitite layer displays undulations (like load structures) as displayed by the undersurface of that chromitite and anorthosite seen in an overhanging slab (**c**). Width of view 20 cm. **d** Thin chromitite layers with sharp upper and lower contacts interlayered with pyroxenite and pegmatitic pyroxenite. Note that the pegmatitic facies can occur directly above a chromitite and also terminate against a pyroxenite of normal grain size (Steelpoort chromite mine). **e** Sharp upper and lower

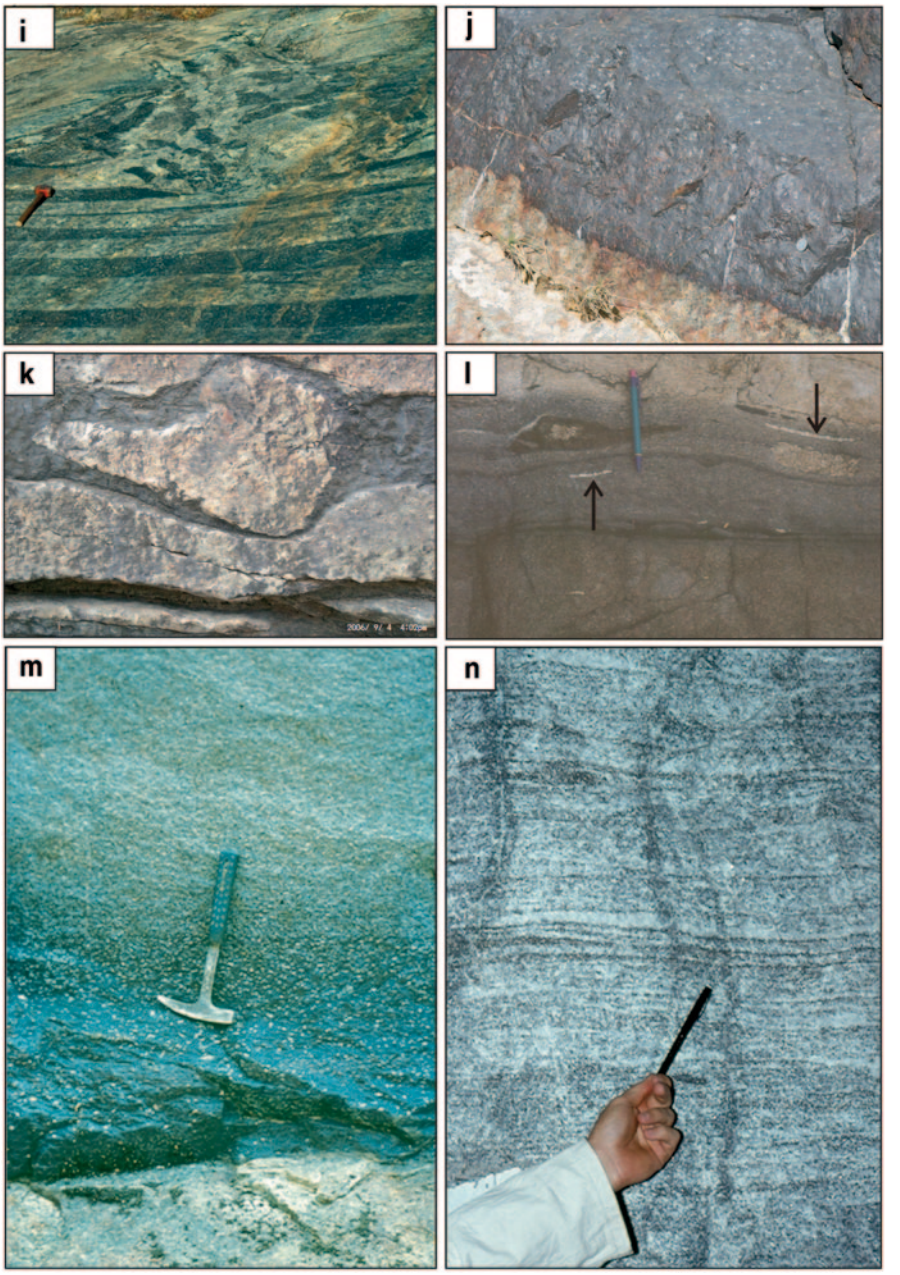

Fig. 12.3 (continued) contacts to thin chromitite layers in poikilitic anorthosite. Note the small lenses of anorthosite and birfurcations of the chromitite layers (Dwars River). **f** Rare outcrop of the Pyroxenite Marker, (on the farm Mooimeissiesfontein) eastern lobe, showing parallel cross bedding in the overlying gabbronorite. Width of view 1 m. The more massive and resistant nature of this rock is due to the inversion of many small grains of pigeonite into large poikiloblasts of orthopyroxene that make a powerful "cement". **g** Random spinifex textured pyroxenite about 10 m from the floor contact (near Burgersfort). Coin is 2.5 cm. **h** Thinly layered melagabbronorite—leucogabbronorite

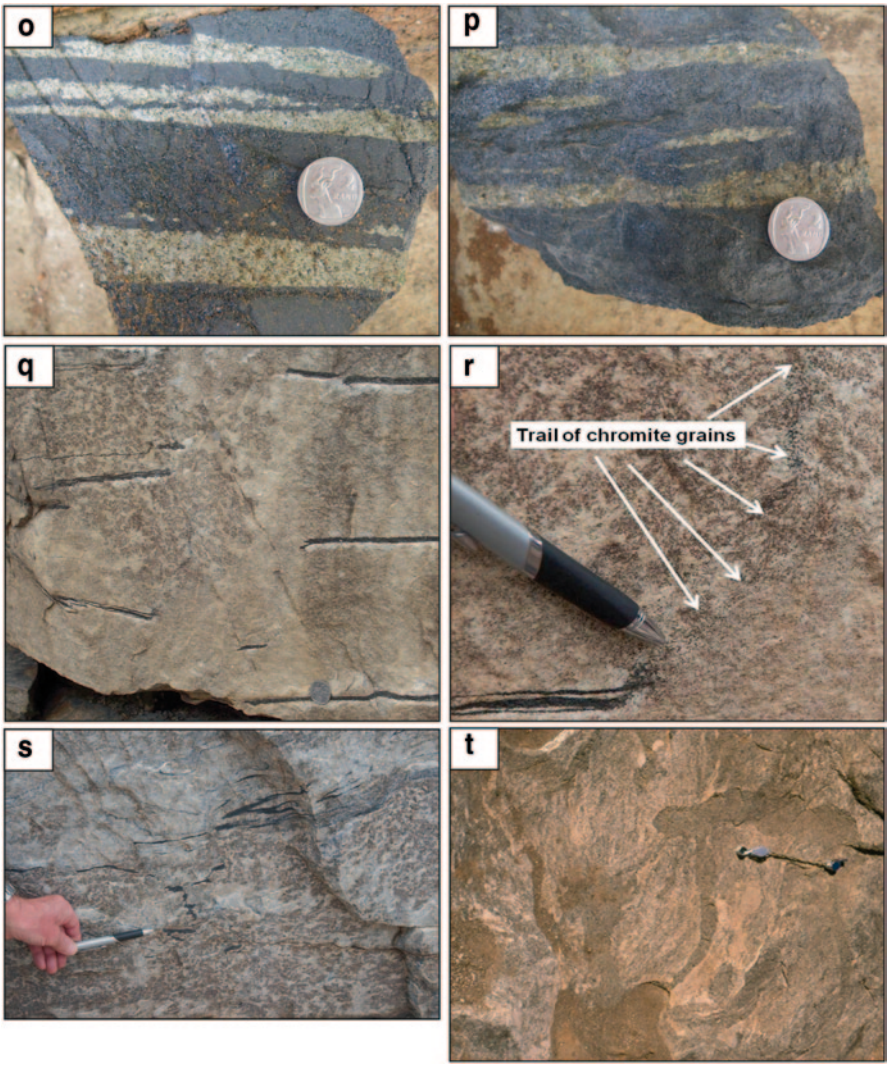

Fig. 12.3 (continued) a short distance below the Pyroxenite Marker, Main Zone. All rocks contain cumulus plagioclase and two pyroxenes, but none are in their cotectic proportions (Quadling and Cawthorn 1994). Note the planar cross-bedded structure and termination of mafic layers. Photo from Dr TG Molyneux. **i** Disruption of thinly layered sequence shown in (**h**) and redeposition of angular fragments testifying to the force of horizontal currents, and the solid nature of the cumulate pile immediately below the mush-liquid interface. **j** Main Magnetitite layer with a sharp, planar contact to underlying anorthosite (Magnet Heights). Width of view 50 cm. **k** Rounded anorthosite fragment in thin chromitite layer. Note depression of the lower contact of the chromitite due to the impingement of the autolith (Dwars River). Width of view 25 cm. **l** Assorted fragments (autoliths) in disseminated MG2 chromitite overlying feldspathic pyroxenite. Two of the fragments are anorthosite, but there are allegedly no rocks with cumulus plagioclase below this level (2 km south of Jaglust). **m** Magnetitite layer 1 (first above the Main Layer) showing abrupt underlying contact with anorthosite and upper contact grading into anorthosite. Note the absence of pyroxene. **n** Thinly layered anorthosite—pyroxenite in footwall to UG2 at Impala Platinum Mines (Rustenburg). **o** and **p** two examples (analogous to the Dwars River locality) showing bifurcation of chromitite (**o**) and

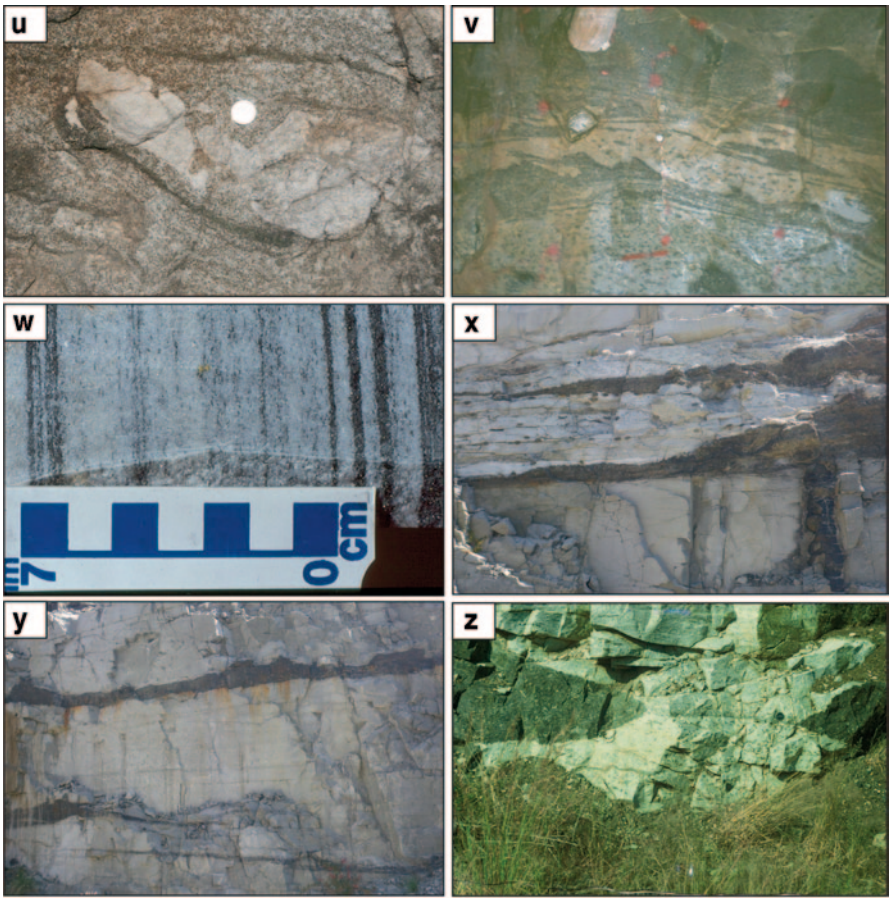

Fig. 12.3 (continued) extremely thin lenses (**p**) of pyroxenite in LG6 Chromitite layer. Coin is 2.5 cm. **q** and **r** Disruption of thin chromitite layers **q** showing brittle fragmentation unlike the plastic deformation shown in **s**. The large oikocryst of orthopyroxene on left has grown across the boundary between the layered chromitite-anorthosite sequence and the disrupted vertical mass of anorthosite. Width of view 50 cm. Close-up (**r**) of edge of the chromitite layer at bottom left of (**q**). Note that where the anorthosite has re-intruded through the chromitite layer a trail of chromite grains has been smeared upward along the contact between the primary anorthosite and the remobilised anorthosite (Dwars River). **s** Extreme deformation emphasized by the thin chromitite layer. Note that the chromitite layer retains extremely sharp contacts despite deformation, and shows no tendency to disaggregate (Dwars River). **t** and **u** Plan view of deformed melanorite—anorthosite (**t**) and brecciation of anorthosite fragments (**u**) and redeposition in norite (below UG3 chromitite, Maandagshoek). Coin is 2.5 cm. **v** Vertical mine face showing "Flame Bed" of variably slumped norite and poikilitic anorthosite layers below the Merensky Reef on Impala Platinum Mines (Rustenburg). Width of view 50 cm. **w** Examples of the extreme thinness of chromitite layers, and even mere heavy disseminations in planar bedding in anorthosite. **x**, **y** and **z** Assorted features of disruptive iron-rich ultramafic bodies. Vertical dyke (**x**) turning into a horizontal structure. Width of view 5 m. Concordant body (**y**) with a perfectly planar basal surface but more irregular upper contact to anorthosite. Width of view 8 m. Highly irregular margins to two discordant bodies (**z**). Width of view 4 m. **x** and **y** are from Lonplats mines, and **z** is from Tweefontein (Tegner et al. 1994)

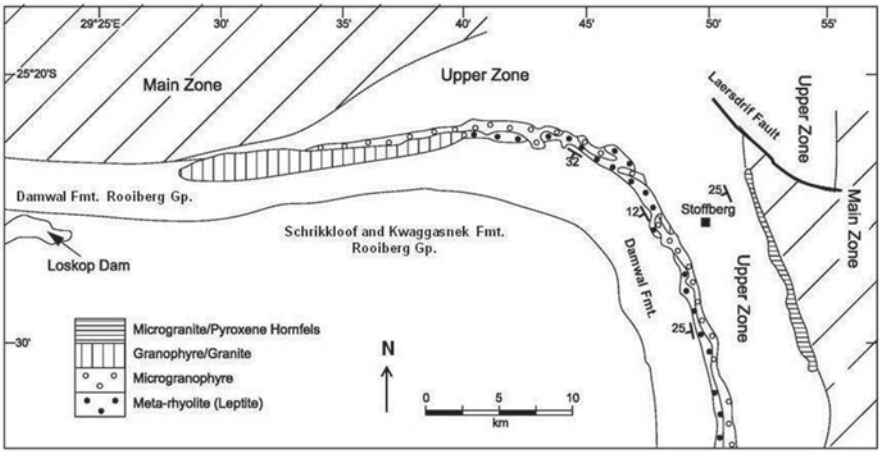

Fig. 12.4 Geological map of the Loskop Dam area in the southeastern Bushveld, showing how the mafic rocks at the upper contact with the roof rock felsites may range from Main Zone in the west to Upper Zone in the east. Mainly from the 1:250,000 maps of the Council for Geoscience, South Africa, and Groeneveld (1970)

comes from a borehole section at Nooitgedacht (Fig. 12.1b), Union Mine (Teigler and Eales 1996). The lateral extents of the Critical, Main and Upper Zones progressively increase (Kruger 2005) as the magma chamber expanded with sequential filling (Fig. 12.1b). This expansion is most obvious in the southeast. The extent to which Lower and Critical Zones may persist below the onlap of the Main Zone there is unknown.

The top contact is also discordant (Fig. 12.4), most obviously near Stoffberg (Fig. 12.1b). From northwest to southeast in this area, the topmost rocks range from Main Zone through Upper Zone to a poorly exposed sequence recorded by Hall (1932) as syenite and Groeneveld (1970) as fayalite diorite, for which the name Residual or Roof Zone (and rock type—monzonite) has recently been proposed (Cawthorn 2013a).

Continuity

Hall's (1932) cross-section from west to east showed the western and eastern lobes as connected in the form of a lopolith. Initial regional gravity interpretations suggested they were not connected, but reinterpretations of the regional gravity data from the Council for Geoscience, shown in Fig. 12.1d by Cawthorn et al. (1998) and Webb et al. (2011) reinstated the connectivity hypothesis (see modelled cross-section in Fig. 12.1e). Apart from demonstrating the isostatic effects of this thick, dense body, causing depression of the continental crust—mantle boundary, Cawthorn et al. (1998) noted the existence of numerous very distinct matching layers of rocks in eastern and western lobes. At the level of the Lower Zone discrete elongate

finger-like bodies may have existed (Uken and Watkeys 1997a), but the occurrence in both lobes of the same number of distinctive chromitite layers of comparable compositions in the Lower Critical Zone suggests consanguinity from that level upward. The southern portion of the northern lobe appears lithologically different from the equivalent levels in the west and east. Lower Zone rocks are recognised, but debate continues as to the extent of equivalent Critical Zone rocks in the north (Kinnaird et al. 2005). The scarcity of chromitite layers suggests a discrete evolution of the northern chamber at this stage. Debate also continues as to whether the Platreef (a coarse-grained platiniferous orthopyroxenite) in the north is the equivalent of the Merensky Reef in the west and east. It is complicated by the fact that the Platreef has been extensively modified at the liquidus and subsolidus stages by interaction with the underlying floor rocks, especially the very reactive Chuniespoort dolomites (Kinnaird et al. 2005). Above this level (into the Main Zone), boreholes studied by Ashwal et al. (2005) and Roelofse and Ashwal (2012) in the northern lobe provide evidence for possible correlations with the east and west lobes, in that the mineral assemblages and compositions in the northern lobe have many similarities with the Main and Upper Zones elsewhere. A difference exists in the middle of the Main Zone where a chemically distinct Pyroxenite Marker in the west and east may have a lateral representation as a troctolite layer in the north. Again, above this layer the mineral compositions and distinctive magnetitite layers, especially in terms of thickness and vanadium content in the north find analogues in the west and east (Cawthorn and Molyneux 1986). Connectivity therefore probably also extended to the northern lobe at this level, but perfect lateral homogeneity may not have been achieved. The southeastern or Bethal lobe is only known from borehole information (Buchanan 1979), and consists of Upper Zone lithologies. It was probably connected with the eastern lobe over a structural arch that was possibly only overflowed by the transgression of Upper Zone magma (Kruger 2005). In the far western lobe, erosion has removed all except Marginal to Lower Critical Zones (Engelbrecht 1985), but the extensive thermal aureole (Engelbrecht 1990) suggests that a very thick and laterally extensive body originally existed here.

Feeders

The location(s) of vertical feeders that must have existed remain elusive. Dyke swarms have variably been proposed (Uken and Watkeys 1997b; Olssen et al. 2010), but none has the right age or distinctive composition (see “Parental Magmas”) to indicate magma injection mechanisms (Maré and Fourie 2012). Eales (2002) proposed a feeder (of undefined shape) in the northwest, based on the gravity high. However, this “high” occupies an extent of more than 30 km north-northeast by several km perpendicularly. Such an enormous area (bigger than almost every other layered intrusion in the World) cannot represent a feeder, but indicates an area underlain by very thick ultramafic rocks. The east-northeast trending Thabazimbi-Murchison lineament (Fig. 12.1d) has also been proposed as a feeder direction, based on the fact that some of the best studied Lower Zone sections occur in the west, east and north close to this structure (Clarke et al. 2009). Apart from this

spatial connection no other evidence exists, specifically, there are no gravity highs along that trend (Fig. 12.1d). Hatton and von Gruenewaldt (1987) documented fundamental differences in the thickness and spacing of most chromitite layers on either side of the Steelpoort lineament (a very straight 60 km-long valley, 2 km wide and devoid of outcrop, Fig. 12.1b). Such a dramatic change in detailed stratigraphic sequence is reminiscent of that observed in the Rum Intrusion where the eastern and western layered sequences cannot be correlated; they are separated by the Long Loch fault within which there is outcrop of chaotic melanges and breccias indicative of a feeder zone. By analogy, in the east (Steelpoort) and in the west (Crocodile and Rustenburg) conjugate faults defining the normal fault directions in a north-south compressive strain ellipsoid (du Plessis and Walraven 1990) could represent potential feeder directions. This issue remains unsolved.

Age

In the last 10 years many age determinations have been undertaken on different minerals from the Rooiberg Group lavas, the mafic layered rocks and the granites. Almost all suggest an age of 2.056–2.060 b.y. These data are reviewed by Scoates et al. (this volume). Intriguingly, they further suggest that there may a time break of 5 m.y. at the base of the Merensky Reef, top of the Critical Zone. Such an assertion creates problems. There is no chill at that level, as expected if there had been such a long time gap. The Sr isotopic evidence for a new magma occurs above the Merensky Reef (as discussed under "Parental Magmas") This disparity needs further investigation.

Stratigraphy

The gross structure of the Bushveld is relatively simple—gently radially inward dipping layered mafic rocks. However, exposure is very poor in the west and north and only generalizations of the stratigraphy are possible there. Exposure is intermittently better in the east. Fortunately, a number of deep boreholes have been drilled by exploration companies and the Council for Geoscience, and provide detailed vertical sections, but lateral variations are known to exist.

The names Marginal, Lower, Critical, Main and Upper Zones have long been used (Hall 1932), but proposed boundaries have changed (and still need reconsideration). The currently used boundaries and subdivisions were formalized by Wager and Brown (1968). Subsequently, the South African Committee on Stratigraphy (SACS 1980) proposed an alternative nomenclature, namely that the mafic layered rocks be termed the Rustenburg Layered Suite. It rejected the zonal nomenclature and proposed names that reflected local geographic features. Thus, the Main Zone was given the names Winnaarshoek Norite-Anorthosite, Leolo Mountain Gabbronorite and Mapochs Gabbronorite for the eastern lobe; Mathlagame Norite-

Table 12.1 Proposed parental magmas to different successions in the Bushveld Complex

	B1	B2	B3	Hendriksplaas Norite	Marginal Zone Rustenburg
SiO_2	5567	50.79	51.33	48.52	50.93
TiO_2	0.33	0.76	0.37	0.20	0.21
Al_2O_3	11.46	15.7	16.14	17.4	18.03
Fe_2O_3	9.96	12.54	10.45	10.19	7.70
MnO	0.17	0.19	0.18	0.23	0.16
MgO	13.36	6.91	7.69	8.53	8.81
CaO	6.32	10.7	11.25	11.92	9.85
Na_2O	1.59	1.94	1.91	1.95	2.28
K_2O	1.07	0.25	0.28	0.11	0.16
P_2O_5	0.06	0.16	0.03	0.03	0.01
LOI	−0.01	0.27	0.17		
(ppm)					
S		177(90)	97(36)		
Ba	293	192	139		91
Cr	1874	201	408		650
Cu	32	76(67)	46 (13)		26
Nb	4.5	3.9	1.4		
Ni	368	106	133		193
Rb	41	4.44	8.86	1	7
Sr	198	348	337	313	295
Y	11.4	19.4	9.92	10	9
Zr	71	54.3	22.9	10	13

Lower Zone (B1) magma—sample from locality described by Davies et al. (1980), with trace elements re-analysed by Barnes et al. (2010). Average B2 and B3 are from Barnes et al. (2010). B2 and B3 are remarkably similar despite the suggestion that they are parental to the Upper Critical and Main Zones respectively. Hendriksplaas norite is from the type locality of the Marginal Zone, eastern lobe (own unpublished data). Marginal Zone, Rustenburg is average from Davies (1982). Both of these two samples are from below Lower and Lower Critical Zones

Anorthosite and Pyramid Gabbronorite for the western lobe, and no proposed name for the same rocks in the northern lobe. I argue that such terminology destroys the important consanguinity of such rocks, and negates attempts to correlate, which I suggest we can do with a high degree of confidence.

The Marginal Zone (called the Hendriksplaas Norite in older literature) is the most enigmatic. Nearly everywhere that it is in contact with the Magaliesberg Quartzite floor rocks, the contact is covered by a thick quartzite scree. Its upper contact with the ultramafic rocks is also rarely exposed. It is a variably fine/medium grained norite showing poor layering, and can reach up to 800 m in the west (Vermaak 1976), based on borehole intersections, but may be totally absent (Wilson 2012). Such thicknesses and variable grain size, suggest multiple injections. However, its depletion in incompatible elements such as Zr (Table 12.1)

suggests that it has partial cumulate characteristics. Its composition is not suitable as a parental magma to the Lower Zone (see "Parental Magmas") and may represent multiple, variably differentiated injections of magma, not directly related to the layered mafic rocks. However, no chilled facies can be found between these rocks and the Lower Zone to demonstrate an age difference.

The Lower Zone has a basal orthopyroxene-rich succession, followed by and interlayered with (thin) olivine-rich sequences (Fig. 12.2). (I know of only two clinopyroxenite layers in the entire intrusion, and so the term pyroxenite henceforth refers to orthopyroxenite.) In the Stillwater Intrusion Cooper (1997) has shown that specific layers within such alternations of dunite-harzburgite-orthopyroxenite packages cannot be traced laterally with confidence (based on many closely-spaced boreholes). The outcropping alternating sequence in the Olifants River Trough (Cameron 1978) provides the only opportunity to test for such similarity in the Bushveld. My attempted detailed mapping was not conclusive due to poor outcrop, but in general, olivine-rich layers could not be traced along strike for more than a very few hundred metres out of 6 km of the trough. (Magnesite—the product of surface breakdown of olivine by acid rain-water was usually the only tracer for such olivine-bearing layers.) In this trough, Cameron (1978) suggested that there was an upper pyroxenite within the Lower Zone above which an increase in interstitial plagioclase defined the top of the Lower Zone. However, in the west, the borehole study by Teigler and Eales (1996) showed no increase in interstitial plagioclase, and they argued for placing the top of the Lower Zone at the top of the uppermost olivine-rich layer. I would subscribe to that view. However, if one could totally redefine units, I would include all ultramafic rocks of the Lower Zone and Lower Critical Zone into a single zone, making it comparable to the Ultramafic Unit of the Stillwater Complex.

The Critical Zone was so named, according to Hall (1932), because of the remarkable layering inferred to result from some unspecified "critical" conditions operating in the magma chamber. Those critical conditions are still not understood. It is divided into a Lower and Upper Critical Zone based on the appearance of cumulus plagioclase. The Lower Critical Zone is dominated by pyroxenite with rare olivine-bearing units and chromitite layers. There is a package that contains up to 7 chromitite layers referred to as the Lower Group chromitites (LG1–LG7, numbered from the base upward), but only the LG6 is thick enough to be economic. The continuity of the lowest layers is not known and may be limited, which may indicate that the chamber was still not fully interconnected at these levels. (Layering in the Lower Critical Zone is not very pronounced, so perhaps it should not be designated as "Critical" Zone, but merely part of an Ultramafic Suite, as suggested above.) In the west there is a considerable gap between the LG chromitites and a Middle Group of chromitites (MG1–MG4), whereas in the east there is only a short vertical interval between the LG and MG. It is above the MG2 layer that cumulus plagioclase appears (Fig. 12.3b). The origin of the features analogous to load structures in sedimentary rocks (Fig. 12.3c) at the lower surface of the thin MG3 chromitite remains enigmatic. The relationship between overlying anorthosite (low density) and underlying pyroxenite (high density) negates the possibility that

such features are density driven. Above this level the spectacular layering is seen in repetitive sequences typically of chromitite, (rarely harzburgite), pyroxenite, norite, and anorthosite. (They are called cycles, but should actually be called rhythmic units. A cycle ought to be of the kind ABCDCBA, whereas a rhythm is ABCD-ABCD, as discussed by Wager and Brown 1968, p. 545). It is thus only the Upper Critical Zone that results from these "critical" conditions of Hall (1932). Near the top of the Upper Critical Zone occur the Upper Group 1 and 2 chromitite layers (there is a third in the northeast). The uppermost chromitites occurs within the Merensky Unit (in which there may be one, two or three chromitite layers around the Bushveld), although a discontinuous chromitite may occur at the base of the uppermost rhythmic unit, known as the Bastard Unit (based on its remarkable similarity to the Merensky Unit in all aspects except being devoid of platinum-group elements).

Variation in thickness of chromitite layers exists within individual lobes, especially across the Steelpoort lineament (Hatton and von Gruenewaldt 1987). In the north of the eastern lobe the LG chromitites are traceable with constant thicknesses for 100 km. However, south of the Steelpoort lineament there are probably no LG chromitites or at most very trivially thin layers. In contrast, the MG chromitites are very robust south of Steelpoort compared to the north. Debate exists among chromite-mining companies as to whether it is the LG6 or MG1 that is the thick layer mined south of the lineament. I would suggest that it is the MG1 on the basis of whole-rock analyses that show the undisputed LG6 layer north of Steelpoort contains interstitial orthopyroxene only, whereas south of Steelpoort the mined layer has both orthopyroxene and plagioclase (Fig. 12.5), consistent with it having an affinity with the Upper Critical Zone. Faulting cannot change the thickness or vertical spacing of rock layers—in this case, chromitite layers, and so the role of this Steelpoort lineament in controlling the thickness of chromitite layers remains to be resolved. In the western lobe, the LG chromitites apparently do not occur to the east of the Spruitfontein structure about 20 km east of Rustenburg (Clarke et al. 2000), but detailed successions in this area have not been made available by the chromite-mining companies and exposure is lacking.

The sequences of pyroxenite-norite-anorthosite in each rhythmic unit are more complicated than the names imply (as discussed in the section "Origin of Layering"). Small-scale layering with modal variations of orthopyroxene and plagioclase exist, with both sharp and gradational contacts between units. Chromitite layers almost always have very sharp lower and upper contacts (Fig. 12.3d and e).

The boundary between the Critical Zone and the gabbronorite-dominated and largely unlayered Main Zone is not clearly defined. It has been taken within the Merensky Unit on the basis of a Sr isotopic break (see section "Parental Magmas"). An alternative boundary is at the top of the highest prominent rhythmic unit, known as the Bastard Unit. The top of this unit is marked by a poikilitic anorthosite with extremely large oikocrysts of pyroxene (the Giant Mottled Anorthosite). Above this layer are leuconorites which are difficult to distinguish from common similar rocks of the Critical Zone, but with a distinctly lower Cr/MgO whole-rock value (see below). Use of the principle espoused by Wager and Brown (1968) of using mineral

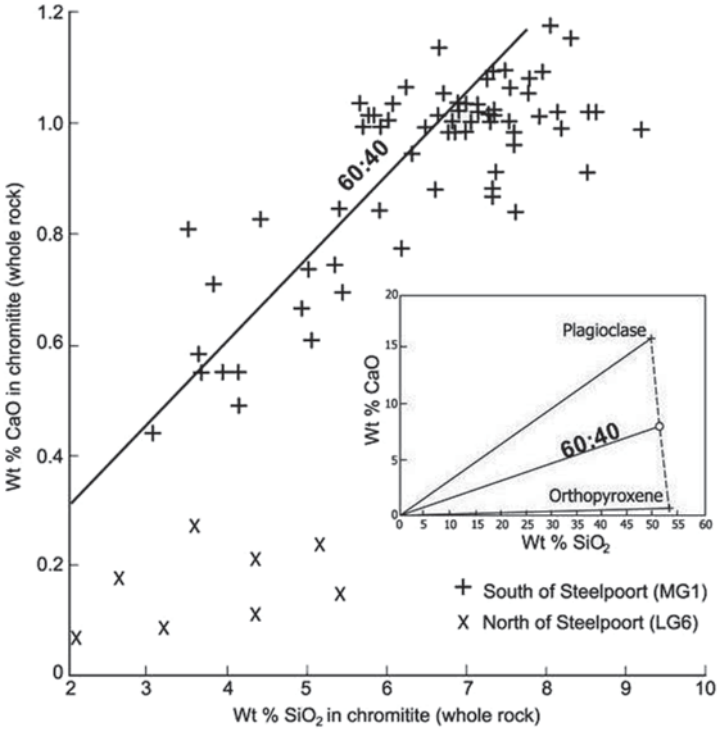

Fig. 12.5 Plot of whole-rock compositions (SiO_2 versus CaO) from the LG6 and MG1 chromitite layers. Note how the LG6 data show a trend toward orthopyroxene as the only interstitial phase, whereas the MG1 data show a trend toward orthopyroxene (40 %) plus plagioclase (60 %) as interstitial phases (as shown in the inset). The LG6 analyses are from north of the Steelpoort lineament where the designation as LG6 is undisputed. The MG1 is from south of the lineament where it has been proposed that this layer may be the same as the LG6 north of the lineament. This chemical difference demonstrates that the MG1 is genuinely different from the LG6. All data with less than 2 % SiO_2 have been excluded. (Data are own unpublished analyses)

(dis)appearance for stratigraphic subdivision would place a boundary some 300 m higher where cumulus clinopyroxene appears (Von Gruenewaldt 1973; Mitchell 1990). Thus, an entirely satisfactory definition for the boundary does not exist. An alternative scheme was proposed by Kruger (1990). He suggested the term Transition Unit for an interval from the Merensky unit up to the Giant Mottled Anorthosite. The reasons were elaborated by Seabrook et al. (2005) who showed that the initial Sr isotope ratio increased a short distance above, but not at, the Merensky chromitite, whereas the Cr content of pyroxene only decreased at the top of this succession. Thus, this interval contains geochemical features of both Critical and Main Zones, and hence the term "transition".

Somewhat higher the primary orthopyroxene is gradually replaced by pigeonite, now inverted to orthopyroxene, producing very large poikiloblasts. Thus, three cumulus pyroxenes appear to co-exist. Even higher, there occurs an important layer,

known as the Pyroxenite Marker (Von Gruenewaldt 1973; Klemm et al. 1985a; VanTongeren and Mathez 2013). It has been traced for about 70 km in the east, but then laterally terminates (Von Gruenewaldt 1973), to be replaced by a magnetite gabbronorite. There is only one (borehole core) example of it in the west (Cawthorn et al. 1991), so its ubiquity must be considered doubtful. A correlatable stratigraphic unit in the northern lobe may be represented by a troctolite layer (Ashwal et al. 2005). In the east and west lobes this marker is overlain by a thick zone where primary orthopyroxene reappears. The mg# of pyroxene and the An value of plagioclase increase upward, and the initial Sr isotopic ratio decreases, all over an interval of about 300 m that straddles the Pyroxenite Marker (Von Gruenewaldt 1973; Klemm et al. 1985a; Cawthorn et al. 1991; VanTongeren and Mathez 2013). Locally developed below this marker the rocks may be quite strongly modally layered (Molyneux 1974; Quadling and Cawthorn 1994; Nex et al. 1998), and above it fine-scale modal layering is observed (Fig. 12.3f). Rare anorthosites occur throughout the Main Zone.

The base of the Upper Zone is defined by the appearance of cumulus titanomagnetite, a short vertical interval above which occur layers of almost monomineralic magnetite. 25 have been identified in the east, slightly fewer in the west and north. Two thick and distinctive layers appear to be continuous throughout all three lobes. Near the base is a 2 m-thick layer, mined for its 1 % vanadium. The uppermost layer is more disseminated and up to 6 m thick with only 0.2 % V. Of the many unresolved issues regarding these layers is the little mentioned fact that almost all layers are over- and underlain by anorthosites; cumulus mafic minerals are generally absent.

A three-fold subdivision of the Upper Zone; subzone (a) containing plagioclase, pyroxenes and magnetite; subzone (b) also with olivine and subzone (c) also with apatite was proposed by Wager and Brown (1968). I suggest this subdivision was strongly influenced by their subdivision of the Skaergaard Intrusion, and also the fact that there is good exposure of such a section near Magnet Heights in the east (Fig. 12.1b). Such a subdivision ignores the conclusions of Hall (1932), who reported rocks that he called syenite in all lobes at the top of the intrusion. They were described in more detail by Groeneveld (1970) from the southeast, but not included into any formal stratigraphy despite being 700 m thick according to him. I have proposed that their existence requires incorporation into the stratigraphy as the Residual or Roof Zone (Cawthorn 2013a). These rocks do not display an obvious cumulus texture, and contain increasing proportions of hornblende, quartz and potassium feldspar. It is relevant here to contrast the Bushveld and Skaergaard successions. The Skaergaard crystallized from bottom, top and sides (albeit different thicknesses). No sides are known for the Bushveld, and the crystallization is unidirectional with no accumulation from the top. This difference is almost certainly due to the nature of the roof rocks. In Skaergaard they are refractory basalt. In the Bushveld they are felsic volcanics that would have been intermittently melted by the underlying basaltic magma and hence, no crystals could have adhered to the upper surface.

Two important discordant features in the Bushveld need mention. The first occurs north of the Pilanesberg Complex (Fig. 12.1b) where the Upper Zone rocks

cut through the Main and Critical Zone and abut the floor rocks. Faulting can be ruled out because the floor rocks are not displaced, and layers of magnetitite drape with centripetal dips into this large depression rather than dipping uniformly toward the centre of the complex. Wilson et al. (1994) presented a detailed study of the mineral compositions and initial Sr isotope ratio of samples from a borehole close to the edge of the northern transgression. They identified xenoliths of Main Zone rocks engulfed in the host Upper Zone and concluded that there had been major injection of the magma that produced the Upper Zone disrupting the original layered succession. The fate of the disrupted Main and Critical Zone rocks is unknown. (Each of these two transgressive Upper Zones lobes is the size of the Skaergaard intrusion.) The second feature is the presence of discordant (perpendicular to the layering) pegmatitic iron-rich ultramafic bodies (Scoon and Mitchell 1994). They are extremely irregularly distributed round the intrusion. They trend from olivine- and clinopyroxene-rich near the base to magnetite-rich near the top.

Mineral Compositions

Mineral compositions define a stratigraphy. Generalized trends of vertical changes in mineral compositions from many studies have been compiled previously, and summarized in Fig. 12.2. The overall fractionation trends of An value in plagioclase and mg# in mafic minerals belies a much more complicated pattern in detail. In strongly modally layered rocks mineral compositions (both major and trace elements) can be modified by reaction with the interstitial magma, especially for the mafic minerals, which greatly complicates interpretation (as discussed in the section "Trapped Liquid Shift Effect").

In the ultramafic rocks of the Lower and Critical Zones the minerals show a pattern of differentiation and reversals (Fig. 12.6), such that through a vertical interval of over 1500 m (at the extreme thickest) only minor net differentiation can be observed. Profiles from west and east are broadly similar, but it is not possible to suggest that any specific reversal can be traced that distance laterally. Recently, a section in the east containing even higher mg# phases ($Fo_{91.5}$) has been identified in borecore (Wilson 2012). In the north, comparable highly Mg-rich compositions have been identified (Hulbert and von Gruenewaldt 1985). The very minor interstitial plagioclase is quite strongly zoned and provides no petrological information.

With regard to Fig. 12.6, near the base of the Lower Zone there is an interval of rocks with cumulus plagioclase. It has been indicated in diagrams by Vermaak (1976) in the southwest, and Cameron (1978) in the northeast, although little information is available apart from its existence. A much more detailed study of these rocks in the northwest was presented by Teigler and Eales (1996), who reported that it was 60 m thick and contained an average of 20% plagioclase. Its location coincides with the most evolved orthopyroxene compositions (Fig. 12.6a and b), and they concluded that its occurrence was consistent with differentiation of the magma. Its existence at three such widely separated places might suggest that mag-

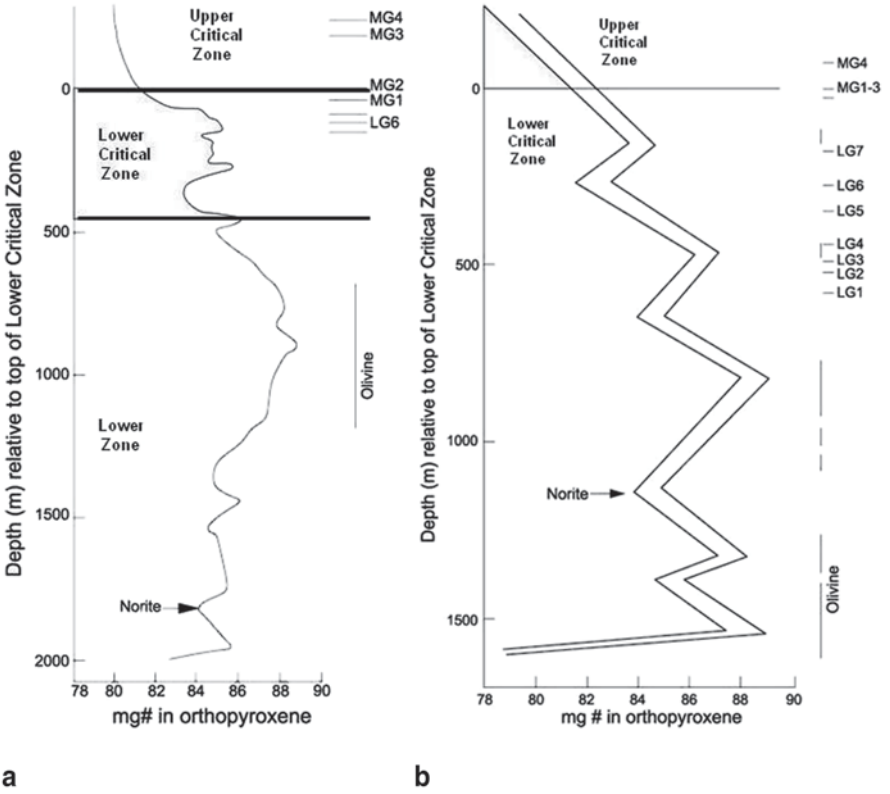

Fig. 12.6 Values of mg# in orthopyroxene in two sections of the Lower Zone and Lower Critical Zone, **a** in the east (Olifants River Trough) from Cameron (1978), and **b** in the west (Nooitgedacht) from Teigler and Eales (1996), showing their zigzag pattern. Localities shown in Fig. 12.1b. Note that there are sections that show differentiation (decreasing mg#), but equally sections with slowly increasing mg# due to slow, sustained recharge. There are no sudden increases in the mg#. In Fig. 12.6c is shown the mg# of orthopyroxene from the two samples immediately below and above each chromitite layer, showing that there is no observable increase in mg# across such layers and hence challenging the model for the origin of chromitite layers by addition of primitive magma

matic continuity existed over such an area early in the evolution of the chamber. Immediately above this unit there is a gradual increase in mg# of the orthopyroxene (over tens to hundreds of metres) from 84 to 88 (together with the appearance of olivine). Despite this convincing evidence of addition of primitive magma there are no chromitic intervals, suggesting that magma addition did not produce chromitite layers. Furthermore, there is no change in the mg# of orthopyroxene from below to above any of the chromitite layers (Fig. 12.6c), again suggesting that addition of primitive magma (and mixing) cannot be the cause of chromitite layer formation.

At the top of the Lower Critical Zone plagioclase becomes a cumulus phase with a composition of An_{80}, and changes little through the entire Upper Critical Zone. In contrast, the orthopyroxene composition oscillates with significant variation in

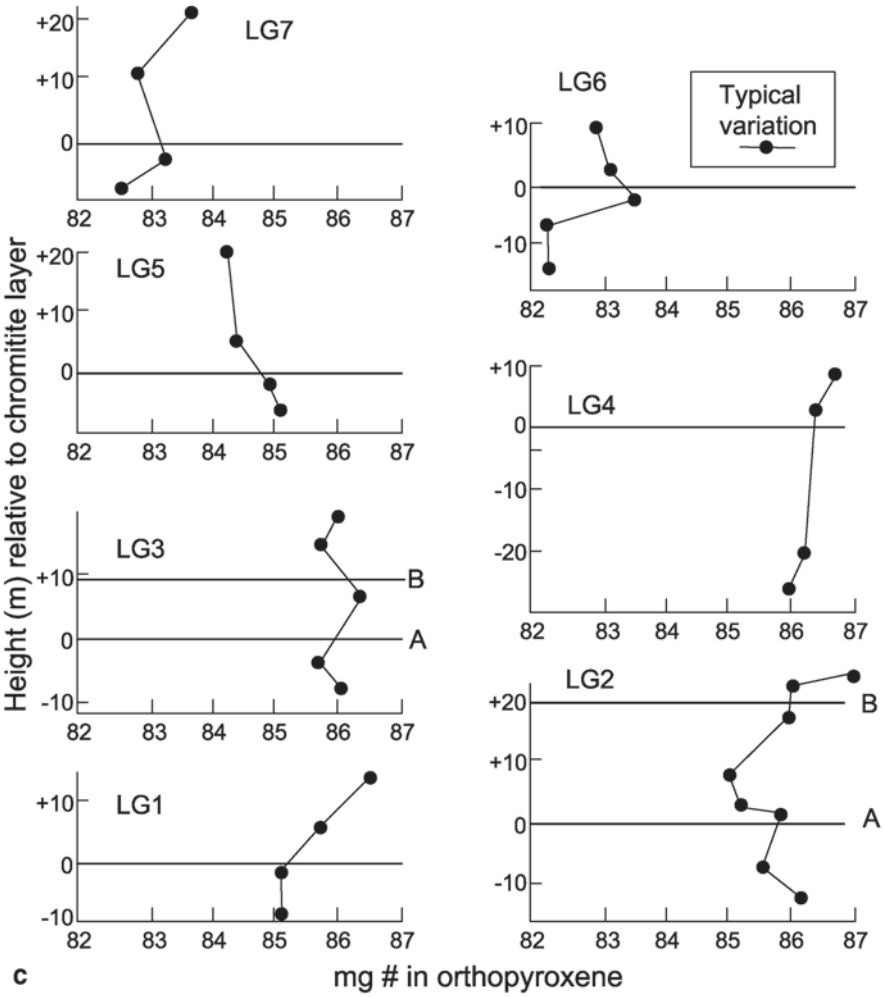

Fig. 12.6 (continued)

mg#. The Cr contents of the cumulus orthopyroxene remain remarkably constant over this interval (Fig. 12.7), despite this mineral being by far the most abundant cumulus phase and having a partition coefficient for Cr of over three and possibly as high as five (Barnes 1986a). Both mg# and Cr contents decrease significantly where the orthopyroxene is an intercumulus phase, especially close to the top of the Upper Critical Zone (Fig. 12.7).

Chromite compositions show a general systematic trend upward (Naldrett et al. 2012). From LG1 to MG2 the trend is one of decreasing mg# and cr#−Cr/(Cr + Al)−due to pyroxene fractionation, but above the MG2 the trend is toward higher cr# due to plagioclase (and pyroxene) fractionation.

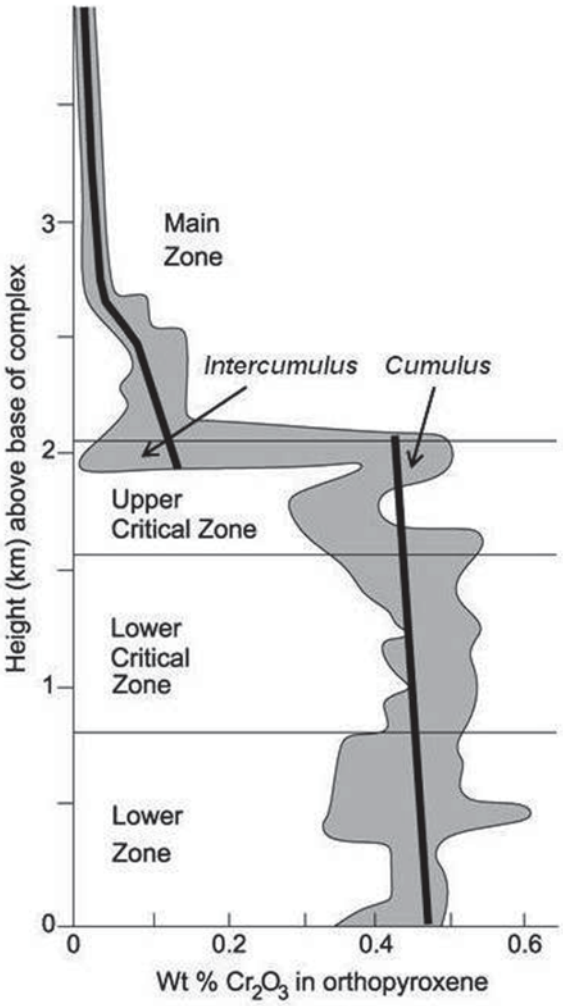

Fig. 12.7 Plot of the general trends in wt % Cr_2O_3 contents in orthopyroxene from the Lower, Critical and Main Zones (mainly from a very large data base summarised by Eales 2000, but also Schürmann 1993, Maier and Eales 1997, and Mitchell and Manthree 2002). The first and last authors did not distinguish between cumulus and intercumulus pyroxene, but the general distinction has been made here based on their reported modal proportions

Across the Critical Zone—Main Zone boundary there is no significant change in An or mg# values of cumulus phases. However, immediately above the Giant Mottled Anorthosite in the Main Zone the Cr decreases (Fig. 12.8a) and the Ti increases markedly in the pyroxenes (Mitchell 1990), and a very detailed study shows the whole-rock Cr/MgO abruptly decreases above this level (Fig. 12.8b). Throughout the overlying 1000 m above the Giant Mottled Anorthosite the extent of fractionation in mineral compositions is very subdued, with many very minor oscillations (Mitchell 1990; Roelofse and Ashwal 2012). A major reversal in mineral compositions occurs gradually across the Pyroxenite Marker interval in the west and east (Fig. 12.9). In the southern part of the eastern limb, a reversal occurs even though there is no Pyroxenite Marker. Such lateral variations suggest inhomogeneity in the magma chamber. Sadly, the borehole cores available for the detailed mineralogical studies of Mitchell (1990) and Roelofse and Ashwal (2012) did not traverse this

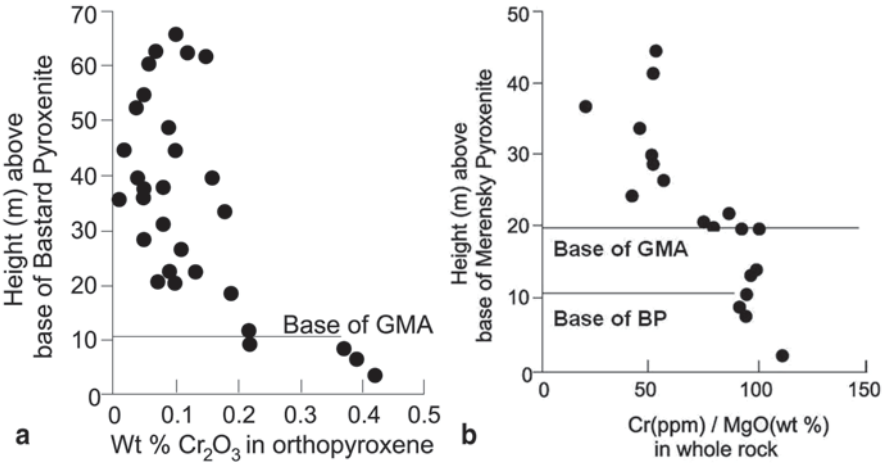

Fig. 12.8 **a** Plot of Cr_2O_3 in orthopyroxene in the section above the Bastard Pyroxenite, which occurs some 10 m above the Merensky Reef (data taken from Mitchell 1990), and **b** of whole-rock Cr/MgO (own unpublished data). GMA is Giant Mottled Anorthosite, the top of which is conventionally considered base of Main Zone

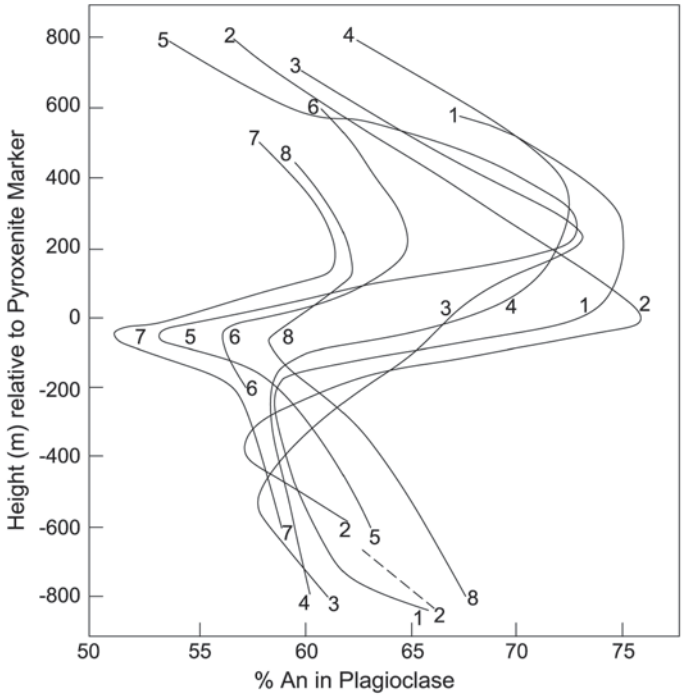

Fig. 12.9 Plot of An content in plagioclase versus height in the Main Zone, relative to the Pyroxenite Marker or top of magnetite gabbronorite, eastern lobe. The profiles are numbered from north to south over a distance of more than 100 km. Profiles 1, 4 and 8 from Lundgaard (2003); profile 2 from vanTongeren and Mathez (2013); profile 3 from von Gruenewaldt (1973); profiles 5, 6 and 7 from Klemm et al. (1985a)

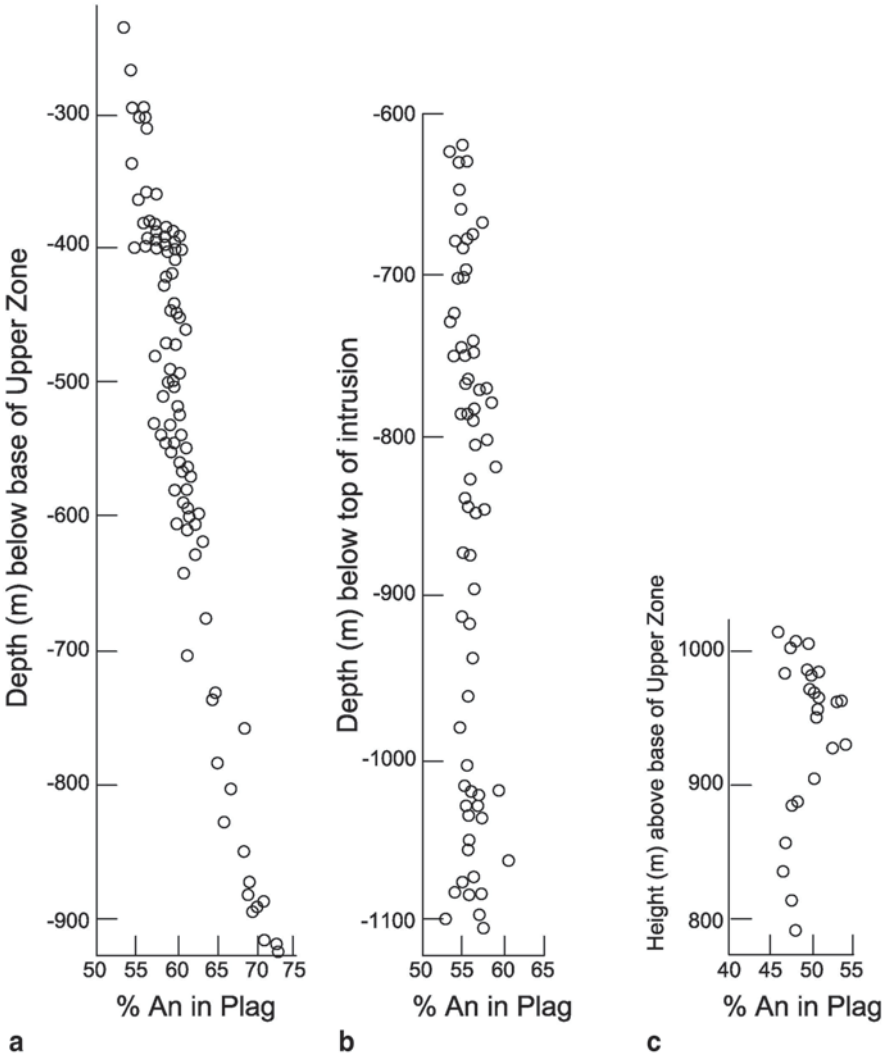

Fig. 12.10 Variations in plagioclase compositions from sections of the Upper Zone from Bellevue borehole (see Fig. 12.1b) using data from Ashwal et al. (2005). **a** shows a section with regular upward decrease in An content, **b** shows a long section with near-constant An content, and **c** shows an interval that includes a slow reversal in An content through about 90 m

interval, and so variability in the western and northern lobes across this interval remains to be investigated.

Oscillations in mineral composition are recognised in the Upper Main and Upper Zones (Ashwal et al. 2005; Tegner et al. 2006, Cawthorn and Ashwal 2009), although there is a distinct overall differentiation upward. The most evolved compositions reported are Fo_3 and An_{37}. But there are distinctly different patterns where the compositions of the plagioclase may show a systematic significant differentiation (Fig. 12.10a), or remain constant for considerable vertical intervals in another

sequence (Fig. 12.10b), or show a slow reversal (Fig. 12.10c). The An content of the plagioclase remains constant across all the magnetitite and anorthosite layers (Cawthorn and Ashwal 2009). The mafic minerals show an even more irregular pattern, which does not coincide with the pattern for plagioclase. Such irregularity may result from re-equilibration with oxide phase and/or the trapped liquid shift effect.

In the magnetitite layers, the V content of magnetite decreases, albeit rather erratically, upward (Klemm et al. 1985b; Cawthorn and Molyneux 1986; Eales and Cawthorn 1996) from about 1% V at the base to 0.2% at the top. However, the analyses of disseminated magnetite between the layers show a more complex pattern, not consistent with differentiation of a single, homogeneous magma (Klemm et al. 1985b). Again, the extent of change of composition of the disseminated magnetite due to reaction with trapped liquid or subsolidus reaction with other silicate minerals has not been adequately investigated (cf. Duchesne 1972). Studies of the Cr content of magnetite in short vertical sections revealed dramatic upward decreases and abrupt reversals over very short intervals, even within single layers of magnetitite (Cawthorn and McCarthy 1980; Klemm et al. 1985b).

Textures

The types of cumulate textures stylised by Wager et al. (1960) are rarely seen in Bushveld rocks. Most rocks are chemically adcumulates, but the extent of overgrowth versus assorted maturation processes (mechanical compaction, annealing) and the depth in the cumulus pile at which those processes occurred are unresolved (Hunter 1996). Monomineralic pyroxenites, anorthosites and rare dunites show highly annealed textures (Figs. 12.11a, b and c), with triple junctions (120°) and planar surfaces (not crystallographic primary surfaces, but the result of annealing). Very small grains such as plagioclase and chromite (Fig. 12.11a) occur at triple point boundaries (Boorman et al. 2004). Preserved intercumulus grains with concave and irregular boundaries do occur but are of very minor modal proportions (Fig. 12.11d). However, evidence of considerable resorption can be identified in olivine-rich (replaced by orthopyroxene) and orthopyroxene-rich (replaced by clinopyroxene) rocks (Fig. 12.11e). In the Lower and Critical Zones the orthopyroxene shows multiple, extremely fine, twin lamellae (much thinner than typical albite twinning), which Wagner (1929) concluded were inverted clinobronzite, but they are generally referred to as orthopyroxene. The gabbronorites of the Main Zone do not display any classic cumulate textures; no mineral appears euhedral; all are variably anhedral and interlocking, suggesting significant post-cumulus modification (Fig. 12.11f). The inversion of pigeonite to orthopyroxene in the Main Zone results in very large poikiloblastic grains (Fig. 12.11g). Multiple different orientations of high-temperature, pre-inversion exsolution lamellae testify to the original (pigeonite) grains (von Gruenewaldt 1970). It is this recrystallization that produces a very powerful “cement”, resulting in extremely strong (and unfractured) rocks that are used in the dimension stone industry from the well-exposed Pyramid Hills. The

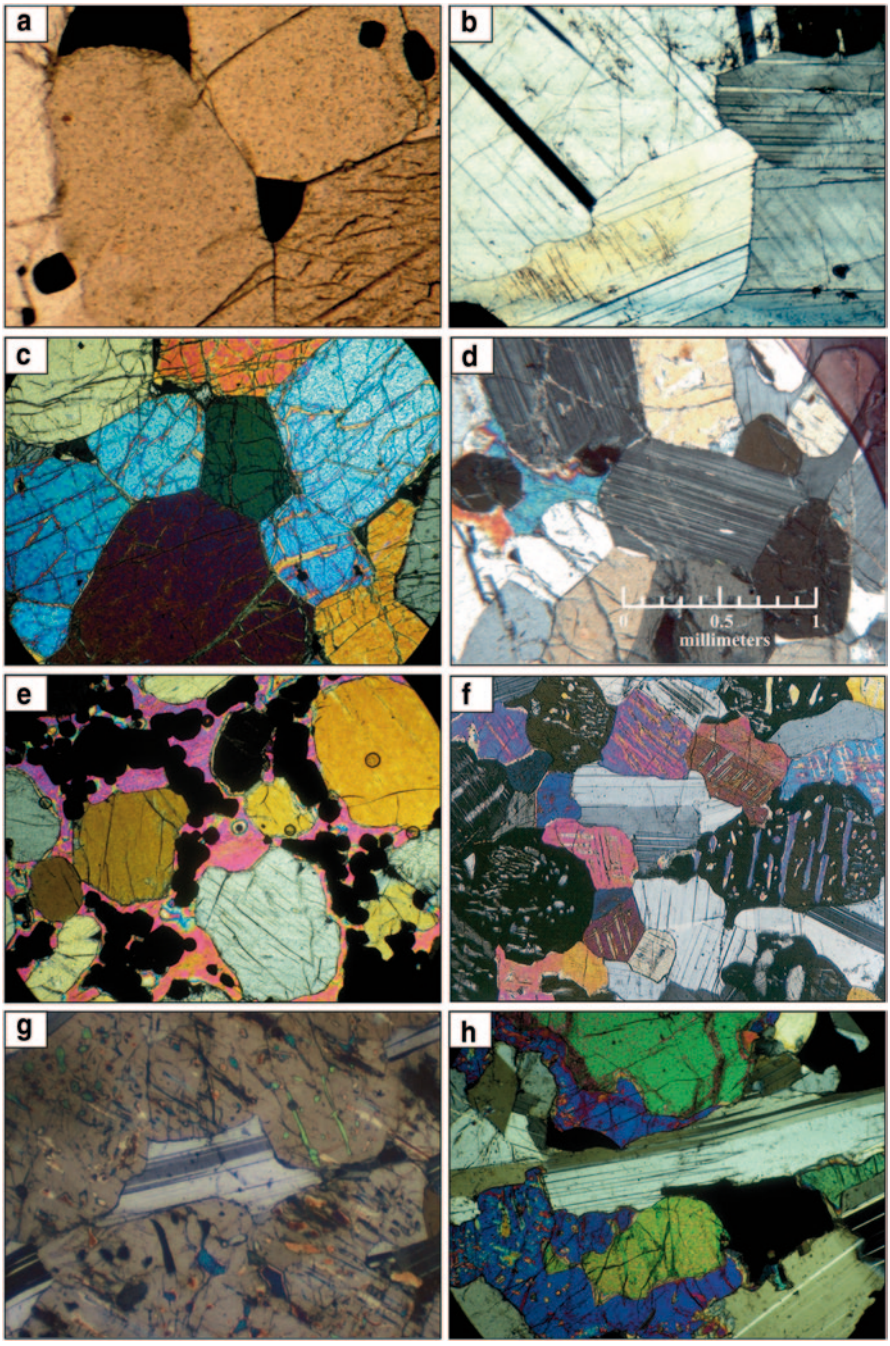

Fig. 12.11 Assorted photographs of textures within the Bushveld Complex. **a**, **b** and **c** Dunite, anorthosite and pyroxenite adcumulates with triple junctions and grain boundaries that are not natural crystal faces. **d** Cumulus orthopyroxene and minor chromite with interstitial plagioclase and clinopyroxene. **e** Cumulus orthopyroxene and chromite, the former showing marked resorption (gaps between orthopyroxene outline and chromite grains) and replacement by large poikilitic clinopyroxene. **f** Main Zone gabbronorite with plagioclase, clinopyroxene (with thin exsolution

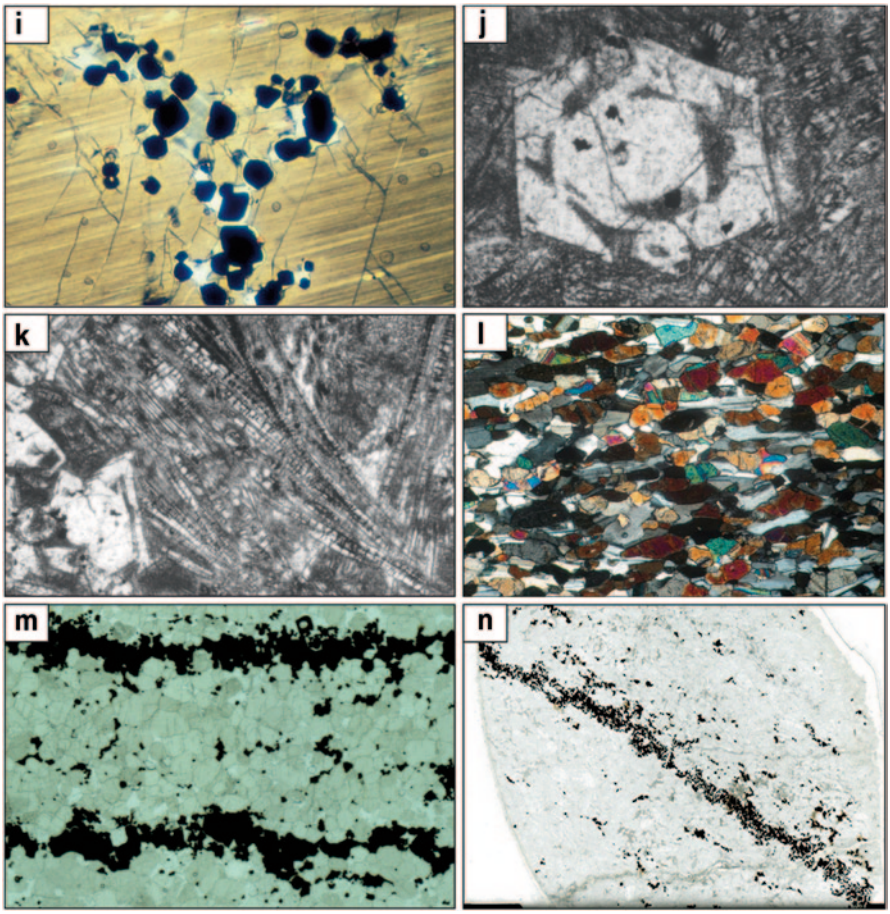

Fig. 12.11 (continued) lamellae) and inverted pigeonite (showing abundant and thick exsolution lamellae). Note that none of the minerals is convincingly euhedral in shape due to significant grain boundary readjustment. **g** A single large optically continuous orthopyroxene grain. However, it can be see that it was originally several grains of pigeonite. Each original grain shows different orientations of lamellae which exsolved prior to inversion to orthorhombic pyroxene. The plagioclase is interstitial to the original pigeonite grains and still preserves its original shape. (*Main* Zone below Pyroxenite Marker). **h** Olivine-magnetite gabbro from Upper Zone. Only plagioclase preserves a relatively euhedral shape. Olivine (three green grains) is irregular in shape and surrounded by anhedral clinopyroxene (blue). A large anhedral magnetite grains is present toward top left. **i** A single large grain of orthopyroxene in pegmatitic pyroxenite from the Merensky Reef. Note that it contains a tricuspate arrangement of chromite grains and anhedral plagioclase. They define the outlines of smaller original orthopyroxene grains that have recrystallized into the single, large grain (Cawthorn and Boerst 2006). **j** Hopper olivine grain in fine matrix from thin sill, the composition of which is considered to be representative of the earliest magma type in floor rocks east of Rustenburg (Cawthorn et al. 1981). **k** Spinifex pyroxene needles in parallel and radiating pattern, with triangular very fine grained matrix at bottom right, from same thin sill as in (j). **l** Microgabbronorite with granular texture of plagioclase and two pyroxenes, the plagioclase defining a weak parallel fabric. (Marginal Zone north of Steelpoort Chromite Mine) **m** Thin chromitic layers in pyroxenite. Note how the grains of chromite drape over and fill between the irregular surface defined by the larger pyroxene grains. **n** Weakly disseminated chromite grains in anorthosite above an extremely thin layer of chromitite

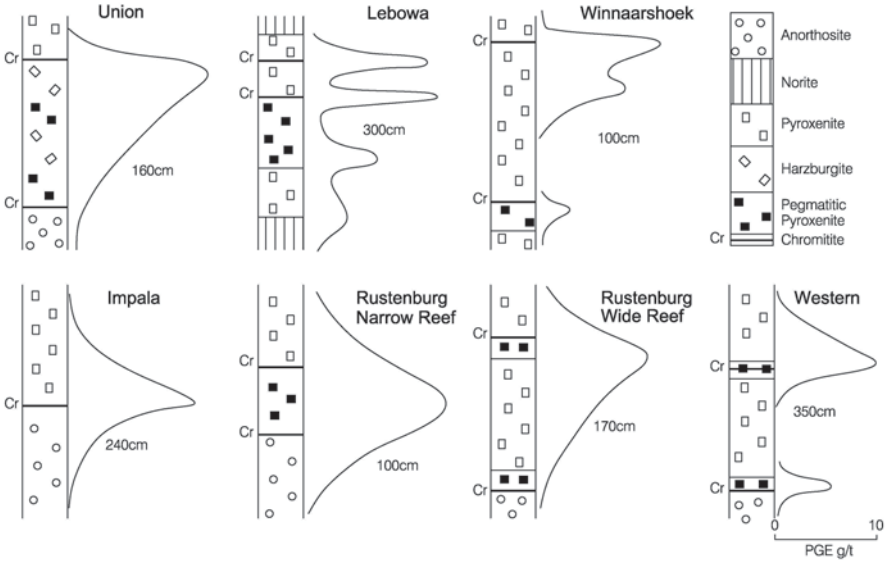

Fig. 12.12 Distribution (semi-quantitative) of platinum-group elements through the Merensky Reef from different mines (updated and modified but mainly from Cawthorn et al. 2002). Note that usually the highest grades do not coincide with pegmatitic pyroxenite and that the highest grade becomes more obviously top-loaded as the reef becomes thicker. The vertical thicknesses of each section in cm are indicated. For specific examples and values in thick reef which show the PGE distribution best, see Mitchell and Scoon (2007)

more massive and resistant nature of this rock is due to the inversion of many small grains of pigeonite into large poikiloblasts of orthopyroxene that make a powerful "cement".

All three lobes have this same thick unit just below the Pyroxenite Marker. In the Upper Zone the distinction between cumulus and intercumulus status deteriorates; only plagioclase has a vaguely euhedral shape; all other minerals are variably anhedral, especially magnetite (Fig. 12.11h). Apatite is euhedral, often very elongate, but always is in igneous rocks, so its texture is no proof of cumulus status.

The oxide minerals possibly show the greatest degree of textural re-equilibration because of their simple structure. Annealing of chromite has been described by Waters and Boudreau (1996). The magnetite also shows re-equilibration with almost monomineralic rocks resulting from massive coarsening of the grain size up to 2 cm (Reynolds 1985; Willemse 1969).

The coarse-grained pyroxenites present major problems in interpretation. They have been reported associated with chromitite layers, but can occur elsewhere. Often they occur below the chromitite where they have been interpreted as the result of trapping of evolved fluids (Mondal and Mathez 2007). However, they do occur within and above chromitites (Fig. 12.3d). They occur within the Merensky Unit (Fig. 12.12), usually above a thin chromitite. Here the texture has been attributed to the trapping of a fluid that caused almost complete hydration melting (Mathez et al.

1997). It is not clear to this author why such an almost totally melted layer did not penetrate the overlying cumulate package. The textures of these rocks pose further problems. The large orthopyroxene grains (up to 2 cm) contain many inclusions of tricuspate plagioclase often associated with trails of similarly clustered chromite grains (Fig. 12.11i) that have been interpreted as the result of textural annealing from many small grains close to the solidus (Cawthorn and Boerst 2006), aided by a temporary cessation in grain accumulation at the grain-liquid interface.

With reference to the genesis of the platinum mineralization it is often stated to be associated with the pegmatitic pyroxenite, an oversimplification, influenced by publications on the earliest mined sections at Rustenburg Platinum Mines (Vermaak 1976). Vermaak himself warned against assuming great lateral uniformity. Where the vertical succession through the Merensky is chromitite—pegmatitic pyroxenite—chromitite there is a convenient cut-off grade and width of 80–100 cm (Fig. 12.12). However, where the unit becomes thinner or thicker the separation between pegmatitic textures and mineralization becomes progressively clearer (Fig. 12.12). Sections that contain no pegmatitic pyroxenite may still contain good grade as shown for Impala mine, specifically its northern portion (Leeb-Du Toit 1986), and in thicker sections the mineralization and pegmatitic pyroxenite need not be correlated, as seen in the sections from Western/Lonplats (Davey 1992) and Winaarshoek/Marula (Scoon and Mitchell 2009) Platinum Mines.

The textures in the fine-grained rocks at the margins of the intrusion and as sills below, proposed as parental magmas deserve highlighting. Spinifex-like textures (random and parallel) of the pyroxenes were described by Davies et al. (1980), Sharpe (1981) and Wilson (2012) as shown in Figs. 12.3g and 12.11j and k. They have been termed the B1 compositions (Table 12.1).

Textures seen in the chilled sampled considered to represent the subsequent magmas, termed B2 or B3 compositions, are totally different. These rocks have microgranular textures with polygonal grain boundaries between the plagioclase and pyroxenes (Fig. 12.11l). They are reminiscent of the textures described by, for example, Latypov et al. (2011) as being the result of partial melting and/or annealing.

A final, cautionary note regarding textures needs to be mentioned. The literature (not just Bushveld) often contains phrases along the lines, “the pyroxenite contains 90% cumulus pyroxene and 10% intercumulus plagioclase”, implying 10% of intercumulus liquid. Texturally, it might be valid to say that there is 10% anhedral or interstitial plagioclase, but the genetic implication is almost certainly wrong. Two alternative descriptions are more plausible. (1) This 10% of plagioclase may have the same composition as the plagioclase in adjacent norite where it is demonstrably cumulus, and hence the rock should be termed heteradcumulate feldspathic pyroxenite (Wager et al. 1960). (2) The liquid forming the 10% of plagioclase is almost certainly saturated in both plagioclase and pyroxene, and those minerals crystallize in approximately the proportions 60% plagioclase and 40% pyroxene (and maybe significant proportions of other minerals). Thus, if there is 10% intercumulus plagioclase then there must also be 7% of intercumulus pyroxene and variable proportions of other minerals. The correct restatement of the above quote would then become “the pyroxenite contains 83% cumulus pyroxene and 10 and 7% of

intercumulus plagioclase and pyroxene respectively (and other minerals).” Both of these mechanisms are plausible (even contributing in the same rock), and both drastically change the implied proportions of cumulus and intercumulus minerals, and intercumulus liquid.

Parental Magmas

First Magma Type

Many dyke swarms are known on the Kaapvaal craton (Uken and Watkeys 1997b; Olssen et al. 2010), but none have the distinctive geochemical signature of the Bushveld. The enigmatic Marginal Zone varies along strike in thickness, in grain size (but generally medium grained) and composition, making rocks of the Marginal Zone unsuitable for predictions of the parental magma(s) compositions. Wager and Brown’s (1968) proposed parental magma emphasized their perceived similarities between the Bushveld and Skaergaard, but whereas the Lower Zone at Skaergaard is dominated by troctolite cumulates, in Bushveld it is dominated by orthopyroxene (and less olivine). Thus, parental magmas cannot have been similar. Experimental work on Wager and Brown’s proposed Bushveld parent magma demonstrated this fallacy (Tilley et al. 1968; Biggar 1974). Sills adjacent to the intrusion offered an alternative for estimating parental magma. Two types of sill were identified by Willemse (1969), one microgabbroic (and extensively metamorphosed) and one micronoritic. Further subtypes were distinguished by (Sharpe 1984). The latter includes a range of compositions characterised by relatively high SiO_2 and MgO. Actual analyses (Table 12.1) of fine-grained and quench textures members of this suite range from 10% MgO (Maier et al. 2000) to 14% MgO (Davies et al. 1980; Wilson 2012), although Wilson argued, on the basis of mg# in olivine, that a magma with 19% MgO must have been parent to at least some of the lowest cumulates. No full analysis was given by him. If it accepted that the most voluminous ultramafic rocks contain olivine and orthopyroxene with mg# not greater than 91 then the parent magma ought to produce such compositions. Magma with 10% MgO would produce less magnesian minerals. Magma with 19% MgO would crystallize abundant olivine before orthopyroxene saturation, yielding dunite (which is very scarce) rather than harzburgite with cumulus orthopyroxene. There was perhaps no single magma composition that was repetitively injected into the chamber, but a suite of related compositions, all being characterised by high Cr, MgO and SiO_2. The orthopyroxene in the Lower and Lower Critical Zones oscillate in mg# up to 88 (Cameron 1978, 1980; Teigler and Eales 1996), which would have crystallized from a magma with about 13% MgO and so that might be considered the dominant added magma composition, at least in the east and west.

Modelling the crystallization of chromite from parental magmas is another contentious issue. This author believes that the use of the MELTS crystallization programme to model these MgO- and SiO_2-rich magmas (as used by Naldrett et al.

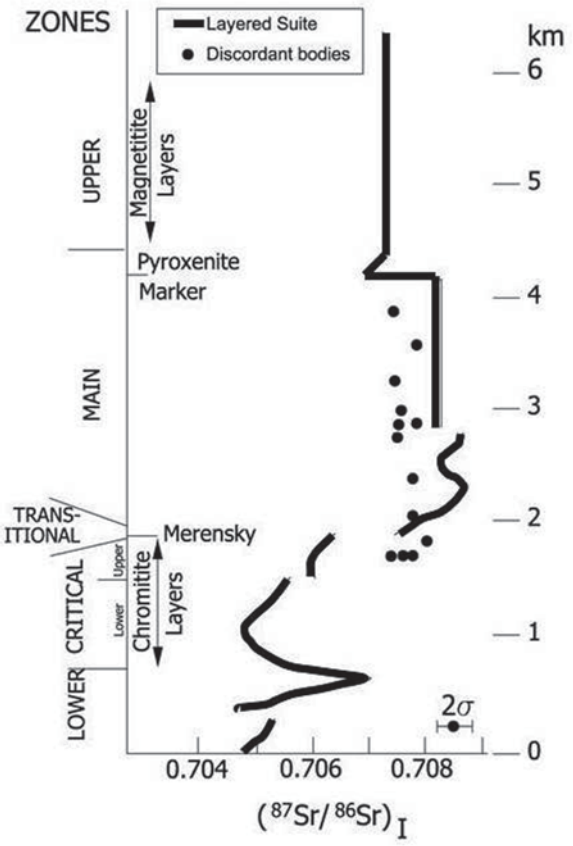

Fig. 12.13 Initial $^{87}Sr/^{86}Sr$ values from the entire succession as compiled by Kruger (1994). Also included are data from the discordant ultramafic bodies that cut the Critical and Main Zones compared to the ratio for the layered rocks (Data from Scoon and Mitchell 1994 and Cawthorn et al. 2000). The distinctive and constant values for these bodies shows that they are not derived from local material

2012; Eales and Costin 2012) to predict the crystallization of chromite is inappropriate. MELTS indicates that such magmas only become saturated in chromite at ±2000 ppm Cr, whereas the actual experimental studies of Barnes (1986a), Murck and Campbell (1986), Cawthorn and Biggar (1993) and Roeder et al. (2006) yielded chromite in equilibrium with magnesian liquid containing only 1000 ppm Cr at the QFM buffer.

Subsequent Magma Types

Wager and Brown (1968) discussed multiple magmatic injections filling the chamber, but implied that all had the same composition. The possibility that injected magmas changed composition fundamentally was proposed by Hamilton (1977) on the basis of variations in initial $^{87}Sr/^{86}Sr$ ratios in the cumulate succession, and refined by Kruger (1992; 1994) as shown in Fig. 12.13 The liquid compositions and the stratigraphic layers which they formed have been much debated. Note that

each magma type may have been repeatedly injected; what is emphasised here is the injection of different compositions.

The Lower Zone and Lower Critical Zone are dominated by orthopyroxenite with minor olivine-rich layers, the mineral compositions and dominance of orthopyroxene over olivine suggest a magma with 13% MgO, using accepted K_D values for Mg and Fe. For magma compositions above the Lower Critical Zone even greater uncertainty exists. Harmer and Sharpe (1985) suggested that there was a different magma for the Upper Critical Zone. It was argued that the appearance of cumulus plagioclase required a different magma type. There was also a transitory increase in the initial Sr isotope ratio (Fig. 12.13). The idea was further developed by Naldrett et al. (2009), who suggested that the bulk rock Th/Nb ratio of the Upper Critical Zone indicated mixing with different magmas. With regard to the former issue it was shown that the mg# of orthopyroxene at this level is exactly that expected at the composition of magma that begins to crystallize plagioclase, based on the experimental studies reviewed by Cawthorn (2002). At this boundary are the Middle Group Chromitite layers. It has been shown that most chromitite layers are associated with increases in initial Sr ratio, but that the value decreases again above these layers (Schoenberg et al. 1999; Kinnaird et al. 2002). The Cr content of the proposed added magma is 200–400 ppm (Barnes et al. 2010), much lower than the underlying magma. Yet the orthopyroxene does not change in Cr content across this boundary (Fig. 12.7). The evidence for addition of a fundamentally different magma at this boundary therefore is very weak.

A fundamental change in initial Sr isotope ratio occurs close to the Merensky Reef. Hamilton (1977, p. 32) stated that the Critical Zone Sr isotopic signature (i.e. R_0 of 0.7065) could be traced to "3 m above the Merensky Reef" (based on a total of 11 samples). That the isotopic break occurs above the Merensky Reef is confirmed by all six subsequent detailed profiles in Fig. 12.14 that shows that all the samples of pegmatitic and normal grain sized pyroxenite in the Merensky Unit have R_0 values typical of the Critical Zone. Thus the inference that the magma addition is at the Merensky Reef is based on a rather-too-casual inspection of the data. The affinity of the Merensky (pegmatitic) pyroxenite is totally Critical Zone in its mineral composition and isotopic chemistry.

As well as this dramatic increase in the R_0 value into the Main Zone, there is also a major expansion of the eastern lobe toward the south at this level (Fig.12.1b), demonstrating the lateral extension of the Bushveld chamber (Kruger 2005). It should be noted that it is at the position of this expansion of Main Zone east of Roossenekal across the floor that Wager and Brown (1968) took their chilled sample of proposed parental magma. The same area was resampled in detail by Sharpe (1981), Maier et al. (2000) and Barnes et al. (2010), who proposed a magma composition similar to that of Wager and Brown (Table 12.1). All these samples from this area have a microgranular texture, with triple point junctions between plagioclase and pyroxenes (Fig. 12.11l). The samples analysed by Maier et al. (2000) have an initial Sr isotopic ratio of 0.706, and so are not suitable to explain the increase in this ratio in the Main Zone to 0.7085. These rocks were described by Sharpe (1981) and Maier et al. (2000) from the eastern Bushveld where the Main Zone abuts the floor. How-

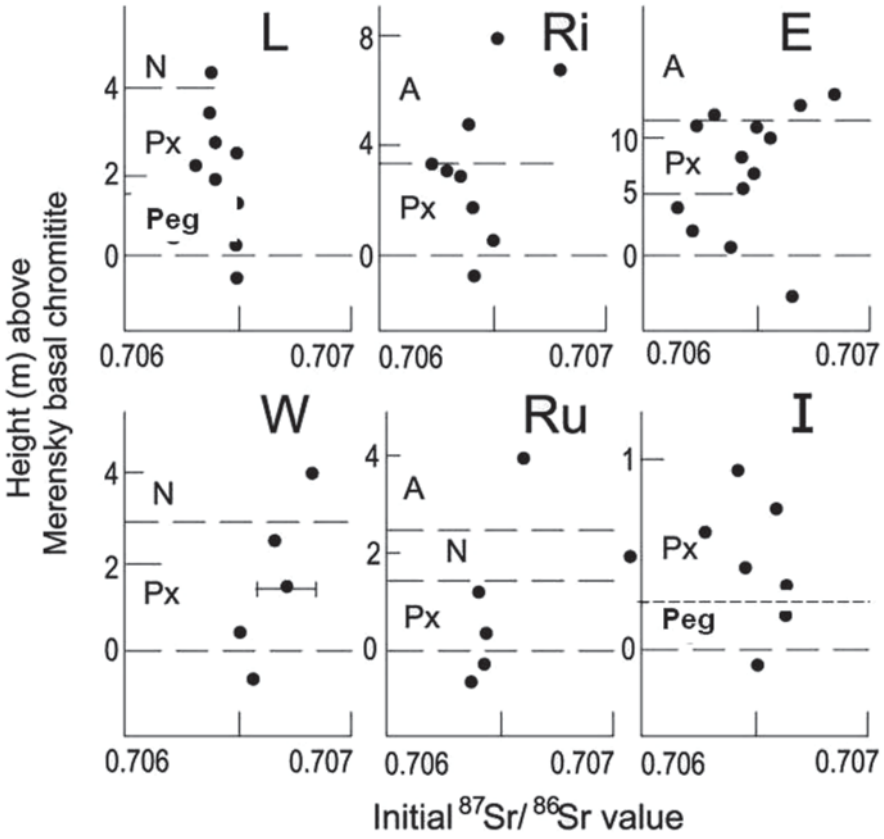

Fig. 12.14 Initial $^{87}Sr/^{86}Sr$ values through several sections of the Merensky Unit. Note that the break in ratio does not occur at the base of the unit as is commonly assumed. Abbreviations: Px and Peg refer to pyroxenite and pegmatitic pyroxenite. Mine names and data sources *L* Lebowa (Lee and Butcher 1990), *Ri* Richmond (Seabrook et al. 2005), *E* Eastern (Carr et al. 1999), *W* Western (Cawthorn 2011), *Ru* Rustenburg (Kruger and Marsh 1985), *I*mpala (Cawthorn and Boerst 2006)

ever exactly the same compositions (and textures) are found in rocks that underlie the Lower and Critical Zones in the east (to the north of Steelpoort) and in the west as described by Vermaak (1976). Analyses are given in Table 12.1. In these two settings they are not consistent with being parental to the Main Zone.

At the Pyroxenite Marker there is a major gradual increase in mg# in pyroxene and An in plagioclase, and a decrease in initial Sr isotope ratio, indicating addition of magma. The nature of this magma was excluded from the discussions of Sharpe (1981) and Cawthorn et al. (1981). The only samples identified as possible added magma was by Davies and Cawthorn (1984), based on complex intrusive relationships seen in the Upper Critical Zone. Sharpe (1981) argued for a very different genesis for this reversal at the Pyroxenite Marker, suggesting that these features do not represent a new magma but the continued crystallization of the stranded magma

that originally overlay the Critical Zone/Merensky Reef, because mineral compositions and initial Sr ratio are similar. In this model the Lower Main Zone resulted from an injection of dense magma that did not mix with the residual magma. The limited range of differentiation in the Lower Main Zone as demonstrated by the decrease in An in plagioclase from 75 to 65 (and similar mg# of the pyroxenes) in more than 1.5 km of cumulates begs the question as to where and what happened to the remaining more evolved magma in this model.

Using initial Sr isotope ratios Kruger et al. (1987) suggested that there were no subsequent major influxes, but Tanner et al. (2014) suggested that there were two further additions based on Cr contents of clinopyroxene in the Upper Zone although other aspects of the chemistry of these magmas was not resolvable.

Mass Balance Models

Given that there are a number of different magmas with no consensus on their compositions or relative proportions, and that the original extent of the intrusion is undefined, attempts at mass balance modelling seem highly conjectural. However, two calculations warrant discussion, one at the base and one at the top. Eales (2002) and Eales and Costin (2012) discussed a mass balance up to the level of the top of the Critical Zone. They focused primarily on the Cr budget, and concluded that there was 8 times more Cr in this section than in the parental magma, and hence that there was an imbalance. This writer would contend that the one-dimensional view adopted in this model is too simplistic. The profile for which the calculation was done was through the section with the thickest Lowest Zone in the western lobe, and with well-developed chromitite layers (Teigler and Eales 1996). It is well-known that the ultramafic layers and the Lower Group chromitites thin away from this vertical section. Indeed, Maier and Eales (1994) suggested the terms proximal and distal to explain the lateral variation in thickness of these sequences. Hence, the validity of this calculation can be questioned. Another issue is important in this regard. At the top of the Critical Zone the plagioclase composition is about An_{78} and the cumulus orthopyroxene has mg# of about 78. These compositions are still relatively primitive (for example, more primitive than the initial Skaergaard magma). A typical basalt may have phenocrysts with those compositions. The extent of differentiation using a Bushveld primary magma (Table 12.1, column 1) and modelled using the MELTS, programme, suggests that there had only been 17% fractionation (Li et al. 2001) up to this level. Hence, 5 times as much magma as the mass that has solidified still remained in the chamber. Thus, the mass balance anomaly is not just for Cr, but for the entire magmatic system. The fate of this volume of magma is still unknown, but may have been intruded laterally or extruded (Cawthorn and Walraven 1998; Naldrett et al. 2012). This enigma offers some support for the proposal of Sharpe (1985) mentioned above that this magma survived as an upper layer that produced the Upper Main Zone and Upper Zone.

A second mass balance calculation was presented for the end of differentiation. A calculation of the concentration of Zr and K_2O in the Upper Main and Upper Zone rocks yielded concentrations much less than found in the various proposed parental magmas (Cawthorn and Walraven 1998). They therefore proposed that a significant volume of evolved magma (with high Zr and K_2O) had escaped from the measured sections of the chamber, either vertically or laterally. Subsequent debates have challenged the vertical escape concept (Eales 2002), but VanTongeren et al. (2010) have resurrected this mechanism. This author claims that the lateral expulsion is a far more plausible model. The recognition of the existence of a Residual Zone with rocks originally called syenites by Hall (1932) may go part way to resolving this mass balance problem. There are few analyses of these Residual Zone rocks, but their Zr and K_2O contents are not high enough to totally account for the missing magma (Cawthorn 2013a). What rocks may have existed laterally, and have now been totally eroded, can never be more than topics of pure speculation.

Magma Mixing

The recognition of multiple pulses of different magma composition leads inevitably to discussion of the behaviour of such magmas once in the chamber, specifically mixing versus stratification. The assumption of magma mixing in Bushveld studies can be traced to two papers by Irvine (1973, 1975), which presented two ways of producing chromitite layers. However, whether magmas of different density (and temperature) would mix remains unresolved. In general, magmas of different density should not mix (as reviewed by Campbell 1996), but should remain stratified. Their subsequent cooling and crystallization, separately or with interaction, then becomes extremely difficult to predict. A review of both volcanic and intrusive examples shows that although stirring may produce extremely intimately convoluted (migmatite-like) textures, contacts between two different magmas remain remarkably sharp (Perugini and Poli 2012) and true homogenisation between mixed magmas is an extremely protracted process. A converse view exists, using observations from plagioclase compositions in calk-alkaline volcanic rocks, where rapid mixing of basic and silicic magmas has been claimed (Kent et al. 2010). Thus, fluid dynamic principles and mineral compositions yield two contrary views on whether magma mixing can occur or not. This writer suggests that resolving this impasse is one of the important challenges in understanding the mineralogical and geochemical evolution of layered complexes.

Three important features in the Bushveld can be re-examined in the light of these debates on magma addition and mixing.

1. Chromitite Layering. The chromitite layers were the issue addressed by Irvine in his magma mixing models. In all except one instance the lower contact of the chromitite layers is extremely sharp (Fig. 12.3d). Campbell and Murck (1993) presented calculations on the thicknesses of magmas that needed to be mixed

to produce such layers. Taking the thickest of the Bushveld layers as 1 m their Fig. 12.10 showed that many kilometres in total needed to be perfectly mixed. These estimates were the optimum for magmas mixed in equal proportions. Unequal proportions would demand even greater vertical thicknesses of magma. This writer would challenge whether several kilometres (vertically) of magma can be mixed as abruptly as would be required to produce the observed sharp contacts over an area of more than 30,000 km^2.

2. Critical Zone—Main Zone transition. The addition of isotopically different magma in the Merensky Unit interval triggered the concept of magma mixing and the formation of the platiniferous Reef itself (Campbell et al. 1983). Whereas magma addition is probably indisputable, the extent of mixing remains debatable. The Cr content of orthopyroxene can be used as a critical parameter for distinguishing Critical Zone versus Main Zone lineage. It was first shown by Mitchell (1990) that the Cr_2O_3 content of the orthopyroxene at the Merensky interval is 0.4 % and decreases abruptly to 0.1 % only 30 m higher in the Lower Main Zone (Fig. 12.8a). The major review by Eales (2002) reinforced this data set with additional profiles. A simple calculation for Cr using these mineral compositions shows that no mixing can have occurred in the approximately 30 m above the Merensky Unit (see Appendix 1).

   This author's view (adapted from the modelling of Cawthorn and Walraven 1998) is that the residual magma was pushed outward by the new injection(s) of magma. However, this non-mixing hypothesis would also be consistent with the previous suggestion of Sharpe (1985), as discussed above.

   In the interval between the Merensky Unit and some 30 m above there is an apparently anomalous sequence. The Sr isotopic ratios indicate that there is a fundamentally new magma at this level, but the Cr in orthopyroxene shows that this sequence has formed from typical Critical Zone liquid. This paradox was resolved by Seabrook et al. (2006) who suggested that the new Main Zone magma formed a layer below the residual Critical Zone magma with no mixing. Orthopyroxene and chromite continued to form and sank from the upper liquid layer whereas the interstitial plagioclase (that contained all the Sr) solidified from the lower liquid layer.

   Further challenging evidence against rapid mixing is based in initial Sr isotope ratios. The Critical Zone has a ratio of 0.7065, and the Main Zone a ratio of 0.7085. If the latter were the result of mixing of equal proportions of magma, then the added magma must have had a ratio of 0.7105. I suggest that is a highly improbable isotopic composition for an enormous volume of basic magma.

3. Pyroxenite Marker. One of the first and most convincing examples of addition of new magma in any intrusion is the Pyroxenite Marker in the Main Zone. It was identified by Lombaard (1934), but it was von Gruenewaldt (1970) who showed that the mg# of pyroxene and the An content of plagioclase increase by about 10 units upward, and there is now also known to be a decrease in the initial Sr isotopic ratio (Sharpe, 1985). A similar study in the western Bushveld (Cawthorn et al. 1991), reached similar conclusions, but they further emphasised that

the change in mineral composition was gradual and could be recognised over a vertical interval of more than 200 m, approximately equally disposed below and above the Pyroxenite Marker. Thus, this most convincing example of magma addition suggests that it was a very protracted process rather than abrupt (as also shown in the Lower Zone rocks discussed above).

Origin of Layering

Layering can range from very abrupt variations in modal proportions over short vertical intervals (as in the Critical and Upper Zones) to so diffuse (visually cryptic) over very many tens of metres that it requires detailed point counting of mode (Roelofse and Ashwal 2012) or detailed density measurements (Ashwal et al. 2005) to recognize.

Possibly the most important observation that must be satisfied by any model for modal layering in the Bushveld is the remarkable continuity of many distinctive layers (chromitites, magnetitites and Merensky Unit in particular) often in both western and eastern limbs, but also in some cases in the northern limb. It was the main argument in the suggestion that the west and east exposures are part of a single lopolith, and not discrete intrusions (Cawthorn et al. 1998).

Two opposing paradigms dominate views of solidification processes; as summarised in the Wager and Brown (1968) model of crystal settling and sorting, and the Marsh (2006) model of in situ crystallization. The analogies would be with clastic versus chemical sedimentary rocks. In the former model, heat would be lost through the roof causing an increase in magma density and/or crystallization at the top resulting in downward plunging packages, the continued crystallization in which would be promoted by the relatively greater steeper slope (δ temperature/δ pressure) of the liquidus than the adiabat with increasing pressure. The latter view would be that nucleation is heterogeneous not homogeneous, and will occur on a pre-existing substrate (floor, walls, roof—if solid) where heat loss occurs. Modelling which of these effects is more dominant is difficult.

Grain Settling

The Wager and Brown (1968) model is summarized on their pages 208–221, in which they envisaged grains nucleating in the magma chamber; this crystal-charged magma (proportion of grains unspecified) slowly circulated by convection, dropping out a steady rain of all cumulus minerals (in their approximate cotectic proportions) and producing the homogeneous successions. Intermittently, super-charged slurries descended the walls (or possibly elsewhere from the roof) of the (Skaergaard) intrusion; lost momentum as they travelled along the instantaneous floor;

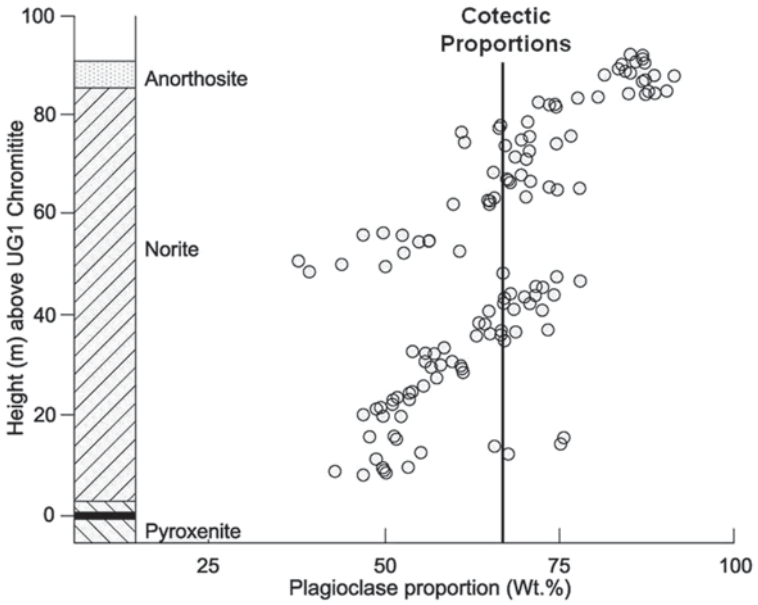

Fig. 12.15 Modal data through part of the Upper Critical Zone. Detailed modal proportions of plagioclase through the MG4 rhythmic unit, taken from a borehole in the western Bushveld Complex (own unpublished data), using the method described by Cawthorn and Spies (2003). The section that is called norite is not homogeneous but contains three sections that show a progressive upward increase in the plagioclase content from 35 to over 75 %. The probable cotectic proportion of plagioclase to orthopyroxene is about 65 %, and there is no tendency for rocks with that proportion to occur. The simplest explanation for the observed modal variations is by crystal settling and sorting

and gradually dropped their load of crystals in order of density (according to Stokes' Law). An intricately amplified development of these views was presented by Irvine et al. (1998; p. 1437). They emphasised the likely non-laminar nature of the horizontal flow of the magma close to the crystal-liquid boundary and suggested that shearing within the liquid permitted intermittent separation and reattachment of the magma close to this boundary that was capable of major redistribution and sorting of minerals of different density.

Can this first model be applied to the Bushveld? Two fundamental expressions of deposition by settling would be (i) a gradual decrease in mafic mineral proportion in the graded layers upward and, if horizontal turbidity currents were involved, in the direction of movement, and also (ii) erosive and possibly channel-like features displaying cross-bedding. Such features do occur in the Bushveld. Evidence for decreasing mafic mineral proportion upward on a large scale is shown in Fig. 12.15. Planar cross-bedding has been recorded (Fig. 12.3h) in the middle of the Main Zone (Quadling and Cawthorn 1994), and is strongly suggestive of horizontal flow of crystal-charged slurries. The disruption of such layering (Fig. 12.3i) demonstrates the erosive power of such currents. Quadling and Cawthorn (1994) also document-

ed linear fabrics suggestive of horizontal flow. They reported alternating layers of gabbronorite with greater and less than the cotectic proportion of plagioclase (and none with the cotectic proportion). The plagioclase defined a linear fabric in the plane of the layering, but with very different orientations in the two layers. In the mafic-rich layer the lineation was parallel to strike, whereas in the felsic-rich layer it was down dip. These features were interpreted to be due to flow of grains in a current, the denser, mafic-rich portion being carried as a bed load, and the less dense, felsic portion being carried as a suspended load. Any plagioclase in the bed load would roll along the bottom with its long axis perpendicular to flow, whereas in the suspended load the long axis would be parallel to flow. The abundance of the lateral terminations of the mafic layers (Fig. 12.3h) suggests that these currents are of relatively limited extent horizontally. Many more studies would be needed to test if linear rather than planar fabrics were common in the Bushveld.

In contrast to the laterally discontinuous nature of the individual layers shown in Fig. 12.3h (although the entire package of layering is many metres thick and very continuous over tens of km), are the examples where modal layering is laterally very continuous. These features indicate a contrast with the Skaergaard layering (Irvine et al. 1998) where the laterally non-continuous layering is strongly suggestive of horizontal flow. Such a mechanism becomes questionable when a specific layer can be traced in the Bushveld for very great distances. Horizontal flow for many tens to possibly one hundred km that would be required by such observations is considered implausible. Such sequences are more consistent with the model of Sparks et al. (1993) where a convecting magma (of chamber-wide dimensions) held ever more grains in suspension until a critical concentration was reached, speed of convection decreased and settling and sorting of the grains from the suspension occurred. As the magma column was depleted of grains, the upper part of the column recommenced convecting, cooling and crystallization and another cycle resumed. A possible example of this effect is shown in Fig. 12.15 where there are three contiguous vertical sections that would all be classified as norite, but showing a regular upward increase in modal plagioclase content.

There is an important consequence of this model. Consider a magma that is crystallizing plagioclase and pyroxene. When settling did commence, pyroxene grains would concentrate at the floor. Such a pyroxene-rich layer has traditionally been inferred to have formed from a magma saturated only in pyroxene. The inference used in reaching such a conclusion is that whatever mineral assemblage crystallized from the magma was immediately and totally preserved by accumulation at the base. Given the concept of crystal settling this inference is invalid. It was shown by Cawthorn (2002) that pyroxenes in several pyroxenites had evolved mg# values (less than 82) that indicated that the pyroxene had crystallized together with plagioclase but that the plagioclase had not accumulated at the base (Fig. 12.16). This observation challenges the view that pyroxenite forms from magma saturated only in pyroxene.

Among the most dramatic exposures in the Bushveld Complex are the oxide-rich layers. They remain relatively constant in thickness for tens to even hundreds

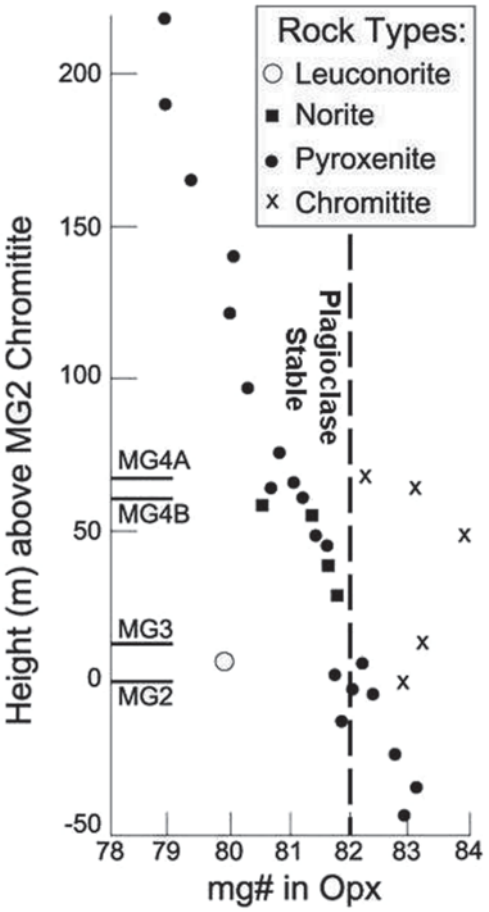

Fig. 12.16 mg# in orthopyroxene from a section above the MG2 (data from Teigler et al. 1992). Note that the mg# in orthopyroxene in pyroxenites is no greater than those in norites. All values in both norites and pyroxenites are less than 82 which is the composition reflecting the stage of crystallization when plagioclase becomes a cumulus phase. Thus, pyroxenites with mg# < 82 are not the result of formation from a liquid crystallizing only pyroxene, but indicate that the crystallizing plagioclase did not accumulate on the floor

of km in the east and west. Some correlatable layers are even of similar thickness and composition in all three lobes, e.g.: the vanadium content of magnetitite layers (Cawthorn and Molyneux 1986). Their substantial thicknesses (especially for the chromitite layers) require formation from a very thick and laterally uniform volume of magma that was driven into the oxide stability everywhere abruptly. The abruptness of the event can be demonstrated by the extremely sharp basal contacts seen for chromitite (Fig. 12.3d) and magnetitite layers (Fig. 12.3j).

A challenge to crystal settling depends upon density considerations. This problem was first recognised by Darwin (1844) where he noted that a lava flow was enriched in albite at its base which he considered contrary to the inferred density of the host lava. When Bottinga et al. (1982) developed a rigorous magma density calculation scheme based on partial molar volumes of oxides they pointed out that basic magma may be denser than plagioclase, which would make an origin of anorthosites by grain settling impossible. With regard to anorthosites in the Upper

Critical Zone, the magma is probably quite siliceous and so could have had a lower density than plagioclase. However, in the Main Zone where the minerals become more evolved, but prior to magnetite formation, the density of the magma may have been greater than plagioclase. However, the original density calculations of Bottinga et al. (1982) and Campbell et al. (1978) and experiments assumed zero water. The subsequent inclusion of the effect of water into magma density calculations indicates a reduction in density of about 0.15 g cm^{-3} for each 1% of water (Lange 1994; Ochs and Lange 1999). Hence, provided this 1% water can be inferred for evolved Bushveld magma, plagioclase would probably have been dense enough to sink. 170 years after Darwin's observation this issue is still not satisfactorily resolved.

A significant feature encountered is the presence of autoliths that almost certainly have been transported before downward accumulation into the succession (Fig. 12.3k). A remarkable example is the presence of anorthosite autoliths in the MG2 chromitite (Fig. 12.3i). It is commonly stated that below the MG2 there is no cumulus plagioclase, yet thin fragments of anorthosite are found in this chromitite layer. Their origin is enigmatic. However, it was shown above that plagioclase may be a crystallizing but not an accumulating phase at levels where pyroxenite layers (with pyroxene having an mg# <82) were being preserved. Teigler and Eales (1993) also reported the presence of resorbed plagioclase inclusions in orthopyroxene grains below the MG2 chromitite, and reached a similar interpretation. Were the non-accumulating plagioclase gains forming rafts or mats that were capable of being deposited either laterally or at some higher level by currents?

In Situ Growth

In the other model for solidification, Marsh (2006) suggested that the most likely site for grain nucleation would be where the magma is coolest and where heterogeneous rather than homogeneous nucleation would occur. The margins of the intrusion are the most conducive to creation of these conditions. Hence, he proposed in situ growth of solid, with fractionation occurring by the remaining liquid migrating inward from the solidifying carapace. In the case of the Bushveld, once a moderate thickness of cumulates had formed at the floor, cooling would be mainly through the roof suggesting that would be the best site for grain formation. But no roof cumulates exist in the Bushveld unlike Skaergaard. This model can be tested against the repetitive sequence of pyroxenite—norite—anorthosite in the Bushveld Complex. In the simple binary pyroxene—plagioclase phase diagram a magma could begin to crystallize pyroxene. It would then reach the eutectic and produce pyroxene and plagioclase (norite), but it could not then produce only plagioclase (anorthosite). Considered another way, with in situ growth all multi-phase assemblages formed ought to be in cotectic proportions. However, the above-mentioned sequences often show perfectly gradational changes in modal proportions over significant vertical intervals that are not constrained by cotectic proportions (Fig. 12.15). A second

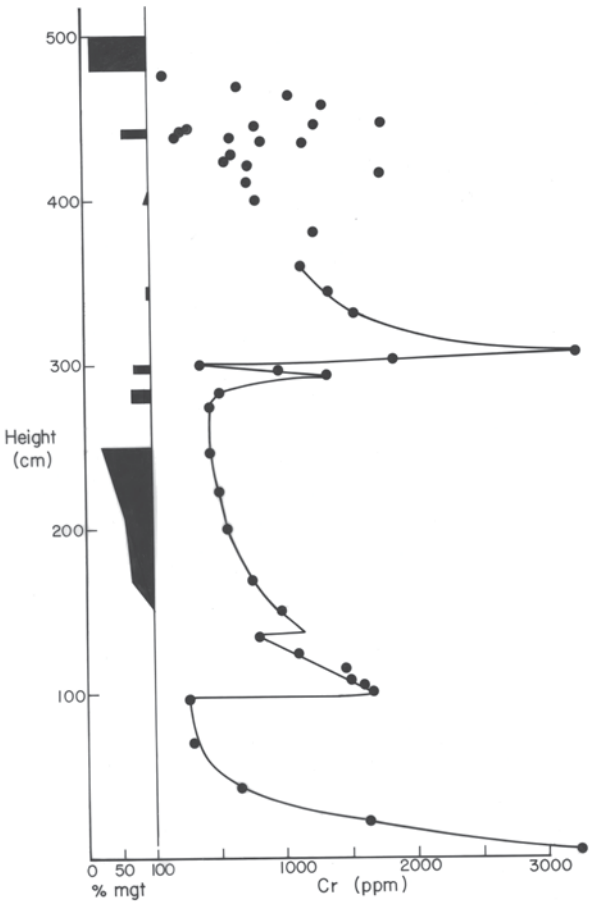

Fig. 12.17 Cr content of pure magnetite mineral separates taken from the Main Magnetitite Layer (from McCarthy and Cawthorn 1983). The proportion of plagioclase in this section is shown on left. The marked gradual decrease in Cr content demonstrates that the magnetite did not form from a large volume of magma or that settling occurred over a large distance. The reversals in Cr content demonstrate that these layers are not formed as one homogeneous layer, but are produced by several discrete layers superposed, in some cases recognisable by the presence of cumulus plagioclase (e.g. at 300 cm height)

example of such gradual changes in modal mineralogy from essentially one mineral to another is provided by the magnetitite layers, almost all of which show massive magnetite (only one cumulus phase) at the base increasing regularly upward in proportion of plagioclase to ultimately produce anorthosite (Fig. 12.3m). The abundance of layers with non-cotectic mineral proportions in the Critical and Upper Zones, especially, is a challenge to the model of in situ growth.

The Cr content of magnetite in magnetitite layers has been used to argue in favour of in situ growth (Cawthorn and McCarthy 1980). They showed a depletion of Cr from several thousand to less than one thousand ppm Cr with a number of abrupt reversals in less than 2 m of magnetitite (Fig. 12.17). Such massive depletion is difficult to model if grains were forming and settling from a large volume of magma. The chromitite and magnetitite provide an interesting contrast. A similar model for the formation of both might seem logical. However, the chromitite layers containing 300,000 ppm Cr do not appear to deplete the magma significantly in Cr based

on the Cr content of overlying orthopyroxene (Teigler and Eales 1996). Junge et al. (2014) showed a number of rather subtle fractionation-reversal cycles in the UG2 chromitite layer qualitatively comparable to the trend identified by Cawthorn and McCarthy (1980) for magnetitite. The explanation for the lack of depletion in Cr in overlying orthopyroxene may be found in the fact that if Cr in magma that was producing chromite decreased slightly, then chromite crystallization would terminate (by reaction relation) or be swamped by cotectic silicate formation. However, if Cr in the magma that was producing magnetite decreased, magnetite could still continue crystallizing (because Cr is merely a trace element) and the magma could become further depleted in Cr.

Latypov et al. (2013) have argued that the thin chromitite layers (in Rum) at the boundaries between anorthosite and peridotite might have resulted from in situ growth. They showed that chromite grains and thin layers could be found on vertical or even overhanging surfaces within potholes, and argued that they could not have accumulated there by vertical settling. With regard to the potholes in the Merensky Reef, Schmidt (1952) presented petrofabric evidence that the pyroxene grains had been plastered with their long axes horizontal against the circular vertical walls of the pothole by swirling currents. Exactly the same process might have applied to the chromite grains. Thus, finding the definitive criteria to constrain mechanisms of grain accumulation remains elusive.

Other Mechanisms

A number of other factors and driving mechanisms have been discussed by Naslund and McBirney (1996). Ultimately, grains must sink or grow in place, but not necessarily exclusively one or the other. One of these processes proposed by Maaløe (1978) involves oscillatory grain growth, with the liquid becoming alternately supersaturated in one phase then another on either side of a cotectic. Possible examples of such features are noted (Fig. 12.3n), but are very rare compared to the gradual change in mode noted in Fig. 12.15. The sequence pyroxenite-norite-anorthosite observed in the Critical Zone is not consistent with oscillatory nucleation. As noted by Wager (1959) nucleation order may be controlled by simplicity of crystal structure, producing an order of oxide, olivine, pyroxene and plagioclase (as seen in the Bushveld rhythmic units). A refinement of that concept was presented by Duchesne and Charlier (2005) who suggested that variations in nucleation rate of plagioclase relative to other phases could produce a single graded unit in terms of increasing plagioclase proportion upward rather than multiple oscillations in modal proportions. Another model for layering involves pressure fluctuations, which, rather than changing the magma composition so it lies in a new mineral stability field, changes the position of phase boundaries relative to a constant magma composition. Naslund and McBirney (p. 27) stated “The effects of a pressure change would be felt nearly simultaneously over the entire magma chamber, and as a result, [is] attractive for explaining layers of great lateral extent”. Closely similar to this model is one of seismic shocks that can trigger extreme rates of nucleation (tap the side

of a glass containing a carbonated drink). Again, Naslund and McBirney (p. 19) concluded that "seismically induced layers should be laterally continuous over the entire chamber". These two quotes from Naslund and McBirney fit perfectly the descriptions of the chromitite and magnetitite layers.

Two further complexities to interpreting modal variations are provided by a consideration of what minerals might be expected to accumulate. In successions of pure anorthosite there is the implication that only plagioclase is accumulating (whether it be by settling or in situ growth). Such a process requires that no mafic minerals be forming anywhere in the magma chamber because they would definitely sink if plagioclase could sink. Hence, there must be periods when no significant nucleation and growth of mafic minerals is occurring anywhere in the chamber. Does such an observation imply that there were pulses of nucleation and grain growth followed by settling with no further nucleation? The second example comes from the Upper Zone that is mainly composed of magnetite gabbronorite. Above the Main Magnetitite Layer there are two closely spaced additional magnetitite layers. The intervals below and between the magnetitite layers consists of anorthosite (with minor oxide), but no cumulus pyroxene., which, being denser than plagioclase, would have sunk if grains of it were present. Hence, why is there no cumulus pyroxene present in this interval? A possible explanation could be that nucleation and growth of magnetite grains removed iron from the adjacent magma. Given the extremely low MgO content of the magma at this level of the intrusion, removal of iron could have destabilised pyroxene and driven the magma into the plagioclase stability field.

UG1 Chromitite at Dwars River

The thin bifurcating chromitite layers in the anorthositic footwall to the UG1 chromitite at the National Monument site, Dwars River, are the most photographed and possibly most enigmatic features in the Bushveld (Fig. 12.3e), and so are highlighted here. Similar bifurcations and lenses are seen wherever the footwall to the UG1 is exposed. However, these features are not unique to the UG1 footwall. They occur in all the chromitite layers, but usually with pyroxenite as the lenses. Two examples are shown in Fig. 12.3o and p. The difference is that the chromitite layers tend to be thicker and the silicate lenses thinner than the Dwars River anorthosite package. In the chromite mines the pyroxenite lenses are known as "internal waste" and "partings", and can range from a few grains to 30 cm thick and up to hundreds of metres long. I would suggest that a purely clastic sedimentological analogy the simplest interpretation, using the Dwars River locality for the explanation. It occurs at the top of the MG4 chromitite rhythmic unit, and only plagioclase was the accumulating phase. Any one of the assorted mechanisms for producing chromitites operated. (I prefer the possibility of tectonic instability triggering earthquakes with associated shock waves.) They initiated nucleation of chromite grains everywhere in the chamber, which accumulated as thin and, importantly, continuous layers. Repeated earthquakes caused the large number of thin layers, as implied by the compositional data for chromite reported by Junge et al. (2014). Between each layer the plagioclase continued to accumulate. Possibly as a result of variably horizontal flow rates

in plagioclase-laden suspensions, the grains sedimented in elongate lenses analogous to braided stream deposition. Thus, the difference between discontinuous plagioclase lenses and perfectly continuous chromitite layers (when they first formed) resulted from the two mechanisms of accumulation, the former separating from horizontally flowing basal suspensions, and the latter from earthquake-triggered nucleation throughout the entire chamber. However, the chromitite layers are essentially devoid of cumulus silicate grains (although there is abundant intercumulus plagioclase and pyroxene). Thus, this model requires that there are no silicate grains accumulating during the period of chromite accumulation. The "sand volcano" model of Nex (2004) is slightly different. He emphasised the discordant upward emplacement of plagioclase suspensions disrupting the originally uniform chromitite layers (Fig. 12.3q and r), and suggested that the upward motion of a plagioclase suspension was promptly transferred into a sub-horizontal collapse as momentum was lost to produce gentle domes of accumulated plagioclase on the chromitite floor. My one reservation with this model is that the width of many of these plagioclase lenses is in the order of a few to many metres. However, the spacing between these (chromitite) disruptive structures is one to two orders of magnitude greater. It is therefore hard to conclude that there is a disruptive feature beneath each plagioclase dome. The search for definitive features to demonstrate any of the proposed models for Dwars River will doubtless continue to occupy geologists' imagination.

The many conjectural interpretations mentioned above demonstrate that there are major uncertainties in determining the origin(s) of layering. Searching for a single mechanism may be unrealistic.

Consolidation

The *in situ* crystallization model of Marsh (2006) envisages a vertical profile (of unspecified thickness) near the base of the magma chamber that ranges from 0% to close to 100% crystalline. Even the crystal settling model envisages a zone that contains variable interstitial liquid proportion. The thickness of that zone is difficult to demonstrate because it is so transitory (see Irvine et al. 1998). Also the fate of that liquid is variably interpreted. Wager and Brown (1968) considered that it might be trapped (and solidify to produce an orthocumulate rock with up to 30% post-cumulus minerals); or, close to the interface (thickness or depth of this zone unspecified), be capable of interaction with the overlying liquid to produce adcumulates (with overgrowth of the cumulus minerals with the cumulus composition). Alternatively, that interstitial liquid may have been driven out by textural annealing/physical compaction (Hunter 1996) as modelled by McKenzie (2011). Unravelling the relative contributions of all these processes is probably almost impossible and can vary within different sections of the same intrusion. Here, I document a number of field observations in the Bushveld that are relevant to this debate.

Compositional convection is a process in which the interstitial liquid changes its density and hence migrates vertically due to gravity, dependant on whether the

crystallizing assemblage decreases or increases the density of the residual magma. As discussed by Naslund and McBirney (1996), metasomatism and zone refining are subtle consequences of this process. Any of these mechanisms could be channelized (and produce distinct discordant bodies), or pervasive (and hence be extremely cryptic). In the Upper Critical and Main Zones of the Bushveld the magma crystallized plagioclase and one or two pyroxenes, and the evolving magma would have become denser (McBirney 1985), and so gravity-driven upward migration would not have occurred. One specific example is also worthy of mention. Tait and Jaupart (1992) suggested that the discordant iron-rich bodies that occur in the Critical and Main Zones are examples of this compositional convection. Not only is the density change of the evolving liquid incorrect (Scoon 1994), but the initial Sr isotopic ratio (Fig. 12.13) of these rocks demonstrates that the iron-rich liquids are not derived from the adjacent cumulate succession (Scoon and Mitchell 1994; Cawthorn et al. 2000).

Most of the textures in the Lower, Critical and Main Zones show evidence of annealing, with triple point junctions and planar edges that are not major crystallographic directions (which tend to dominate crystal growth in a magma). Hence, they are not the product of just grain overgrowth as in the adcumulus model of Wager et al. (1960). Some combination of Ostwald ripening and other compaction processes has clearly been operative. The three most important factors are time, proportion of liquid and temperature gradient. These collectively result in a crystal pile with interstitial liquid, the thickness of which will depend upon the rate of cooling. Cooling of the magma produces grains that accumulate on the floor with quicker cooling producing a thicker mush zone. Being such a thick intrusion the Bushveld crystallized very slowly. Using the cooling curves of Cawthorn and Walraven (1998) the rate at which the crystal mush advanced decreased per zone in cm y^{-1}, from 40 (Lower) to 10 (Critical) to 4 (Main) to 2.5 (Upper). These rates are about ten times faster than calculated by Morse (1979; p. 578) for the Kiglapait Intrusion which is of comparable thickness to the Bushveld. The reason for this discrepancy is not obvious to me. Using our quicker cooling rates, the accumulation rate ranges from one grain (2 mm in size) per day to one grain per 16 days. The rate at which grains will anneal and so compact and exclude remaining liquid is not known, because it is the combination of a number of different processes. It will be quickest in monomineralic rocks because all touching grains are the same mineral, and slower when more cumulus minerals are present. Plagioclase would be the slowest mineral to recrystallize because of its tectosilicate structure and oxides the fastest. Hence, the relationship between depth in the crystal pile and proportion of liquid is difficult to predict. However, the rate of annealing toward a solid rock is probably significant compared to the rate of arrival of the grains at the floor (for Bushveld), and so only a thin zone of crystal mush is inferred to have existed from these considerations. Thus Ostwald ripening may be more significant than compaction forces.

Structures in the layered rocks provide some limiting examples. Below the UG1 chromitite at Dwars River is a zone of slumping (Fig. 12.3s) of alternating melanocratic and leucocratic norite. The thickness of this slumped zone is less than 3 m, and is then overlain by multiple thin chromitite layers devoid of this deformation.

A similar package of variably slumped and brecciated noritic rocks occurs between the UG2 and UG3 chromitites on Maandagshoek (Fig. 12.3t and u, and described in detail by Maier et al. 2012), underlain and overlain by UG2 and UG3 that are perfectly planar and undisturbed. An interpretation of these structures is that these very few m-thick zones contained sufficient liquid to be capable of soft-sediment slumping possibly due to floor instabilities driven by loading by this huge mass of magma. They may be interpreted as seismic-triggered instability structures (Carr et al. 1994) in a plastic mush. Deeper layers were unaffected. The slumping event pre-dated the formation of the overlying, planar chromitite layers. The thickness of this zone of soft-sediment therefore may be in the order of a few metres.

Below the Merensky Reef at Impala Platinum mine there is an area that has been significantly deformed. Locally on the mine it was called the "flame bed" (Fig. 12.3v). All the "flames" show evidence of slumping in the same direction, down the dip. These flames are much more regular than at the Dwars River UG1 locality and may indicate a greater degree of cohesion of the grains and less liquid (or a less powerful seismic trigger). Below and above that layer is an undeformed planar layered package limiting the slumped package to very few metres.

In the Main Zone there is a sequence of strongly planar layered rocks. There is one outcrop where they can be seen to have been brecciated into blocks tens of cm across and typically ten cm thick (Fig. 12.3i). The fragments are quite angular. The maximum thickness of this layered package is 10 m (Quadling and Cawthorn 1994). Hence, one infers that these crystal-charged slurries that produced this brecciation broke up layered rocks that were sufficiently rigid to produce angular blocks, and so contained very little liquid. This feature also shows that the layering was of a primary nature and not due to any post-depositional process. These four examples suggest that the rate at which loose uncompacted grains annealed into progressively more rigid bodies occurred within a few metres of the upper boundary with the magma (with most to least liquid suggested in the order presented).

In the Upper Zone the fractionating magma would have become less dense due to oxide segregation (McBirney 1985), and so compositional convection might be envisaged. Magnetite has a large partition coefficient for Cr and patterns of fractionation and importantly abrupt reversals in Cr content of magnetite within the magnetitite layers are observed (Fig. 12.17). Had there been significant upward migration of liquid through these layers these reversals would have been smoothed into more gentle upward increases or completely eliminated, using the interpretation of Irvine (1980) for upward displacement and smoothing of reversals in the Muskox Intrusion.

Another example from the Upper Zone provides a different test for these models. Below Magnetitite Layer number 1 (the first above the Main Magnetitite Layer) there is a xenolith of Dullstroom basalt that has been metamorphosed into a granular texture. Along the outcrop it is at least 20 m long. Its extent at right angles is obviously unknown. It is 40 cm thick. Such a large xenolith would be expected to have trapped upward percolating residual magma if such a process were operative. Six short vertical profiles were taken along the strike, three from below the xenolith and three where the normal succession of footwall anorthosite overlain by magnetite oc-

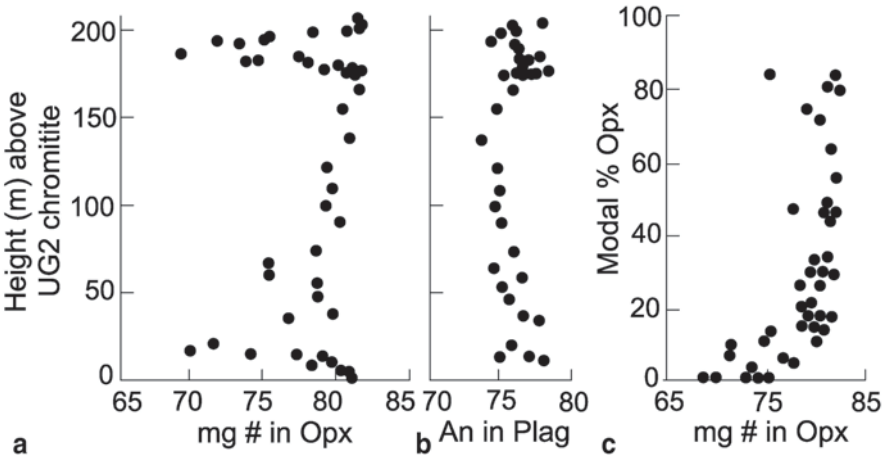

Fig. 12.18 **a** mg# in orthopyroxene and **b** An content in plagioclase versus height through the UG2 rhythmic unit. **c** mg# in orthopyroxene versus proportion of orthopyroxene showing that there is a pronounced decrease in mg# of the pyroxene where it is present at less than 20% by mode, and hence is composed of a significant proportion of intercumulus material. These trends suggest that the orthopyroxene has been markedly affected by the trapped liquid shift effect where its abundance is low. (Data from Schürmann 1993)

curs. There is no evidence for accumulation of residual magma beneath the xenolith based on incompatible trace element abundances (Cawthorn and Street 1994).

It has been suggested that upward percolation of liquid could have caused the concentration of chromitite layers within anorthosite in the Upper Critical Zone (Boudreau 1994). At Dwars River there is another definitive outcrop (Fig. 12.3q and r). Thin layers of chromitite have been disrupted by intrusion of an anorthosite mush. Layers of chromitite beneath this feature are continuous and suggest that the anorthosite in the mobilized mush is very locally derived (Nex 2004). Along the near-vertical boundary between the layered anorthosite and the discordant anorthosite is a thin zone of chromite grains (Fig. 12.3r), smeared out from the layer by the intruding anorthosite mush. The two observations, that the chromitite layer is truncated by the anorthosite mush and the smearing of the chromite grains, show that the chromitite layers are syn-depositional features.

Models that envisage large-scale vertical melt migration and metasomatism or zone refining can be tested with detailed mineralogical trends in the uppermost Critical Zone. A section of 200 m of layered plagioclase and orthopyroxene-bearing rocks is shown in Fig. 12.18. The An content of the plagioclase is near-constant at $An_{75–78}$. However, the mg# of the orthopyroxene varies greatly, notably in two sections with very leucocratic rocks (Fig. 12.18). If there had been metasomatism that had equilibrated with the sequence as the liquid passed upward, all the mg# values should be the same. The extent of variation on quite small scales is more consistent with the trapping of liquid, as discussed below, than with zone refining.

The overall conclusions suggested by these assorted observations are that fine-scale layering is a primary feature, and that consolidation of a very slowly accumulating pile of grains, from a mush to a very coherent, essentially rigid body of rock, occurs within a few metres of the magma interface, and that pervasive interaction between grains and a migrating residual liquid is minimal.

The Trapped Liquid Shift Effect (TLSE)

Ideally, the compositions of cumulus minerals in layered intrusions ought to define processes such as fractionation and recharge of the magma. However, their interpretation is hampered by the need to consider the post-cumulus effect of the interstitial liquid. Cooling and crystallization of this liquid should produce zoned margins to grains. The rate of exchange between NaSi and CaAl in plagioclase is extremely slow (Morse 1984), even at magmatic temperatures and so any original zoning is preserved, and the cores of grains can be analysed to give a true reflection of the cumulus composition. However, Mg–Fe exchange in mafic minerals is fast, resulting in homogenisation of grains (at least, in the Bushveld), and variable distortion away from the original cumulus composition. Barnes (1986b) showed that the effect could be quantified provided that the liquid fraction was trapped. If pervasive migration of liquid occurred then reaction between cumulus grains and this liquid would occur but the magnitude of the effect would be completely random. Trace element concentrations can also be influenced by this effect, and examples for major oxides and compatible and incompatible elements in minerals are given below.

Major Oxides

Two examples are used here to demonstrate the TLSE for mg#. The variation in mg# in orthopyroxene in the uppermost Critical Zone is shown in Fig. 12.18. The near-constancy of the plagioclase composition shows that a very large volume of magma existed, such that 200 m of cumulates produced no change in plagioclase composition. However, the mg# of the orthopyroxene is apparently randomly variable. The value of the mg# in orthopyroxene can be compared with its modal proportion in those rocks (Fig. 12.18c). It can be seen that the mg# decrease correlates with the decrease in modal content below 20%. In samples with abundant orthopyroxene there is a relatively large proportion of cumulus mineral compared to that formed from the trapped liquid. As a result, the final analysed mineral has a composition still close to that of the true cumulus phase. However, where there is little orthopyroxene, the rock contains a much larger relative proportion of the intercumulus component and the final mg# of the pyroxene (and the whole-rock) composition decreases. A comprehensive study of the mineral compositions in the Main Zone in the northern lobe was presented by Roelofse and Ashwal (2012). It showed irregular variability vertically of the mg# of the mafic minerals (Fig. 12.19), but

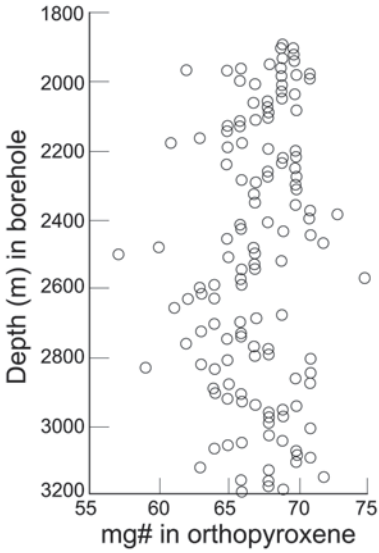

Fig. 12.19 Plot of mg# in orthopyroxene for a 1400 m thick section of the Main Zone. (Data taken from Roelofse and Ashwal 2012)

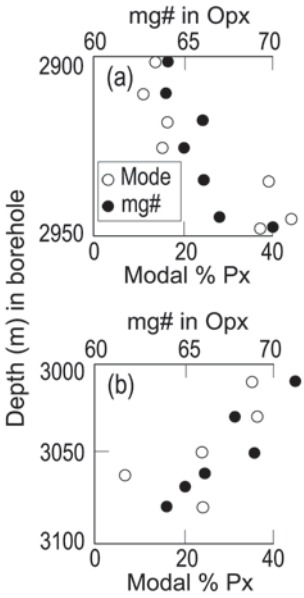

Fig. 12.20 Two short sections taken from Fig. 12.19 showing an upward decrease **a** and an upward increase **b** in mg# with height. Also plotted are the modal proportions of pyroxene in these sections. High mg# correspond to rocks with a high content of (cumulus) pyroxene, and the mg# is lower where there is less pyroxene and the trapped liquid contribution becomes more significant

little variation in the An content of plagioclase. Two detailed sections are shown in Fig. 12.20, illustrating this variability in mg#. In Fig. 12.20a there appears to be an upward decrease in mg# in orthopyroxene. Conversely, in Fig. 12.20b there is an upward increase. Such trends might be interpreted as due to fractionation and recharge respectively. However, when the modal proportion of pyroxene is considered in these plots it can be seen that there is a strong positive correlation between

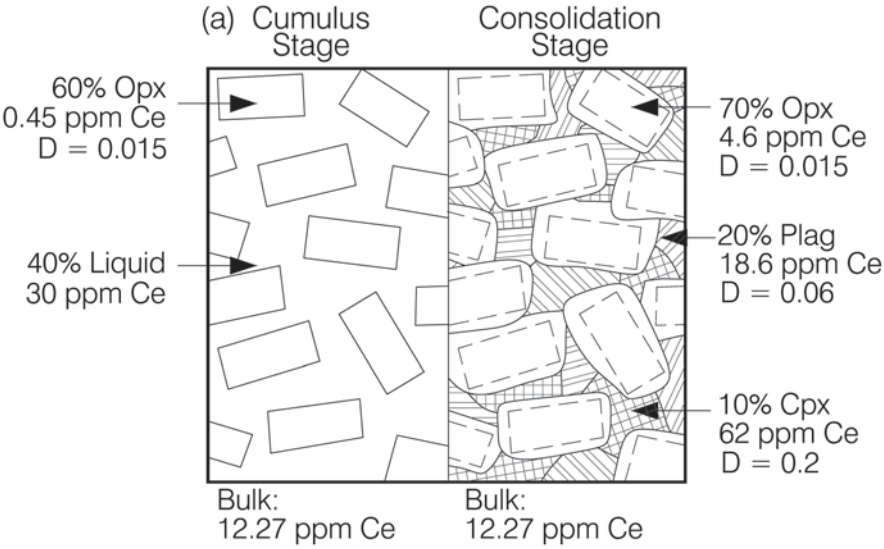

Fig. 12.21 Model showing the effect of the trapped liquid shift on the Ce abundance in mineral compositions. The cumulus orthopyroxene in equilibrium with liquid contains 0.45 ppm Ce, but after solidification of the trapped liquid its composition has increased to 4.6 ppm

mg# and modal pyroxene content, with the more evolved pyroxene compositions in pyroxene-poor rocks. Such a correlation is exactly that predicted by the trapped liquid shift model.

I conclude that using the mg# value of minerals is not a reliable method for modelling fractionation and recharge in a magma chamber. The An content of plagioclase may provide a better parameter for such modelling because the cores are not reset by reaction with interstitial liquid. However, inhomogeneity within the cores of plagioclase grains is typically ± 2 % An (Cawthorn and Ashwal 2009) and so only sustained changes larger than that may be considered significant.

Trace Elements

The incompatible trace element contents in minerals behave in an analogous way to the mg# as a result of the TLSE. The trapped liquid contains very much higher concentrations of such elements than the cumulus minerals, and so contribute very disproportionately to the bulk rock concentration. On solidification of the trapped liquid these incompatible elements have to be partitioned between the cumulus and any new intercumulus minerals (according to their individual partition coefficients). Thus, the final minerals would contain a much higher concentration of such elements than the original cumulus phase. This effect is shown in Fig. 12.21 for Ce in orthopyroxene. The liquid may have contained 30 ppm Ce and so the cumulus pyroxene contained 0.45 ppm (D = 0.015). A model rock is considered, containing

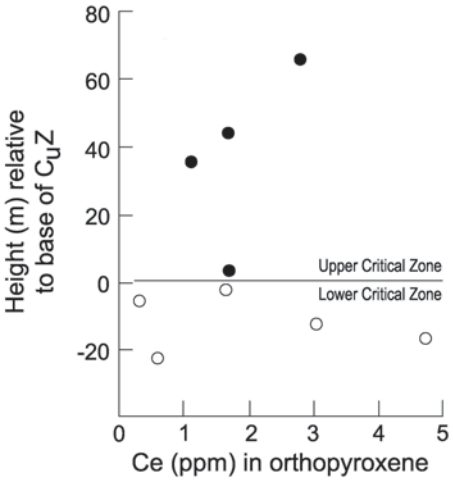

Fig. 12.22 Ce contents in orthopyroxene across the boundary between Lower (open symbols) and Upper (closed symbols) Critical Zone. (Own unpublished data)

60% cumulus pyroxene and 40% trapped liquid. The total Ce content is 12.27 ppm Ce. On solidification, the rock now contains 20% plagioclase, 10% clinopyroxene (both formed from the trapped liquid) and 70% orthopyroxene. The 12.27 ppm Ce has distributed itself between the three minerals to yield Ce contents of 4.6, 62 and 18.6 ppm (for orthopyroxene, clinopyroxene and plagioclase, respectively, using the D values shown in Fig. 12.21). Thus the cumulus orthopyroxene with 0.45 ppm Ce has changed to contain 4.6 ppm, a ten-fold increase. (Smaller proportions of trapped liquid would yield smaller increases in final Ce concentration.) The precision of these calculations depends upon a knowledge of the D values and the proportion of trapped liquid (and the modal proportions produced by the trapped liquid).

This principle was used by Cawthorn (1996b) to show how the large variations observed in REE content of orthopyroxene in the Critical Zone could be explained. A similar demonstration of this effect in the Lower Zone was shown by Godel et al. (2011). Its effect is also shown in Fig. 12.22. The orthopyroxene and whole-rock concentrations from a section traversing the Lower Critical to Upper Critical Zones were determined. The Ce content of the orthopyroxene varies irregularly by a factor of 10 (0.3–5 ppm). If these values for Ce in orthopyroxene were considered the true cumulus compositions then they would demand that the liquid from which they formed also varied erratically by a factor of 10, which I suggest is implausible. The Zr whole-rock content varies considerably, and can be considered a proxy for the proportion of trapped liquid. A plot of the final Ce content in the pyroxene versus the whole-rock Zr content shows a strong positive correlation (Fig. 12.23). Hence, I suggest that the variation in Ce in pyroxene results from the variable proportions of and extent of re-equilibration with trapped liquid. By extrapolation to 8 ppm Zr (the likely content of Zr in pyroxene) the true cumulus pyroxene can be inferred to have less than 0.5 ppm Ce (as used in Fig. 12.21). If there had been infiltration and variable metasomatism during final compaction and solidification, as proposed by Mathez et al. 1997) for the Bushveld and McKenzie (2011) with specific reference to the Skaergaard Intrusion, such a correlation as seen in Fig. 12.23 would not result.

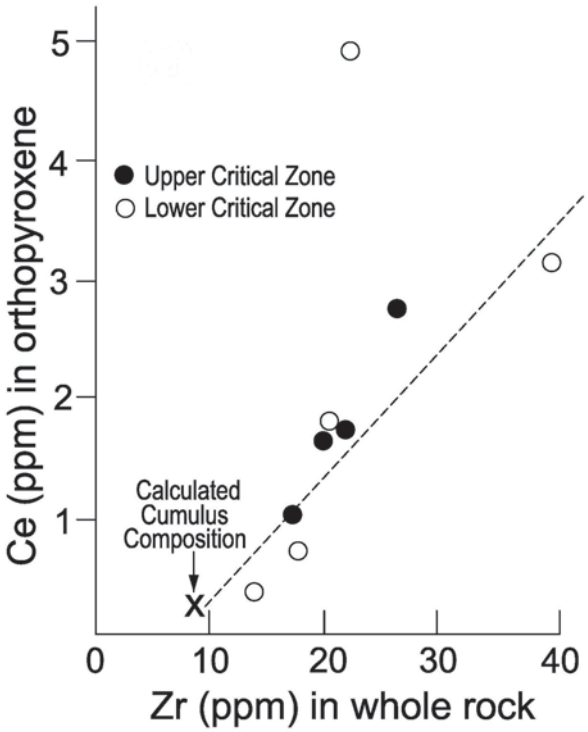

Fig. 12.23 Relationship between Ce content in orthopyroxene and Zr content in whole rock that proxies for the proportion of trapped liquid. Extrapolation to 8 ppm Zr yields the cumulus orthopyroxene composition. (Own unpublished data)

The same principle can be applied to the REE in apatite, even though they are highly compatible in apatite. The effect is shown in Fig. 12.24, which is analogous to Fig. 12.21. For simplicity of demonstration, it is assumed that the other minerals

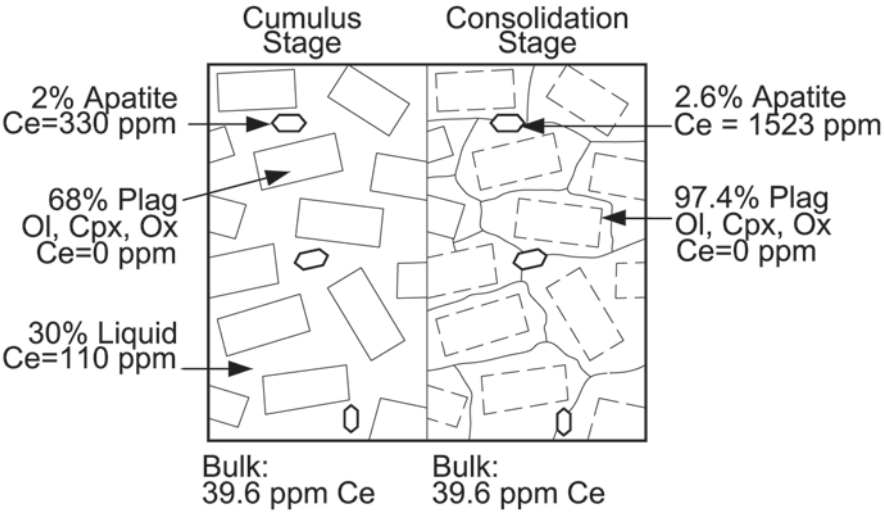

Fig. 12.24 Behaviour of Ce in apatite, analogous to that shown in Fig. 12.21 for orthopyroxene

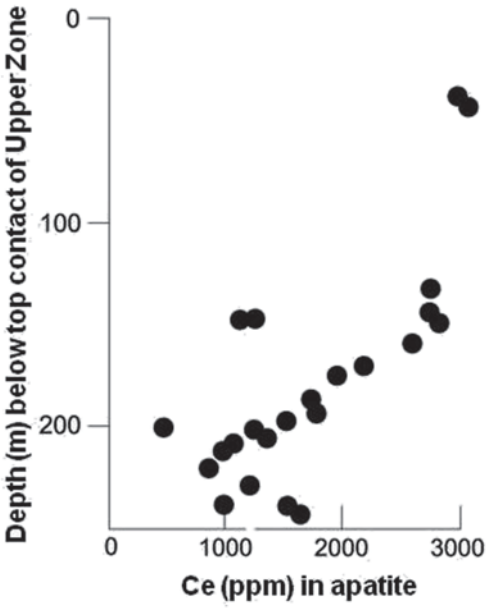

Fig. 12.25 Plot of Ce in apatite versus height below upper contact in Bierkraal borehole BK1 (Own unpublished whole-rock data, and calculated by the method described by Tollari et al. 2008)

contain no Ce. The Ce in apatite in a cumulate rock with 2% cumulus apatite and 30% trapped liquid will increase by a factor of 5 due to the TLSE. The concentration of Ce in apatite in a vertical section through the Upper Zone is shown in Fig. 12.25 and indicates a general upward increase, and a decrease in the normative proportion of apatite. This relationship is predicted by application of the TLS principle and has been used by Cawthorn (2013b) to explain the variations in REE in apatite in the Upper Zone, and is shown in Fig. 12.26. Data previously published was interpreted to have resulted from liquid immiscibility (VanTongeren and Mathez 2012). As can be seen, the proportions of apatite and the trapped liquid are crucial in determining the final apatite composition. The exact proportion of trapped liquid in these rocks is difficult to quantify. The inclusion into these calculations of the minor concentrations of Ce that enter the other minerals is of trivial significance to this principle.

Slurries

In the debate concerning the origin of cumulus grains the concept of injection of a slurry into the presently observable Bushveld is becoming increasingly promoted. The general principle of this model was presented by Marsh (2006). Whereas it is well-known that many lavas erupt carrying some crystals, in none of the models presented below do the authors state the proportion of grains in their proposed slurries. The density of such a slurry would increase linearly as the proportion of mafic phases increases, and the viscosity would increase exponentially (McKenzie 2011).

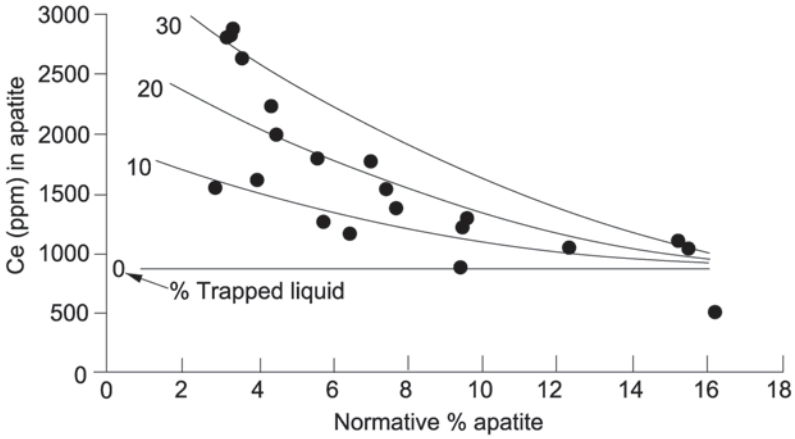

Fig. 12.26 Plot of normative apatite versus Ce content in apatite, showing the effect of changes in Ce content due to reaction with trapped liquid. (Own unpublished data and using the method described by Cawthorn 2013b). Where there is abundant cumulus apatite it buffers the effect of the trapped liquid shift effect and samples with high apatite content approximate to the true cumulus Ce content. However, where there is little cumulus apatite the trapped liquid shift effect becomes very pronounced

Hence, the ability of a slurry to be transported upward would become severely restricted. There are three variants to this model: (i) upward emplacement from a deeper chamber, (ii) lateral transport from the edges of an originally much wider Bushveld chamber, and (iii) injection into (not onto) the cumulate pile. They are discussed below.

Injection from a Deeper Chamber

Maier and Barnes (1998) compared the REE contents of Main Zone cumulates with the proposed parental magma to these rocks, and found them to be closely similar (Fig. 12.27). They proposed that the Main Zone must have been injected as a slurry of the pyroxene and plagioclase grains. The logic of this argument is not clear. If the proposed composition (referred to as B3 or B2) to this zone is a true liquid (i.e. not itself a crystal mush), then a rock that consists of an unspecified proportion of that liquid plus grains of plagioclase and pyroxene (which would be much lower in their REE contents than the liquid from which they formed) should be depleted in REE relative to the liquid. The similarity between the purported liquid (B2 or B3) and the Main Zone cumulates argues against this model. Furthermore, the proposed B2 and B3 compositions have a lower initial $^{87}Sr/^{86}Sr$ value (<0.706) than the Main Zone rocks (Maier et al. 2000).

Roelofse and Ashwal (2012) developed the idea of the injection of slurries. They proposed that the pyroxenes and the plagioclase came from two different magma

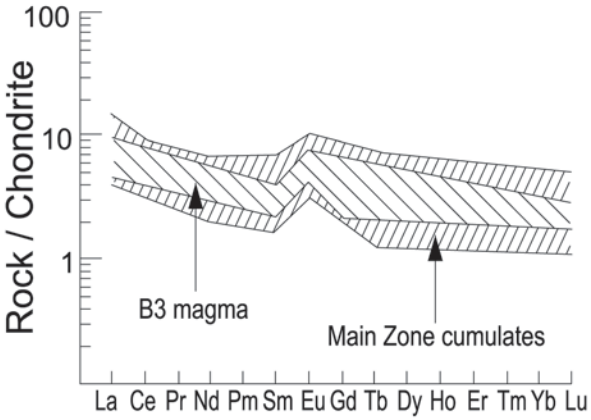

Fig. 12.27 Plot of REE abundance in typical Main Zone cumulates and of the purported parental magmas to the Main Zone (known as B2 or B3) taken from Maier and Barnes (1999). Their very similar abundances demonstrate that the one cannot be a cumulus-enriched assemblage and the other a true liquid. If there were about 10% trapped liquid in a cumulate rock and if the D values for these REE are low, then the liquid should contain almost 10 times as much as any crystal mush or cumulus rock

chambers at depth and then mixed to produce the gabbronorites in the Bushveld chamber. It needs to be questioned why the dense pyroxenes did not settle (in the deeper magma chamber) to produce a solid layer of rock that would not be capable of being remobilized into a slurry. It must further be questioned how a dense slurry of pyroxene (pre-supposing it existed) could be so effectively and completely mixed with a less dense slurry of plagioclase, because clustering of the pyroxenes or plagioclase grains together has never been reported, as would be expected if the process had not been extremely efficient. The extent of liquids of different density mixing was discussed above. The proposed crystal mushes would have had much higher density contrast and much higher kinematic viscosities than between two liquids, and so I question whether they could mix efficiently. Finally, it is well-known that the Al content of pyroxene co-existing with an aluminous phase (and hence being saturated in Al) increases with increasing pressure (Charlier et al. 2010). Data from assorted experimental studies at crustal pressures are shown in Fig. 12.28. At the mid-crustal pressure envisaged by Roelofse and Ashwal (2012) the orthopyroxene ought to contain at least 3% Al_2O_3. All Bushveld orthopyroxene grains contain less than 1.5%, and most less than 1% (Teigler and Eales 1996; Mitchell 1990; Schürmann 1993; Roelofse and Ashwal 2012).

One of the reasons for the proposed model by Roelofse and Ashwal (2012) was the fact that there was no mineral differentiation in terms of An content of plagioclase for their long vertical section of the Main Zone. They argued that differentiation should have occurred in the Bushveld chamber. They therefore proposed the existence of a deeper chamber providing grains of a constant composition. However, how this deeper magma chamber failed to differentiate, but provided minerals of

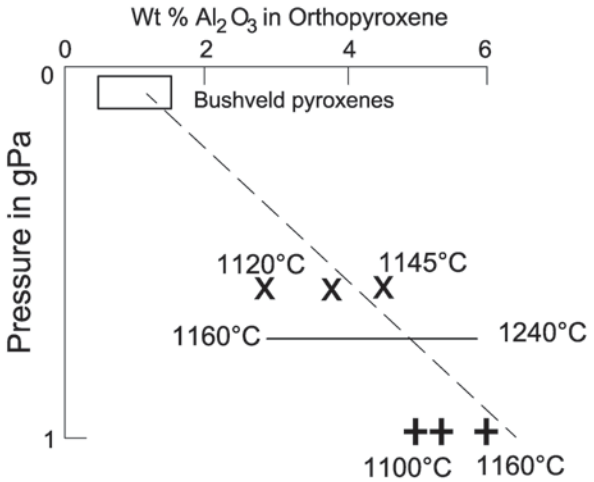

Fig. 12.28 Plot of weight % Al_2O_3 in orthopyroxene (in plagioclase-saturated assemblages) as a function of pressure, taken from assorted natural examples (the dashed line is a semi-quantitative trend from the data of Charlier et al. 2010 for anorthosites) and experimental studies (horizontal line is range of concentrations as a function of temperature from Chalott-Prat et al. 2010, and crosses and squares are individual data points from Vander Auwera et al. 1994 and Gudfinnsson and Presnall 2000)

constant composition was not discussed. The constancy of mineral composition can be explained by reference to lava compositions in large igneous provinces. In the Karoo and east Greenland, Marsh et al. (1997) and Tegner et al. (1998) showed that very many successive liquid compositions were erupted with a very constant composition. By analogy, for the Bushveld chamber, uniform liquids rather than grain mushes, could have been repeatedly injected producing minerals of near-constant composition.

Eales (2002) and Mondal and Mathez (2007) proposed that the chromite in the Critical Zone had been injected as a slurry. The validity of the summation undertaken by Eales has been discussed above. Given the high density of chromite relative to the magma, the possibility of it being so uniformly distributed over such large areas if injected at some point or line as a slurry seems implausible. In an expanded version of this concept, Eales and Costin (2012) suggested that olivine, orthopyroxene and chromite all accumulated in a deeper chamber to be injected as slurries. Given the high density of all three minerals it is not clear how this enormous mass of grains could have been held in suspension in this deeper chamber without coagulating on the floor. The model requires that the grains remain totally separated from each other because, upon injection, all the chromite grains were able to settle to the floor of the Bushveld chamber to form the chromitite layers. Paradoxically, the application of Stokes' Law clearly shows that the very small chromite grains, despite having higher density, would settle much more slowly than the much larger olivine and orthopyroxene. Hence, the order of accumulation proposed by them—chromite

before the mafic silicates—contradicts the settling rates. Again, the Al content of orthopyroxene in the Critical Zone argues against this model (Cameron 1980; 1982; Teigler and Eales 1996; Schürmann 1993). Finally, a slurry existing at the bottom of a large funnel-shaped chamber would not be erupted until all the overlying magma had been pumped out (and presumably into the Bushveld magma chamber), and so this model does not avoid the problem of the mass of magma in the Bushveld chamber.

Lateral Injection

A variation of this slurry model has been presented by Maier et al. (2012). They suggested that there was inward slumping of a semi-consolidated (and mineralogically unsorted) grain mush from the periphery of the intrusion (beyond the present outcrop limit) into the centre (the observable Bushveld area) and that as the grains resettled they separated into the observed modal layers. This model raises a number of questions. If these grains were accumulating around the periphery of the intrusion what was accumulating in the centre of the intrusion (which is the area now preserved)? The known extent of the intrusion (300 km wide) does not contain any of the original unsorted material. Did the accumulated slurry form in a ring all round the margins of the original chamber and all slump inward (everywhere at the same time) from the outside to produce layers of constant thickness everywhere? Or did the mass slumping occur from one side only and hence had to traverse many hundreds of km right across the preserved Bushveld, again producing layers of constant thickness? How did the huge mass of grains remain in a semi-aggregated state such that it could be totally disaggregated into single grains that were then able to sort themselves based on Stokes' Law? A calculation of the mass involved is given in Appendix 2. I suggest that all the examples of deformation seen (Fig. 12.3s to v, and in Maier et al. 2012) show that a semi-consolidated mush existed in the known Bushveld (not some peripheral area) and that tectonic disturbance caused intense deformation (Carr et al. 1994). The horizontal distances moved during such disturbances and deformation were in the order of metres to many tens of metres, not many hundreds of kilometres. Most importantly, these semi-consolidated layers remained largely intact and coherent, and did not disaggregate despite the intensity of their deformation. As shown above, the thickness of the unconsolidated mush was probably in the order of metres, and so the total masses involved in such disturbances was trivial compared to that required to redistribute material to form thick layers over many tens of thousands of square kilometres. Also the model contradicts Stokes Law, again requiring that chromite sank more rapidly than the mafic silicates. Further, the absence of cumulus pyroxene associated with the magnetitite-anorthosite sequences (discussed above) is inconsistent with this model. Finally, both models of redeposition of a slurry fail to explain the observation that the interstitial silicate phases in chromitite layers have higher $^{87}Sr/^{86}Sr$ values than the immediately overlying silicate-rich layers (Kinnaird et al. 2002).

Both the chromitite and the magnetitite layers show evidence of systematic vertical variations in composition, which is not explicable if they formed by remobilisation of an unconsolidated mush either from below or the periphery.

Injection into the Cumulate Pile

Yet another set of views on slurries has evolved that relates primarily to chromitites. The bifurcating UG1 chromitite and its footwall stringers seen at Dwars River (Fig. 12.3e), but present everywhere that the UG1 is exposed (especially underground) have been taken as evidence that the chromitite was a slurry that was injected (discordantly) into an already formed sequence, not emplaced at the mush—magma interface as with the above models (Voordouw et al. 2009). This principle has been applied to the UG2 chromitite as well (Maier and Barnes 2008). I have to debate this model on the grounds that a dense crystal mush cannot be laterally distributed with uniform thickness over an area of 30,000 km^2 (for the UG1 and UG2, which have so many unique features that they are demonstrably the same layer in the east and west). A second issue relates to whether this mechanism only applies to the UG1 and UG2 or all chromitites. If the model applies only to these two layers are all other chromitites formed by accumulation at the mush-magma interface? If so, what criteria distinguish the two different mechanisms of formation? There are many chromitite layers, often associated with the thicker, named layers, that are only mm in thickness (Fig. 12.3w), and yet are traceable over great distances. I question if they could have been intrusive. When viewed in thin section it is clear that small grains of chromite have settled on top of grains of orthopyroxene, not as an intrusion through the middle of a pyroxenite package (Fig. 12.11m). Many of the thin chromitite stringers show a zone of disseminated chromite grains, usually above the chromitite layer (Fig. 12.11n), which cannot be explained by an intrusive origin. Further, the relations at Dwars River (Fig. 12.3q) clearly show that the chromitites can be cut by anorthosite bodies, demonstrating the primary accumulation of chromite.

Finally, the geometry observed in the well-known potholes in the UG2 chromitite, disproves the intrusive relationship. In a pothole, the footwall succession is variably removed and the subsequently accumulating chromitite layer drapes itself into the pothole. Directly above the pothole the overlying layers are thickened relative to the normal succession. These features are shown in Fig. 12.29. Figure 12.29a shows a slightly stylised normal succession of (upward) footwall pyroxenite (FP) and anorthosite (FA), overlain by the UG2 chromitite (chr), then hangingwall pyroxenite (HP), norite (HN) and anorthosite (HA). Figure 12.29b shows the relations observed in a pothole (Hahn and Ovendale, 1994) where FA and part of PF have been truncated, and HP and HN thickened. Figures 12.29c and d show the situation envisaged in models that propose later intrusion of the chromitite between FA and HP; Fig. 12.29c shows the situation before chromitite injection, and Fig. 12.29d after the postulated injection with slight discordances producing the pothole. Note

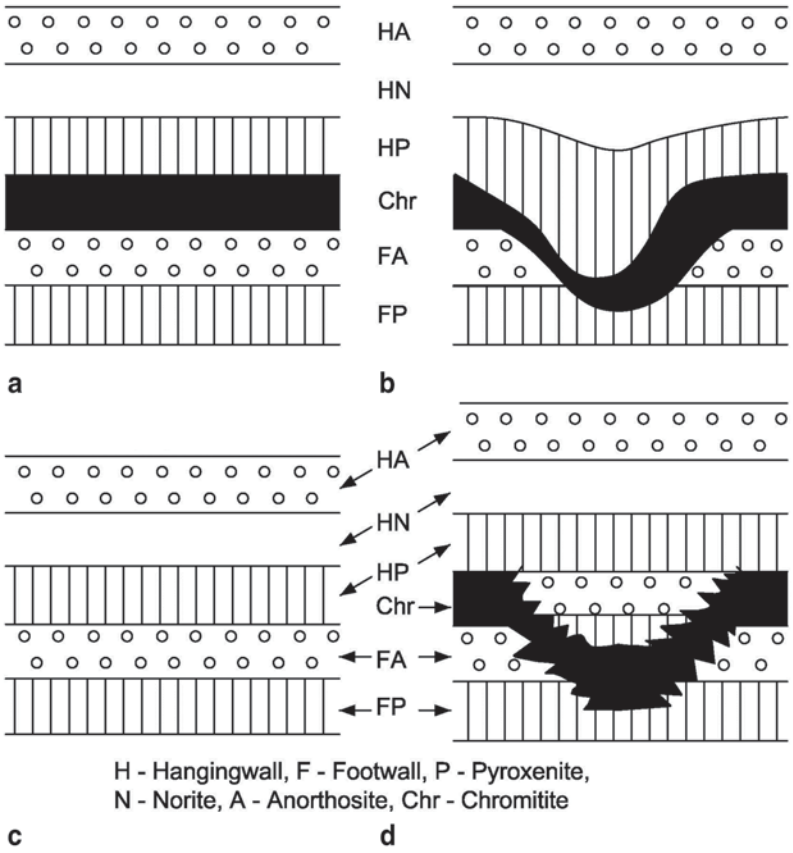

Fig. 12.29 Evidence against intrusive chromitites using observations from the UG2. **a** Illustration of typical layered succession. **b** Cross-section through a typical pothole at the level of the UG2 Chromitite layer (generalized from author's own observations and Hahn and Ovendale 1994). **c** Hypothetical succession pre-emplacement of intrusive chromitite. **d** Geometrical relations in a pothole demanded if chromitite is intrusive. Note that some typical footwall rocks(FP and FA) would be expected above the chromitite with this model. See text for explanation

that some of FP and FA are now displaced above the chromitite, and that HP and HN have not changed in thickness. The observed relations (Fig. 12.29b) show thickening of hangingwall layers and no preservation of footwall layers above the chromitite. All the observed features are very simply explained in a stratigraphic accumulation model, where the layers FA and FP were eroded by current activity. The chromitite was deposited on that eroded surface. The hanging wall layers infilled the depression and eventually obliterated the topographic effects of the pothole erosion event. Such (clastic) sedimentary processes to smooth temporary topographic irregularities were emphasised by Irvine et al. (1998) in the Skaergaard intrusion, although in their case there were autoliths forming positive features that were buried, with the layers becoming horizontal a very short vertical distance above the

autoliths. For exactly the same reasons, the pothole geometry seen at the level of the Merensky Reef invalidates models (Mitchell and Scoon 2007) that propose an intrusive origin for the Merensky Reef.

Density Inversions

The association of anorthosite (density 2.75 g cm^{-3}) and overlying magnetitite (density >5), as shown in Fig. 12.3j, represents the biggest density contrast between any two layers of rock above the core-mantle boundary. Furthermore, they are gravitationally unstable (denser above less dense). If the two layers had existed as mushes with a considerable proportion of interstitial liquid it would be expected that diapiric structures ought to have developed. The remarkably planar boundary between such paired layers suggests that the underlying anorthosite was extremely rigid before any significant accumulation of magnetite occurred. This same observation applies to the MG3, MG4, UG1 and UG2 chromitites that are underlain by anorthosite have remarkably planar undeformed interfaces.

Discordant Bodies

The remarkably laterally extensive layering is interrupted by very irregularly distributed pegmatitic ultramafic bodies ranging from olivine- and clinopyroxene-rich to magnetite-dominated vertically. Vertical continuity of any single body cannot be established, except for the 300-m vertical exposure in the Kennedys Vale vanadiferous magnetitite plug, near Dwars River along the Steelpoort structure (Viljoen and Scoon 1985). Many are pipe-like, but many also are dyke-like (Fig. 12.3x) or are planar and concordant (Fig. 12.3y). Whereas most are iron-rich, those bodies in the Critical Zone are quite magnesian (Viljoen and Scoon 1985; Tegner et al. 1994). Exposures of contacts are limited to mining activities and road cuttings. They do not displace the surrounding rocks but clearly replace them. For example, opposing sides of bodies and not planar and do not match (Fig. 12.3z). They are replacive, and relic features such as remains of thin chromitites and platinum mineralisation at the level of the Merensky Reef have been recorded in them (Viljoen and Heiber 1986). Scoon and Mitchell (1994) interpreted them as either evolved magmas or iron-rich immiscible liquids derived from the Upper Zone. The initial Sr isotope ratio of these rocks is inconsistent with them having been derived from a local source (Fig. 12.13). If they had originated in the Upper Zone as immiscible liquids then they had to melt their way downward for distances of over 2 km through cumulates that would have a very high liquidus temperature, and that remelted material had to be expelled upward without mixing with the descending liquid. Where sill-like bodies are exposed, it is the upper contact that is irregular, not the lower contact, challenging the view that they were emplaced downward. Thus, the mechanism of emplacement must be considered unresolved.

Summary

The Bushveld Complex shows the most complete differentiation sequence of any layered intrusion with olivine Fo_{90} at the base, through iron-rich successions to monzonite with olivine Fo_1, and containing 65 % $SiO_{2\,at}$ the top. In preserved lateral extent (more than 60,000 km^2) the Bushveld Complex is by far the World's largest layered mafic intrusion. Many distinctive layers (chromitites, Merensky and Bastard Reef, and Pyroxenite Marker) can be traced in the east and west lobes; and the magnetitite layers traced also in the northern lobe. Identifying processes that explain the uniformity of such layers is probably the single biggest challenge to modelling this intrusion. Whether most of the accumulation of grains and modal layering is by settling and gravity sorting or by in situ growth is still totally unresolved, although great thicknesses showing gradual modal changes independent of cotectic proportions suggest the former. The rate of accumulation of grains on the floor of the intrusion was extremely slow, permitting textural re-equilibration close to the mush-liquid interface. Many features suggest that the vertical column in which there was considerable liquid was restricted to a few metres at maximum. The remaining ±10 % of interstitial liquid became trapped and as it solidified it modified mg# in mafic minerals when that mineral was present as a minor cumulus phase, and increased the incompatible trace element contents of all minerals. Interpretations based on mg# to model fractionation processes, and of trace elements to model instantaneous liquid compositions are extremely unreliable. The remarkable state of preservation of this 2.06 b.y. old body permits studies (especially geochemical) that are impossible on many old igneous rocks, and provides an insight into the processes that have operated, but which still require conclusive resolution.

Acknowledgements I have been fortunate to have been based at the University of the Witwatersrand for 40 years, which has provided support for my research into the Bushveld Complex in many ways. Financial support has been generously provided by NRF (South Africa), Anglo-platinum, Impala Platinum and Lonplats. Many mining company geologists have willingly given of their knowledge and their bore cores, without which many of my Bushveld studies would be impossible. Also academic geologists (many of whose names appear in the reference list below) have shared ideas and debates, variably enlightening and challenging in my attempts to grasp inklings into the genesis of the Bushveld. Richard Wilson, Jean-Clair Duchesne and James Roberts undertook very thorough reviews of earlier versions of this manuscript. Lyn Whitfield and Di du Toit drafted many diagrams. To all of them—very many thanks.

Appendix

1. Calculation to demonstrate that mixing cannot have occurred between resident and new magma at the base of the Main Zone.

Mitchell (1990) showed that the Cr_2O_3 content of the orthopyroxene below and in the Merensky interval is 0.4 % and decreases abruptly to 0.1 % 30 m higher in the

Lower Main Zone (Fig. 12.8a). Using partition coefficients that Barnes (1986a) showed to be temperature- and MgO-dependant, the Cr content of the magmas may be inferred. At the top of the Critical Zone the liquid contained about 7% MgO (Cawthorn 1996a), yielding a partition coefficient of 5. Thus the liquid contained 500–600 ppm Cr. The Main Zone liquid may have had similar or slightly less MgO. The partition coefficient may have been 6, yielding a liquid with 100 ppm Cr. (Uncertainties in the exact values of these numbers can be seen below to be irrelevant.) If it is assumed that the Main Zone is the product of mixing of residual Critical Zone and added Main Zone liquids an equation may be derived.

M (Cr in mixed magma in ppm) = R (Cr in residual Critical Zone magma)*F (fraction of residual magma involved) + A (Cr in added magma) * (1-F).

M = 100 (see above); R = 500 (see above); A = 100–200 ppm (Maier et al. 2000; Barnes et al. 2010). Hence, F < 0! There can be no mixing!

Note that the actual analyses of purported parental magma to the Main Zone (B2 or B3 in Table 12.1) contain 200 and 400 ppm Cr. These concentrations are implausible, based on the Cr content of the pyroxenes, even if no mixing had occurred.

2. Calculation of mass of material needed to make a 1 m thick layer of chromitite in the slumping model of Maier et al. (2012).

There would need to be a mass of chromite, pyroxene, (?) plagioclase and (?) olivine. One assumes that they are present in their cotectic proportions. Bulk density would be about 3 $t \cdot m^{-3}$. Suppose the cotectic proportion of chromite in that assemblage is 0.2%. To make 1 m of chromitite therefore requires 500 m of grain mush. The area over which the chromitite layers are preserved is at least 30,000 km^2. Hence, the mass of unconsolidated material would need to be $3 * 500 * 30000 * 10^6$ or $4.5 * 10^{13}$ t. All this material must remain in a completely disaggregatable state so that chromite grains could separate from silicate grains. This mass must have accumulated elsewhere for every 1 m-thick chromitite layer.

References

Ashwal LD, Webb SJ, Knoper MW (2005) Magmatic stratigraphy in the Bushveld northern lobe: continuous geophysical and mineralogical data from the 2950 m Bellevue drillcore. S Afr J Geol 108:199–232

Barnes SJ (1986a) The distribution of chromium among orthopyroxene, spinel and silicate liquid at atmospheric pressure. Geochim Cosmoschim Acta 50:1889–1909

Barnes SJ (1986b) The effect of trapped liquid crystallization on cumulus mineral compositions in layered intrusions. Contrib Miner Petrol 93:524–531

Barnes S-J, Maier WD, Curl E (2010) Composition of the marginal rocks and sills of the Rustenburg layered suite, Bushveld Complex, South Africa: implications for the formation of the PGE deposits. Econ GeoI 105:1491–1511

Biggar GM (1974) Phase equilibrium studies of the chilled margins of some layered intrusions. Contrib Mineral Petrol 46:159–167

Boorman S, Boudreau AE, Kruger FJ (2004) The lower zone-critical zone transition of the Bushveld Complex—a quantitative textural study. J Petrol 45:1209–1235

Bottinga Y, Weill DF, Richet P (1982) Density calculations for silicate liquids: I. Revised method for aluminosilicate liquids. Geochim Cosmochim Acta 46:909–919
Boudreau AE (1994) Mineral segregation during crystal aging in two-crysal, two-component systems. S Afr J Geol 97:473–485
Buchanan DL (1979) A combined transmission electron microscope and electron microprobe study of bushveld pyroxenes from the Bethal area. J Petrol 20:327–354
Button A (1976) Stratigraphy and relations of the Bushveld floor in the eastern Transvaal. Trans Geol Soc S Afr 79:3–12
Cameron EN (1978) The lower zone of the eastern Bushveld Complex in the olifants river trough. J Petrol 19:437–462
Cameron EN (1980) Evolution of the lower critical zone, central sector, eastern Bushveld Complex. Econ Geol 75:845–871
Cameron EN (1982) The upper critical zone of the eastern Bushveld Complex—precursor of the merensky reef. Econ Geol 77:1307–1327
Campbell IH (1996) Fluid dynamic processes in basaltic magma chambers. In: Cawthorn RG (ed) Layered intrusions. Elsevier, Amsterdam, pp 45–76
Campbell IH, Murck BW (1993) Petrology of the G and H chromitite zones in the mountain view area of the stillwater complex, Montana. J Petrol 34:291–316
Campbell IH, Roedder PL, Dixon JM (1978) Plagioclase buoyancy in basaltic liquid as demonstrated with a centrifuge furnace. Contrib Miner Petrol 67:369–377
Campbell IH, Naldrett AJ, Barnes SJ (1983) A model for the origin of the platinum-rich sulfide horizons in the bushveld and stillwater complexes. J Petrol 24:133–165
Carr HW, Groves DI, Cawthorn RG (1994) The importance of syn-magmatic deformation in the formation of merensky reef potholes in the Bushveld Complex. Econ Geol 89:1398–1410
Carr HW, Groves DI, Kruger FJ, Cawthorn RG (1999) Petrogenesis of merensky reef potholes at the western platinum mines: Sr-isotopic evidence for synmagmatic deformation. Miner Deposita 34:335–347
Cawthorn RG (1996a) Re-evaluation of magma compositions and processes in the uppermost critical zone of the Bushveld Complex. Miner Mag 60:131–148
Cawthorn RG (1996b) Models for incompatible trace-element abundance and their application to plagioclase and pyroxene compositions in the Bushveld Complex. Contrib Miner Petrol 123:109–115
Cawthorn RG (1998) Geometrical relations between the Transvaal Supergroup, the Rooiberg Group and the mafic rocks of the Bushveld Complex. S Afr J Geol 101:275–280
Cawthorn RG (1999) The discovery of the platiniferous merensky reef in 1924. S Afr J Geol 102:178–183
Cawthorn RG (2002) Delayed accumulation of plagioclase in the Bushveld Complex. Miner Mag 66:881–893
Cawthorn RG (2011) Geological interpretations from the PGE distribution in the bushveld merensky and UG2 chromitite reefs. South Afr Inst Min Metall 11:67–79
Cawthorn RG (2013a) The residual or roof zone of the Bushveld Complex. J Petrol 54:1875–1900
Cawthorn RG (2013b) Rare earth element abundances in apatite in the Bushveld Complex—a consequence of the trapped liquid shift effect. Geology 41:603–606
Cawthorn RG, Ashwal LD (2009) Origin of anorthosite and magnetite layers in the Bushveld Complex, constrained by major element compositions of plagioclase. J Petrol 50:1607–1637
Cawthorn RG, Biggar GM (1993) Crystallization of titaniferous chromite, magnesian ilmenite and armalcolite in tholeiitic suites in the Karoo Province. Contrib Miner Petrol 114:221–235
Cawthorn RG, Boerst K (2006) Origin of pegmatitic pyroxenite in the merensky unit, Bushveld Complex, South Africa. J Petrol 47:1509–1530
Cawthorn RG, McCarthy TS (1980) Variations in Cr content of magnetite from the upper zone of the Bushveld Complex—evidence for heterogeneity and convection currents in magma chambers. Earth Planet Sci Lett 46:335–343
Cawthorn RG, Molyneux TG (1986) Vanadiferous magnetite deposits of the Bushveld Complex. In: Anhaeusser CR, Maske S (eds) Mineral deposits of Southern Africa. Geol Soc S Afr Johannesburg 2:1251–1266

Cawthorn RG, Spies L (2003) Plagioclase-rich cyclic units in the Bushveld Complex. Contrib Miner Petrol 145:47–60
Cawthorn RG, Street J (1994) Vertical migration of residual magma in the Bushveld Complex. Miner Petrol 51:345–354
Cawthorn RG, Walraven F (1998) Emplacement and crystallization time for the Bushveld Complex. J Petrol 39:1669–1687
Cawthorn RG, Davies G, Clubley-Armstrong A, McCarthy TS (1981) Sills associated with the Bushveld Complex, South Africa. Lithos 14:1–15
Cawthorn RG, Meyer PS, Kruger, FJ (1991) Major addition of magma at the Pyroxenite Marker in the western Bushveld Complex, South Africa. J petrol 32:739–763
Cawthorn RG, Cooper GRJ, Webb SJ (1998) Connectivity between the western and eastern limbs of the Bushveld Complex. S Afr J Geol 101:291–298
Cawthorn RG, Harris C, Kruger FJ (2000) Discordant ultramafic pegmatoidal pipes in the Bushveld Complex. Contrib Miner Petrol 140:119–133
Cawthorn RG, Merkle RKW, Viljoen MJ (2002) Platinum-group element deposits in the Bushveld Complex, South Africa. In: Cabri LJ (ed) Geology, geochemistry, mineralogy and mineral beneficiation of platinum-group elements. Can Inst Min Metal Petrol 54:389–430
Chalot-Prat F, Falloon TJ, Green DH, Hibberson WD (2010) An experimental study of liquid compositions in equilibrium with plagioclase-spinel lherzolite at low pressures (0.75 gPa). J Petrol 51:2349–2376
Charlier B, Duchesne JC, Vander Auwera J, Storme JY, Maquil R, Longhi J (2010) Polybaric fractional crystallization of high-alumina basalt parental magmas in the Egersund-Ogna massif-type anorthosite (Rogaland, SW Norway) constrained by plagioclase and high-alumina orthopyroxene megacrysts. J Petrol 51:2515–2546
Clarke BM, Uken R, Watkeys MK (2000) Intrusion mechanisms of the southwest Rustenburg Layered Suite as deduced from the Spruitfontein inlier. S Afr J Geol 103:120–127
Clarke BM, Uken R, Reinhardt J (2009) Structural and compositional constraints on the emplacement of the Bushveld Complex, South Africa. Lithos 111:21–36
Cooper RW (1997) Magmatic unconformities and stratigraphic relations in the Peridotite zone, Stillwater Complex, Montana. Can J Earth Sci 34:407–425
Darwin C (1844) Geological observations on the volcanic islands. Appleton, London
Davey SR (1992) Lateral variation within the upper critical zone of the Bushveld Complex on the farm Rooikoppies 297JQ, Marikana, South Africa. S Afr J Geol 95:141–149
Davies G (1982) The petrogenesis of the peripheral zone of the Rustenburg layered suite and associated sills between Hartbeestpoort and Buffelspoort dams, western Bushveld Complex. Unpubl PhD thesis Univ Witwatersrand, Johannesbg, p 444
Davies G, Cawthorn RG (1984) Mineralogical data on multiple intrusion in the Rustenburg layered suite of the Bushveld Complex. Miner Mag 48:469–480
Davies G, Cawthorn RG, Barton JM, Morton M (1980) Parental magma to the Bushveld Complex. Nature 287:33–35
Du Plessis CP Walraven F (1990) The tectonic setting of the Bushveld Complex in Southern Africa, part 1. Structural deformation and distribution. Tectonophysics 179:305–319
Duchesne JC (1972) Iron-titanium oxide minerals in the Bjerkreim-Sokndal massif, south-western Norway. J Petrol 13:57–81
Duchesne JC, Charlier B (2005) Geochemistry of cumulates from Bjerkreim-Sokndal layered intrusion (S. Norway). Part I: constraints from major elements on the mechanism of cumulate formation and on the jotunite liquid line of descent. Lithos 83:229–254
Eales HV (2000) Implications of the chromium budget of the western limb of the Bushveld Complex. S Afr J Geol 103:141–150
Eales HV (2002) Caveats in defining the magmas parental to the mafic rocks of the Bushveld Complex, and the manner of their emplacement: review and commentary. Miner Mag 66:815–832
Eales HV, Cawthorn RG (1996) The Bushveld Complex. In: Cawthorn RG (ed) Layered intrusions. Elsevier, Amsterdam, pp 81–229

Eales HV, Costin G (2012) Crustally contaminated komatiite: primary source of the chromitites and marginal, lower, and critical zone magmas in a staging chamber beneath the Bushveld Complex. Econ GeoI 107:645–665

Eales HV, Reynolds I (1986) Cryptic variations within chromitites of the upper critical zone, northwestern Bushveld Complex. Econ Geol 81:1056–1066

Engelbrecht JP (1985) The chromites of the Bushveld Complex in the Nietverdient area. Econ Geol 80:896–910

Engelbrecht JP (1990) Contact metamorphic processes related to the aureole of the Bushveld Complex in the Marico district, western Transvaal. S Afr J Geol 93: 339–349

Godel B, Barnes S-J, Maier WD (2011) Parental magma composition inferred from in situ trace elements in cumulus and intercumulus silicate minerals: example from the lower and lower critical zones of the Bushveld Complex (South-Africa). Lithos 125:537–552

Groeneveld D (1970) The structural features and the petrography of the Bushveld Complex in the vicinity of Stoffberg, eastern Transvaal. In: Visser DL, von Gruenewaldt G (eds) Symposium on the Bushveld Igneous Complex and other layered intrusions, Geol Soc South Africa, Johannesbg, pp 36–45

Gudfinnsson GH, Presnall DC (2000) Melting behaviour of model lherzolite in the system CaO–MgO–Al_2O_3–SiO_2–FeO at 0.7 to 2.8 gPa. J Petrol 41:1241–1269

Hahn UF, Ovendale B (1994) UG2 chromitite layer potholes at Wildebeestfontein North Mine, Impala Platinum Limited, XVth CMMI Congress, Johannesburg. S Afr Inst Min Metall 3:195–200

Hall AL (1932) The Bushveld Igneous Complex in the central Transvaal. Geol Surv S Afr Mem 28:544

Hamilton PJ (1977) Sr isotope and trace element studies of the great dyke and Bushveld mafic phase and their relation to early proterozoic magma genesis in Southern Africa. J Petrol 18:24–52

Hargar HS (1934) An early Transvaal geological map by Carl Mauch. Trans Geol Soc S Afr 37:1–4

Harmer RE, Sharpe MR (1985) Field relations and strontium isotope systematics of the marginal rocks of the eastern Bushveld Complex. Econ Geol 80:813–837

Hatton CJ, von Gruenewaldt G (1987) The geological setting and petrogenesis of the Bushveld chromitite layers. In Stowe CW (ed) Evolution of chromium ore fields. Van Nostrand, New York, pp 109–143

Hulbert LJ, von Gruenewaldt G (1985) Textural and compositional features of chromite in the lower and critical zones of the Bushveld Complex. Econ Geol 80:872–895

Hunter RH (1996) Texture development in cumulate rocks. In: Cawthorn RG (ed) Layered intrusions. Elsevier, Amsterdam, pp 77–102

Irvine TN (1975) Crystallization sequences in the Muskox intrusion and other layered intrusions: II origin of chromitite layers and similar deposits of other magmatic ores. Geochim Cosmochim Acta 39:991–1020

Irvine TN (1977) Origin of chromitite layers in the Muskox intrusion and other stratiform intrusions: a new interpretation. Geology 5:273–277

Irvine TN (1980) Magmatic infiltration metasomatism, double diffusive fractional crystallization and adcumulus growth in the muskox intrusion and other layered intrusions. In: Hargraves RB (ed) Physics of magmatic processes. Princeton University Press, NJ 325–384

Irvine TN, Andersen JCØ, Brooks CK (1998) Included blocks (and blocks within blocks) in the Skaergaard intrusion; geological relations and the origins of rhythmically modally graded layers. Geol Soc Am Bull 110:1398–1447

Johnson TE, Gibson RL, Brown M, Buick IS, Cartwright I (2003) Partial melting of metapelitic rocks beneath the Bushveld Complex, South Africa. J Petrol 44:789–813

Junge M, Oberthür T, Melcher F (2014) Cryptic variation of chromite chemistry, platinum group element and platinum group mineral distribution in the UG-2 chromitite: an example from the karee mine, western Bushveld Complex, South Africa. Econ Geol 109:795–810

Kent AJ, Darr C, Koleszar AM, Salisbury MJ, Cooper KM (2010) Preferential eruption of andesitic magmas through recharge filtering. Nat Geosci 3:631–636
Kinnaird JA, Kruger FJ, Nex, PAM, Cawthorn RG (2002) Chromite formation—a key to understanding processes of platinum enrichment. Trans Inst Miner Min Metal 111:B23–B35
Kinnaird JA, Hutchinson D, Schürmann L, Nex PAM, De Lange R (2005) Petrology and mineralization of the southern Platreef: northern limb of the Bushveld Complex. Miner Depos 40:576–597
Klemm DD, Ketterer S, Reichhardt F, Steindl J, Weber-Diefenbach K (1985a) Implication of vertical and lateral compositional variations across the Pyroxenite Marker and its associated rocks in the upper part of the main zone in the eastern Bushveld Complex. Econ Geol 80:1007–1005
Klemm DD, Henckel J, Dehm R, von Gruenewaldt G (1985b) The geochemistry of titanomagnetite in magnetite layers and their host rocks of the eastern Bushveld Complex. Econ Geol 80:1075–1088
Knowles RA (1978) A bibliography of the geology of the Bushveld Complex. Uni Pretoria Res Rep 12:1–20
Kruger FJ (1990) The stratigraphy of the Bushveld Complex: a reappraisal and relocation of the main zone boundaries. S Afr J Geol 93:376–381
Kruger FJ (1992) The origin of the merensky cyclic unit: Sr isotopic and mineralogical evidence for an alternative orthomagmatic model. Aust J Earth Sci 39:255–261
Kruger FJ (1994) The Sr-isotopic stratigraphy of the western Bushveld Complex. S Afr J Geol 97:393–398
Kruger FJ (2005) Filling the Bushveld Complex magma chamber: lateral expansion, roof and floor interaction, magmatic unconformities and the formation of giant chromitite, PGE and Ti-V magnetitite deposits. Miner Depos 40:451–472
Kruger FJ, Marsh JS (1985) The mineralogy, petrology and origin of the Merensky cyclic unit in the western Bushveld Complex. Econ Geol 80:958–974
Kruger FJ, Cawthorn RG, Walsh KL (1987) Strontium isotopic evidence against magma addition in the upper zone of the Bushveld Complex. Earth Planet Sci Lett 84:51–58
Lange RA (1994) The effect of H_2O, CO_2 and F on the density and viscosity of silicate melts. In: Carroll MR, Holloway Jr (eds) Volatiles in magmas. Rev Miner 30:331–369
Latypov R, Hanski E, Lavrenchuk A, Huhma H, Havela T (2011) A 'three-increase model' for the origin of the marginal reversal of the Koitelainen layered intrusion Finland. J Petrol 52:733–764
Latypov R, O'Driscoll B, Lavrenchuk A (2013) Towards a model for the in situ origin of PGE reefs in layered intrusions: insights from chromitite seams of the rum eastern layered intrusion, Scotland. Contrib Miner Petrol 166:309–327
Lee CA, Butcher AR (1990) Cyclicity in the Sr isotope stratigraphy through the merensky and bastard reefs, atok section, eastern Bushveld Complex. Econ Geol 85:877–883
Leeb-Du Toit A (1986) The Impala platinum mines. In: Anhaeusser CR, Maske S (eds) Mineral deposits of Southern Africa. Geol Soc S Afr Johannesburg 2:1091–1106
Li C, Maier WD, de Waal SA (2001) The role of magma mixing in the genesis of PGE mineralization in the Bushveld Complex: thermodynamic calculations and a new interpretation. Econ Geol 96:653–662
Lombaard BV (1934) On the differentiation and relationships of the rocks of the Bushveld Complex. Trans Geol Soc S Afr 37:5–52
Lundgaard KL (2003) Magma chamber processes studied in two layered intrusions. PhD thesis, Aarhus University, Denmark
Maaløe S (1978) The origin of rhythmic layering. Miner Mag 42:337–345
Maier WD, Barnes SJ (1998) Concentrations of rare earth elements in silicate rocks of the lower, critical and main zones of the Bushveld Complex. Chem GeoI 150:85–103
Maier WD, Barnes SJ (2008) Platinum-group elements in the UG1 and UG2 chromitites, and the bastard reef, at impala platinum mine, western Bushveld Complex, South Africa: evidence of late magmatic cumulate instability and reef constitution. Geol Soc S Afr 111:159–176

Maier WD, Eales HV (1994) Facies model for interval between UG2 and merensky reef, western Bushveld Complex, South Africa. Trans Inst Min Metal 103:B22–B30
Maier WD, Eales HV (1997) Correlation within the UG2-Merensky reef interval of the western Bushveld Complex, based on geochemical, mineralogical and petrological data. Geol Surv S Afr Bull 120:56
Maier WD, Arndt NT, Curl EA (2000) Progressive crustal contamination of the Bushveld Complex: evidence from Nd isotopic analyses of the cumulate rocks. Contrib Miner Petrol 140:316–327
Maier WD, Barnes SJ, Groves DI (2012) The Bushveld Complex, South Africa: formation of platinum, palladium, chrome- and vanadium-rich layers via hydrodynamic sorting of a mobilized cumulate slurry in a large, relatively slowly cooling, subsiding magma chamber. Miner Depos 48:1–56
Maré LP, Fourie CJS (2012) New geochemical and palaeomagnetic results from neoarchaean dyke swarms in the Badplaas-Barberton area, South Africa. S Afr J Geol 115:145–170
Marsh BD (2006) Dynamics of magmatic systems. Elements 2:287–192
Marsh JS, Hooper PR, Rehacek J, Duncan RA, Duncan AR (1997) Stratigraphy and age of Karoo basalts of Lesotho and implications for correlations within the Karoo Igneous Province. Geophys Monogr 100:247–272
Mathez EA, Hunter RH, Kinzler R (1997) Petrologic evolution of partially molten cumulates: the atok section of the Bushveld Complex. Contrib Miner Petrol 129:20–34
McBirney AR (1985) Further considerations of double-diffusive stratification and layering in the skaergaard intrusion. J Petrol 26:993–1001
McCarthy TS, Cawthorn RG (1983) The geochemistry of vanadiferous magnetite in the Bushveld Complex: implications for crystallization mechanisms in layered complexes. Miner Depos 18:505–518
McKenzie D (2011) Compaction and crystallization in magma chambers: towards a model of the Skaergaard intrusion. J Petrol 52:905–930
Mitchell AA (1990) The stratigraphy, petrography and mineralogy of the main zone of the northwestern Bushveld. S Afr J Geol 93:818–831
Mitchell AA, Manthree R (2002) The giant mottled anorthosite: a transitional sequence at the top of the upper critical zone of the Bushveld Complex. S Afr J Geol 105:15–24
Mitchell AA, Scoon RN (2007) The merensky reef at winnarshoek, eastern Bushveld Complex: a primary magmatic hypothesis based on a wide reef facies. Econ Geol 102:971–1009
Molengraaff GAF (1901) Géologie de la République Sud Africaine du Transvaal. Bull Soc Geol France 4:13–92
Molyneux TG (1974) A geological investigation of the Bushveld Complex in Sekhukuneland and part of the Steelpoort valley. Trans Geol Soc S Afr 77:329–338
Molyneux TG, von Gruenewaldt G, Knowles RA (1976) A bibliography of the geology of the Bushveld Complex. Uni Pretoria Res Rep 2:1–63
Mondal SK, Mathez EA (2007) Origin of the UG2 chromitite layer, Bushveld Complex. J Petrol 48:495–510
Morse SA (1979) Kiglapait geochemistry I; systematics, sampling, and density. J Petrol 20:555–590
Morse SA (1984) Cation diffusion in plagioclase feldspar. Science 225:504–505
Murck BW, Campbell IH (1986) The effects of temperature, oxygen fugacity and melt composition on the behaviour of chromium in basic and ultrabasic melts. Geochim Cosmo Acta 50:1871–1888
Naldrett AJ, Wilson AH, Kinnaird J, Chunnett G (2009) PGE tenor and metal ratios within and below the Merensky Reef, Bushveld Complex: implications for genesis. J Petrol 50:625–659
Naldrett AJ, Wilson A, Kinnaird J, Yudovskaya M, Chunnett G (2012) The origin of chromitites and related PGE mineralization in the Bushveld Complex: new mineralogical and petrological constraints. Miner Depos 47:209–232
Naslund HR, McBirney AR (1996) Mechanisms of formation of igneous layering. In: Cawthorn RG (ed) Layered intrusions. Elsevier, Amsterdam, 1–44

Nex PA (2004) Formation of bifurcating chromitite layers of the UG1 in the bushveld igneous complex, an analogy with sand volcanoes. J Geol Soc Lond 161:903–909
Nex PA, Kinnaird JA, Ingle LJ, Van der Vyver BA, Cawthorn RG (1998) A new stratigraphy for the main zone of the Bushveld Complex, in the Rustenburg area. S Afr J Geol 101:215–223
Nguuri TK, Gore J, James DE, Webb SJ, Wright C, Zengeni TG, Gwavava O, Snoke JA (2001) Crustal signature beneath southern Africa and its implication for the formation and evolution of the Kaapvaal and Zimbabwe cratons. Geophys Res Lett 28:2501–2504
Ochs FA III, Lange RA (1999) The density of hydrous magmatic liquids. Science 283:1314–1317
Olsson JR, Söderlund U, Klausen MB, Ernst RE (2010) U-Pb baddelyite ages linking major Archean dyke swarms to volcanic rift forming events in the Kaapvaal craton (South Africa), and a precise age for the Bushveld Complex. Precamb Res 183:490–500
Perugini D, Poli G (2012) The mixing of magmas in plutonic and volcanic environments: analogies and differences. Lithos 153:261–277
Quadling K, Cawthorn RG (1994) The layered gabbronorite sequence, Main Zone, eastern Bushveld Complex. S Afr J Geol 97:442–454
Reynolds IM (1985) Contrasted mineralogy and textural relations in the uppermost Ti-magnetite layers of the Bushveld Complex in the Bierkraal area north of Rustenburg. Econ Geol 80:1027–1048
Roeder P, Goften E, Thornber C (2006) Cotectic proportions of olivine and spinel in olivine-tholeiitic basalt and evaluation of pre-eruptive processes. J Petrol 47:883–900
Roelofse F, Ashwal LD (2012) The lower main zone in the northern limb of the Bushveld Complex—a >1.3 km thick sequence of intruded and variably contaminated crystal mushes. J Petrol 53:1449–1476
SACS (South African Committee for Stratigraphy) (1980) Kent LE (compiler) Stratigraphy of South Africa. Geol Surv S Afr Pretoria, Handbook, 8:690
Schmidt ER (1952) The structure and composition of the merensky reef and associated rocks on the Rustenburg platinum mine. Trans Geol Soc S Afr 55:233–279
Schoenberg, R, Kruger FJ, Nägler F, Meisel T, Kramers JD (1999) PGE enrichment in chromitite layers and the merensky reef of the Bushveld Complex, a Re–Os and Rb–Sr isotope study. Earth Planet Sci Lett 172:49–64
Schürmann LW (1993) The geochemistry and petrology of the upper critical zone in the boshoek section of the western Bushveld Complex. Geol Surv S Afr Bull 113:88
Scoon RN (1994) Comment on compositional convection in a reactive crystalline mush and melt differentiation. J Geophys Res 99:11913–11917
Scoon RN, Mitchell AA (1994) Discordant iron-rich ultramafic pegmatites in the Bushveld Complex and their relationship to iron-rich intercumulus and residual liquids. J Petrol 35:881–917
Scoon RN, Mitchell AA (2009) A multi-stage orthomagmatic and partial melting hypothesis for the driekop platiniferous dunite pipe, eastern limb of the Bushveld Complex, South Africa. S Afr J GeoI 112:163–186
Seabrook CL, Cawthorn RG, Kruger FJ (2005) The Merensky reef, Bushveld Complex: mixing of minerals not mixing of magmas. Econ GeoI 100:1191–1206
Seabrook CL, Cawthorn RG, Kruger FJ (2006) The Merensky Reef, Bushveld Complex: Mixing of minerals not mixing of magmas. Econ Geol 100:1191–1206
Sharpe MR (1981) The chronology of magma influxes to the eastern compartment of the Bushveld Complex, as exemplified by its marginal border group. J Geol Soc Lond 138:307–326
Sharpe MR (1984) Petrography, classification and chronology of mafic sill intrusions beneath the eastern Bushveld Complex. Geol Surv S Afr Bull 77:40
Sharpe MR (1985) Strontium isotope evidence for preserved density stratification in the main zone of the Bushveld Complex. Nature 316:119–126
Sparks RSJ, Huppert HE, Koyaguchi T, Hallworth MA (1993) Origin of modal and rhythmic igneous layering by sedimentation in a convecting magma chamber. Nature 361:246–249
Tait S, Jaupart C (1992) Compositional convection in a reactive crystalline mush and melt differentiation. J Geophys Res 98:6735–6756

Tanner D, Mavrogenes JA, Arculus RJ, Jenner FE (2014) Trace element stratigraphy of the belleview core, northern bushveld: multiple magma injections obscured by diffusion processes. J Petrol 55:859–882

Tegner C, Wilson JR, Cawthorn RG (1994) The dunite-clinopyroxenite pegmatoidal pipe, Tweefontein, eastern Bushveld Complex, South Africa. S Afr J Geol 97:415–430

Tegner C, Lesher CE, Larsen LM, Watt WS (1998) Evidence from rare-earth element record of mantle melting for cooling of the tertiary Iceland plume. Nature 395:591–594

Tegner C, Cawthorn RG, Kruger FJ (2006) Cyclicity in the main and upper zones of the Bushveld Complex, South Africa: crystallization from a zoned magma sheet. J Petrol 47:2257–2279

Teigler B, Eales HV (1993) Correlation between chromite composition and PGE mineralization in the critical zone of the western Bushveld Complex. Miner Depos 28:291–302

Teigler B, Eales HV (1996) The lower and critical zones of the western limb of the Bushveld Complex, as indicated by the nooitgedacht boreholes. Geol Surv S Afr Bull 111:126

Teigler B, Eales HV, Scoon RN (1992) The cumulate succession in the critical zone of the Rustenburg layered suite at brits, western Bushveld Complex. S Afr J Geol 95:17–28

Tilley CE, Yoder HS Jr, Schairer JF (1968) Melting relations of igneous rock series. Carnegie Inst Wash Yrbk 66:450–457

Tollari N, Barnes SJ, Cox RA, Nabil H (2008) Trace element concentrations in apatite from the sept-iles intrusive suite, Canada—implications for the genesis of nelsonites. Chem Geol 252:180–190

Uken R, Watkeys MK (1997a) Diapirism initiated by the Bushveld Complex. Geology 25:723–726

Uken R, Watkeys MK (1997b) An interpretation of mafic dyke swarms and their relationship with major mafic magmatic events on the Kaapvaal craton and limpopo belt. S Afr J Geol 100:341–348

Vander Auwera J, Longhi J (1994) Experimental study of a jotunite (hypersthenes monzodiorite): constraints on the parental magma composition and crystallization conditions (P, T, f_{O2}) of the Bjerkreim-Sokndal layered intrusion (Norway). Contrib Miner Petrol 118:60–78

VanTongeren J, Mathez EA (2012) Large-scale liquid immiscibility at the top of the Bushveld Complex, South Africa. Geology 40:491–494

VanTongeren JA, Mathez EA (2013) Incoming magma composition and style of recharge below the pyroxenite marker, eastern Bushveld Complex, South Africa. J Petrol. 54:1585–1605

VanTongeren JA, Mathez EA, Keleman PB (2010) A felsic end to Bushveld differentiation. J Petrol 51:1891–1912

Vermaak CF (1976) The Merensky reef—thoughts on its environment and genesis. Econ Geol 71:1270–1298

Viljoen MJ, Hieber R (1986) The Rustenburg section of Rustenburg Platinum Mines Limited, with reference to the merensky reef. In: Anhaeusser CR, Maske S (eds) Mineral deposits of Southern Africa. Geol Soc S Afr Johannesburg 2:1107–1134

Viljoen MJ, Scoon RN (1985) The distribution and main geological features of discordant pegmatoid in the Bushveld Complex. Econ Geol 80:1109–1128

Von Gruenewaldt G (1970) On the phase change orthopyroxene-pigeonite and resulting textures in the main and upper zones of the Bushveld Complex in the eastern Transvaal. In Visser DJL, von Gruenewaldt G (eds) Symposium on the bushveld igneous complex and other layered intrusions. Geol Soc S Afr Spec Publ 1:67–73

Von Gruenewaldt G (1972) The origin of the roof rocks of the Bushveld Complex between tauteshoogte and paardekop in the eastern Transvaal. Trans Geol Sof S Afr 75:121–134

Von Gruenewaldt G (1973) The Main and upper zones of the Bushveld Complex in the Roossenekal area, eastern Transvaal. Trans Geol Soc S Afr 76:207–227

Voordouw R, Gutzmer J, Beukes NJ (2009) Intrusive origin for Upper Group (UGI, UG2) stratiform chromitite seams in the Dwars River area, Bushveld Complex, South Africa. Miner Petrol 97:75–94

Wager LR (1959) Differing powers of crystal nucleation as a factor producing diversity in layered igneous intrusions. Geol Mag 96:75–80

Wager LR, Brown GM (1968) Layered igneous rocks. Oliver and Boyd, Edinburgh, p 588
Wager LR, Brown GM, Wadsworth WJ (1960) Types of igneous cumulate. J Petrol 1:73–85
Wagner P (1929) Platinum deposits and mines of South Africa. Oliver and Boyd, Edinburgh, p 326
Waters C, Boudreau AE (1996) A re-evalaution of crystal-size distributions in chromitite cumulates. Am Miner 81:1452–1459
Webb SJ, Ashwal LD, Cawthorn RG (2011) Continuity between eastern and western Bushveld Complex, confirmed by xenoliths from kimberlite. Contrib Miner Petrol 162:101–107
Willemse J (1964) A brief outline of the geology of the Bushveld Igneous Complex. In: Haughton SH (ed) The geology of some ore deposits in Southern Africa. Geol Soc S Afr Johannesburg 2:91–128
Willemse J (1969) The vanadiferous magnetic iron ore of the Bushveld Igneous Complex. Econ Geol Monogr 4:137–208
Wilson AH (2012) A chill sequence to the Bushveld Complex: insight into the first stage of emplacement and implications for the parental magmas. J Petrol 53:1123–1168
Wilson JR, Cawthorn RG, Kruger FJ, Grundvig S (1994) Intrusive origin for the unconformable upper zone in the northern gap area, western Bushveld Complex, South Africa. S Afr J Geol 97:462–472